Towards informing a data-driven approach to marine bioregionalization in South Africa: A case study using benthic epifaunal datasets from the southern Benguela shelf

by

Donia Hela Wozniak[1]

Supervisor: Natasha Karenyi[1]

Co-supervisor: Lara Atkinson[2]

Dissertation submitted in fulfilment of the requirements for the degree of Master of Science to be awarded by the Department of Biological Sciences at University of Cape Town

April 2023

[1]Department of Biological Sciences, University of Cape Town, Private Bag X3, Rondebosch 7701 Cape Town, South Africa

[2]South African Environmental Observation Network (SAEON), Egagasini Offshore Node, Foretrust Building, Martin Hammerschlag Way, Foreshore 8002, Cape Town, South Africa

Declaration

I, Donia Hela Wozniak, hereby declare this thesis, submitted in fulfilment of the degree of Master of Science, is my own work, all sources referenced, and that it has not been previously submitted for assessment to another University or for another qualification.

Signed by candidate

Donia Hela Wozniak Date: April 2023

Acknowledgements

This masters research would not have been possible without the help and support of many people and institutions, all of whom I am extremely grateful to. I would like to thank the National Research Foundation (NRF) for funding this research, and to the University of Cape Town (UCT) and the South African Environmental Observation Network (SAEON) for funding conference attendances and travel costs.

This research made use of existing datasets collected by the Department of Fisheries, Forestry and Environment (DFFE) and SAEON over several years, for which I am very grateful for having been given access to. I would like to thank Zoleka Filander for the access to datasets collected from DFFE towed camera surveys and to Hermann Engel for countless meetings on advising and assisting with accessing and processing CTD datasets collected by various research trawl surveys. I would like to thank Luther Adams, Lara Atkinson, DFFE and SAEON for the use of their photos in this master's research.

Many skills were learnt along this journey, and I would like to thank all the people who shared their time and knowledge so willingly with me. I would specifically like to thank Jock Currie for providing help with R scripts and extracting data and to Skip Woolley for help and advice with troubleshooting several queries.

I would like to thank UCT and SAEON for providing the research support and access to workspaces needed to complete this research. I am particularly grateful for the support and kindness of the people within these institutions who I have had the pleasure of working with. I would like to thank Grant van der Heever for always being willing to assist with anything, and to Jordan von Stavel, Silke Brandt and Mari-Lise Franken for the support and help during shared data processing and analyses. To the entire SAEON Egagasini team and the UCT Marine Benthic Ecology Lab, your uplifting energies, and friendly smiles each week were a pleasure to be around, particularly during the challenges of hard COVID lockdown.

I would like to thank my supervisors, Lara Atkinson and Natasha Karenyi, for their endless support and encouragement along the way. I am truly grateful for the devotion both of you show to your students, the effortless guidance and many words of wisdom I have received.

Lastly, I would like to thank my family and friends for their constant love, support and encouragement that make it all worth it.

Table of Contents

List of Tables

List of Figures

Abstract

Marine bioregional, ecosystem and habitat classifications and maps are important for understanding and managing the marine environment. Benthic epifaunal assemblages often inform marine ecosystem classifications and maps, being recognized as good surrogates for broad benthic biodiversity patterns. In South Africa, ecosystem classification and mapping follow an expert-derived data-informed hierarchical approach. A move towards employing data-driven approaches to bioregionalization using quantitative biological and environmental datasets is underway. However, quantitative datasets collected with different sampling methods cannot easily be combined in analyses. It is also unknown whether available biological and environmental datasets can sufficiently define bioregions using existing data-driven approaches. As a case study, this research focuses on the southern Benguela shelf, located on the western margin of South Africa, where research trawl and towed camera sampling methods regularly collect quantitative data on epifaunal assemblages. This research therefore aims to 1) quantify congruency of epifaunal abundance patterns detected by a research trawl and a towed camera, so that their datasets can be appropriately weighted or prioritised in data-driven approaches and to 2) classify and predict epifaunal bioregions by applying a data-driven approach to bioregionalization using abundance data collected by research trawling.

Various univariate and multivariate analyses were used to compare differences in species composition, diversity and assemblage structure at 18 sites (50–700 m) collected between 2017 and 2020 by towed camera and research trawl sampling methods. To quantify congruency in multivariate assemblage patterns between sampling methods, a symmetric co-correspondence analysis (Co-CA) was used on the log+1 transformed abundance matrices. Univariate patterns of diversity were not significantly correlated between sampling methods, which detected mostly different subsets of epifaunal assemblages. The towed camera detected small and patchily distributed epifauna (e.g. the small brittle star *Ophiura trimeni*) and Anthozoans better than the trawl, while the trawl captured patterns of larger, highly motile Decapoda (e.g. the hermit crab *Sympagurus dimorphous*) and burrowing Asteroidea better than the towed camera. Though broad similarities in assemblage structure were evident between sampling methods, with high correlations found between important Co-CA axes ($r = 0.93, 0.93, 0.79, 0.80$), patterns were not significantly similar ($p > 0.05$).

To statistically determine epifaunal bioregions across the study area, Regions of Common Profile (RCP) models were applied, using abundance data collected by research trawling between 2017 and 2020 from 325 sites. An RCP modelling approach was selected as a

potential data-driven method for marine bioregionalization in South Africa, since classification and prediction are performed simultaneously, thereby quantifying uncertainty in estimated bioregions. Research trawl datasets were used due to their systematic sampling design which covers a greater spatial and temporal extent than other sampling methods across the study area. Rare species and collinear predictors were removed prior to modelling, resulting in 46 species and three environmental predictors (bottom temperature, dissolved oxygen and slope) used in the final model. Five bioregions were identified, based on lowest Bayesian Information Criterion (BIC). Low values of dissolved oxygen (< 0.3 ml/l) and low bottom temperature (3.76–5.24 ˚C) were important predictors for bioregions which aligned with the inner shelf (RCP 5, < 150 m) and upper slope (RCP 1, > 500 m) respectively. These bioregions were associated with the highest confidence in spatial predictions. The highest uncertainty was attributed to bioregions across intermediate depths (RCP 2, 3 and 4, ~150–500 m) where species richness was highest.

This study recommends the use of both towed camera and research trawl datasets to describe epifaunal assemblages holistically, though consideration should be given to the strengths and limitations of each dataset for specific applications. A low sample size of sites available for comparison between sampling methods may have influenced findings to be inconclusive, and further comparisons are recommended. However, findings suggest the strength of congruence between sampling methods is dependent on the species, habitat and spatial scale (resolution) of interest. Bioregions defined in this study aligned with broad depth breaks and known biogeographical patterns, though further effort is required to source and test relevant environmental predictors for species distributed across intermediate depth ranges (~150–500 m). Data-driven approaches to bioregionalization which can quantify uncertainty in spatial predictions of bioregions and utilise quantitative datasets provide more information for management applications. As such, RCP models informed by research trawl datasets could be a viable option when delineating marine bioregions for South Africa, though validation with independent datasets is strongly recommended.

This study highlights the importance of context, method and spatial resolution when detecting ecological patterns. When collecting data, different sampling methods may detect patterns with varying degrees of congruence depending on location, species sampled or the spatial scale of interest. When analysing data, the type and quantity of environmental predictors and species used to inform data-driven approaches likely influence bioregional patterns produced. The importance of long-term monitoring using a variety of sampling methods is emphasised to reliably compare and quantify bioregional patterns. Rigorous comparisons between datasets and analytical approaches are encouraged to improve understanding of their

advantages and limitations. This study contributes methodological advances towards informing a data-driven approach to marine bioregionalization in South Africa.

CHAPTER 1: Introduction and background

Marine ecosystem classification and mapping have many management implications and are necessary for evaluating the extent of threats that ecosystems face (Diaz et al., 2004). Benthic epifauna can be useful environmental indicators, and their spatial patterns are often included when informing ecosystem classifications (e.g. Buhl-Mortensen et al., 2020; Howell, 2010; Stephenson et al., 2021). Benthic sampling methods differ between the fauna they target, and the patterns they detect may vary depending on the spatial resolution of interest (Reiss et al., 2010; Silberberger et al., 2019). As such, ecosystem classifications should ideally be informed by data collected across multiple scales and sampling methods (Bowden, 2011; Buhl-Mortensen et al., 2012; Clark & Rowden, 2004; Lecours et al., 2015). While ecosystem classifications have usually been expert-derived (including in South Africa), more recent advancements to data-driven approaches can achieve mapped outputs which are less subjective and have greater ecological relevance (Rowden et al., 2018), particularly when informed by quantitative data (e.g. abundance) (Stephenson et al., 2021). However, quantitative datasets collected by different sampling methods cannot be readily combined in analyses. Different quantitative datasets therefore require appropriate prioritisation or weighting when used in data-driven approaches, depending on the patterns they detect across spatial resolutions or species (Sink et al., 2023). The patterns inferred by different sampling methods are not necessarily consistent between one another and may be largely context dependent (Flannery & Przeslawski, 2015), as is the choice of statistical analyses (Norberg et al., 2019). Quantification of patterns observed across various sampling methods, using appropriate statistical analyses, are therefore required to assist South Africa's transition to a data-driven marine ecosystem classification and map.

Ecosystem classification and mapping refer to the delineation and plotting of ecologically relevant spatial units (also referred to as groups or classes) over a spatially continuous area (Brown et al., 2011; Costello, 2009; Diaz et al., 2004). These groups attempt to reflect relatively distinct spatial distributions of biological assemblages (groups of co-occurring species) and their physical environments. Depending on the spatial scale (extent or resolution) and the data used to inform the classification, spatial units defined have been referred to as 'habitats' (Davies et al., 2004; Greene et al., 1999; McQuaid et al., 2020; McQuaid et al., 2023), 'biotopes' (Buhl-Mortensen et al., 2020; Connor et al., 2004; Davies et al., 2017), 'ecosystem types' (Keith et al., 2020; Sink et al., 2019b), 'assemblages' (Howell, 2010), 'ecoregions' (Spalding et al., 2007) and 'bioregions' (Woolley et al., 2019). It should be noted though that terms are not always dependent on scale or consistently applied across studies (Costello, 2009). Here, 'biological or species assemblages' refers to co-occurring groups of

species, ‘habitat’ refers to the environmental characteristics associated with biological assemblages, and ‘ecosystem type’ is used to refer to ecosystem units delineated using biotic and/or abiotic variables (e.g. Sink et al., 2019a). While only spatial distribution patterns of species assemblages and their environmental predictors are considered here, classifications and maps may be produced based on patterns of e.g. taxonomic diversity indices (Murillo et al., 2020a; O'Hara et al., 2020) or functional diversity (Murillo et al., 2020b).

Classifying and mapping of ecosystem types have many implications for conservation and marine spatial planning (Harris et al., 2022b; McQuaid et al., 2023), such as supporting ecosystem-based management practices (Davies et al., 2017; Last et al., 2010), identifying ecologically and biologically significant areas (Gregr et al., 2012; Harris et al., 2022a), assessing levels of ecosystem protection (Clark et al., 2011; Howell, 2010; Kirkman et al., 2021; McQuaid et al., 2020; Roff & Taylor, 2000; Ross & Howell, 2013; Rubidge et al., 2016; Spalding et al., 2007; UNESCO, 2009) and evaluating ecosystem threat status (Kirkman et al., 2019; Pitcher et al., 2018; Sink et al., 2019a). Since sampling the vastness of the marine environment thoroughly is impractical, due to high associated costs, technological challenges and difficulty accessing certain areas (Diaz et al., 2004; Jamieson et al., 2013), maps provide a means to estimate and assess biodiversity in areas that are data deficient (Jetz et al., 2019; Woolley et al., 2019). The classification and mapping of biodiversity in general aids understanding by simplifying complexity (Woolley et al., 2019), inherent in ecological processes and relationships (Levin, 1998). However, this process of simplification results in spatially distinct units which are ultimately human constructs with artificial boundaries (Kreft & Jetz, 2013) which can be especially vague and dynamic in the marine environment (Brown et al., 2011). As a result, numerous approaches to ecosystem classification and mapping exist, depending on the methods and data used to define them, the spatial extent and resolution of interest, and their intended applications (Brown et al., 2011; Diaz et al., 2004; Harris, 2020; Hill et al., 2020; Shumchenia & King, 2010).

While ecosystem classification assumes that spatial units are representative of biologically and environmentally distinct regions, classifications and maps may not always be informed by both biological (biotic) and environmental (abiotic) data. This is due to the general sparsity of *in-situ* biological data compared to environmental data, which are easier to measure remotely using e.g. satellite imagery, acoustic or multi-beam data (McArthur et al., 2010). When only environmental characteristics are considered as surrogates for biological assemblages, the mapped habitats may be referred to as ‘seascapes’ (Roff et al., 2003). At global extents and broad spatial resolutions, seascapes have also been termed ‘ecoregions’ (Spalding et al., 2007), ‘provinces’ (UNESCO, 2009) or ‘habitats’ (McQuaid et al., 2023). While seascapes are

useful at representing broad spatial scales, the ecological relevance of spatial units at finer scales is improved when biological data are explicitly incorporated (Brown et al., 2011; Eastwood et al., 2006; Przeslawski et al., 2011; Shumchenia & King, 2010).

Ecosystem classification and mapping may be informed by data to various extents, and many different approaches have been used to define the groupings in a classification. Expert-derived classification schemes are hierarchical classifications (multi-level) derived through expert workshops, peer review and/or extensive literature (Connor et al., 2004; Davies et al., 2004; FGDC, 2012; Howell, 2010; Keith et al., 2020; Last et al., 2010; Lombard et al., 2004; Montefalcone et al., 2021; Roff & Taylor, 2000; Sink et al., 2012b; Spalding et al., 2007; Sutton et al., 2017; UNESCO, 2009). Expert-derived schemes may be informed by data, such as by 'ground-truthing' with *in-situ* biological data, usually at lower levels of the classification e.g. habitats (Greene et al., 1999), biotopes (Davies et al., 2017) and ecosystem types (Sink et al., 2019b). Data-driven (or numerical) approaches to classification, on the other hand, classify ecosystem types or habitats which are either directly informed by clustering environmental variables (Clark et al., 2011; McQuaid et al., 2020; McQuaid et al., 2023; Snelder et al., 2007) which may be biologically informed, or by directly classifying and predicting relationships between biological and environmental data (Buhl-Mortensen et al., 2015; Buhl-Mortensen et al., 2020; Hill et al., 2017; Leathwick et al., 2012; Neumann et al., 2017; Pitcher et al., 2018; Rubidge et al., 2016; Stephenson et al., 2022). The term 'bioregionalization' is used to describe mapped outputs of classifications directly informed by biological and environmental data, using data-driven approaches (Woolley et al., 2019). 'Bioregion' is therefore used in this study to refer to a region which has been spatially explicitly defined by both biological and environmental data, using data-driven approaches, and is relatively more homogenous in species' assemblage structure and environmental characteristics than neighbouring regions (Woolley et al., 2019) at a particular scale of interest.

Expert-derived approaches to classification are simpler and easier to understand, particularly for non-scientists, because there is essentially only one method for deriving hierarchical classification schemes (Rowden et al., 2018). While the usefulness of expert input cannot be denied, expert-derived classifications can have some drawbacks. They tend to be more subjective with respect to deciding where boundaries should be drawn and what constitutes a group (Jetz et al., 2019; Rowden et al., 2018). Expert-derived approaches can also be more time-consuming to update and less reproducible than data-driven approaches (Woolley et al., 2019). Instead of largely relying on experts to define groupings, data-driven approaches to classification make use of statistical methods to produce groupings which are directly informed by georeferenced observations. When biological and environmental data are used to inform

bioregionalizations, clearer inferences into species-environment relationships associated with bioregions are provided (Rowden et al., 2018; Woolley et al., 2019). Quantifying uncertainty in predictions, validating models, and predicting bioregions across different spatial and temporal scales are easier to achieve with numerical approaches (Woolley et al., 2019). However, due to the vast number of statistical methods available for classifying and predicting biological and environmental data the choice of analysis and number of bioregions defined can be somewhat subjective (Rowden et al., 2018). Ultimately, the purpose of the mapped outputs should define what data to use or approach to implement (Costello, 2009; Strong et al., 2019). Other factors which may be considered include the type/s of data available, the analytical skills required (Brown et al., 2011; Diaz et al., 2004) and whether mapping practices are institutionally established or nationally mandated (Strong et al., 2019).

Three broad approaches to data-driven bioregionalization have been recognised, based on the order that classification and prediction steps occur (Ferrier & Guisan, 2006). The 'group first, then predict' approach, as applied by Rubidge et al. (2016), initially defines biological groupings, often using a method of ordination such as hierarchical cluster analysis, whereafter groups are related against environmental predictors using a species distribution modelling (SDMs) technique (Guisan & Zimmermann, 2000). The 'predict first, then group' approach either uses multiple single SDMs or joint SDMs (JSDMs) which model multiple species simultaneously to relate species to their environment, after which clustering is performed to identify similar groups e.g. single-species SDMs (O'Hara et al., 2011) and JDSMs (Stephenson et al., 2021). There are fewer methods currently available for executing both classification and prediction steps simultaneously (Woolley et al., 2019), and existing methods have taken a finite mixture modelling approach e.g. Regions of Common Profile (RCPs, Foster et al., 2013) or a Bayesian approach (ter Braak et al., 2003). Both methods make use of latent class analysis (e.g. Weller et al., 2020) which assume a discrete number of unobserved groups (latent classes) exist that can explain patterns of species-environment relationships (details discussed in chapter 3). The most appropriate statistical method differs depending on the context, and ideally, multiple methods should be tested for a specific dataset to identify which analyses is better suited for a particular application (Norberg et al., 2019).

Epifauna are defined in this study as invertebrates living on or protruding from the sediment and as those which are large enough to be visible from camera imagery, approximately > 2 cm (Rex, 1981). For the purposes of this study, the hyper-fauna (crustaceans living in the upper sediment or swimming just above) are broadly included in this definition due to their close relationship with the seafloor (Buhl-Mortensen et al., 2012). Epifaunal patterns often inform benthic maps (collectively with other faunal groups) as surrogates for biological diversity

(Bowden, 2011; Buhl-Mortensen et al., 2015; Buhl-Mortensen et al., 2020; Howell, 2010; Limongi et al., 2023; Sink et al., 2019b; Stephenson et al., 2022), being recognized as sensitive indicators which respond relatively fast to environmental change or disturbance (Atkinson et al., 2011a; de Juan et al., 2007; Jørgensen et al., 2011). They have been acknowledged as important links between benthic and pelagic environments by performing crucial roles in nutrient and carbon cycling (Renaud et al., 2007), as food sources for many benthic and pelagic fish and invertebrates (Jørgensen et al., 2011), and as habitat forming structures which provide support and protection to other organisms (Buhl-Mortensen et al., 2010; Kaiser et al., 1999). Their biological interactions also serve crucial functions by structuring assemblages through competition, predation and bioturbation of sediments (Osman & Whitlatch, 2004; Smith et al., 1986).

Benthic epifauna respond to a variety of environmental drivers across scales (Levin et al., 2001), and multiple predictors are likely relevant when predicting distributions of assemblages. Indirect gradients, which have no direct influence on species distribution but are correlated with those that do, can be adequate predictors for benthic assemblages at broad spatial scales (McArthur et al., 2010). These include variables such as latitude, longitude and depth which are easier to measure than direct gradients (variables that influence a species' physiology) or resource gradients (variables consumed) (McArthur et al., 2010). Depth, in particular, has been consistently useful in predicting benthic distributions (Basford et al., 1990; Buhl-Mortensen et al., 2012; Buhl-Mortensen et al., 2020; González-Irusta et al., 2015; Howell, 2010; Lange & Griffiths, 2014; Leathwick et al., 2012; Snelder et al., 2007). However, since fauna respond to multiple factors which covary with depth (Rex, 1981), depth is a less reliable predictor at finer scales (de Juan et al., 2013; Howell, 2010; Lange & Griffiths, 2014).

Direct gradients, such as seafloor salinity range, dissolved oxygen and bottom temperature, which are properties associated with different water masses (Buhl-Mortensen et al., 2020; Limongi et al., 2023; Neumann et al., 2017), have been shown to play a role in predicting epifaunal distributions, though also at broad spatial scales (Callaway et al., 2002; Leathwick et al., 2012; Rubidge et al., 2016; Stephenson et al., 2022). Sediment grain size (or substratum type) is considered to be a good predictor of epifaunal assemblages (Buhl-Mortensen et al., 2012; Callaway et al., 2002; de Juan et al., 2013; Makwela, 2017; Pitcher et al., 2012), since sediment characteristics are correlated with direct drivers such as oxygen concentration and organic or microbial content (Snelgrove & Butman, 1995). Current speed, which affects food availability, has been shown to be an important predictor of epifaunal assemblages (Leathwick et al., 2012; Stephenson et al., 2022). In turn, seafloor variables derived from bathymetry (e.g. slope) which affect current speeds also influence epifaunal distributions (Bouchet et al., 2015;

Davies et al., 2009; Durden et al., 2015; Mohn & Beckmann, 2002; Wilson et al., 2007; Yesson et al., 2012).

Resource gradients which affect energy available to species drive species' distributions most directly by influencing their physiology and metabolism (Woolley et al., 2016). Particulate organic carbon (POC) flux and nutrient input related to surface primary production are thought to be significant in driving species distributions and maintaining diversity, especially in deeper environments (Levin et al., 2001; O'Hara et al., 2020; Rex, 1981; Woolley et al., 2016). Anthropogenic disturbances, such as bottom trawling, have also been shown to impact epifaunal distributions (Atkinson et al., 2011a; Callaway et al., 2002; Collie et al., 2000; de Juan et al., 2007; de Juan et al., 2013; Hiddink et al., 2017). Increased fishing effort is usually negatively correlated with diversity of epifaunal assemblages, though some burrowing and scavenging species can be found in higher abundances after fishing (Atkinson et al., 2011a; de Juan et al., 2007; de Juan et al., 2013). While biotic interactions are acknowledged as important drivers of epifaunal distributions (Ovaskainen et al., 2017), they are not considered in this study.

Ideally, marine bioregionalizations incorporate data from a wide variety of faunal assemblages across multiple scales (Bowden, 2011; Buhl-Mortensen et al., 2012; Lecours et al., 2015; Silberberger et al., 2019), providing a view of benthic biodiversity patterns that is as holistic as possible (Jørgensen et al., 2011). No one type of sampling method can aptly target all benthic fauna, or even all epifauna, resulting in a wide range of methods (or gear types) with different advantages, limitations and applications (Jamieson et al., 2013; Przeslawski et al., 2018). Commonly used epifaunal sampling methods can either employ visual or direct sampling techniques (Costello et al., 2017). Visual sampling methods can reveal information on species behaviour and habitat associations e.g. remotely operated vehicles (ROVs, Adams et al., 2020; de Mendonça & Metaxas, 2021), autonomous underwater vehicles (AUVs, Meyer et al., 2019), towed camera systems (McIntyre et al., 2015) and drop cameras (Cooper et al., 2019). Direct sampling techniques can provide more reliable species identifications and cover greater extents e.g. beam trawls (Jørgensen et al., 2011), otter trawls (Cailliet et al., 1999), commercial bottom trawls (Trenkel et al., 2004), and benthic sleds and dredges (Clark & Stewart, 2016; Filander et al., 2022a) (discussed in more detail in Chapter 2).

Different sampling methods may operate across multiple spatial and temporal extents with varying degrees of sampling effort which can create challenges for combining quantitative datasets (such as abundance or biomass) using classical statistical analyses. To combat this issue, occurrence data (presence-only or presence-absence) are generally used when

informing data-driven bioregionalizations, being more easily modelled and readily available (characterizing open-source databases e.g. OBIS) (Reiss et al., 2014). However, bioregionalizations based on abundance data are far more informative, revealing greater detail about species-environment relationships and identifying regions where species may thrive (as opposed to only tolerate) which is particularly useful for management applications (Stephenson et al., 2021). While some benthic sampling methods have been found to be more likely to detect congruent (i.e. similar) ecological patterns than others, comparisons across/between sampling methods have been inconsistent, and the degree of congruency appears largely contextual (Przeslawski et al., 2018). Quantifying biases and patterns collected between sampling methods is therefore necessary to inform the optimal combination and prioritisation of sampling methods to best describe biodiversity most effectively at multiple scales (Przeslawski et al., 2018). This enables decisions on how to weight different datasets for classifying and mapping bioregions when using a data-driven approach (Sink et al., 2023).

A South African perspective

The classification and mapping of marine ecosystem types in South Africa forms the basis of evaluating their protection and threat status and has implications for conservation and marine spatial planning (Harris et al., 2022b; Kirkman et al., 2021; Sink et al., 2019a; Sink et al., 2023). The current classification is hierarchical (4 levels) and follows an expert-derived data informed approach (SANBI, 2022; Sink et al., 2023). A new iteration of the South African national classification and map, informed by more datasets each time, has been produced every 5 to 7 years as part of the National Biodiversity Assessment (Lombard et al., 2004; Sink et al., 2012b; Sink et al., 2019b; Sink et al., 2023). An update with minor edits has recently been produced (SANBI, 2022) for improved alignment with the International Union for Conservation of Nature (IUCN) global ecosystem typology (Keith et al., 2020). At the lowest level, representing fine-scale biodiversity patterns and their drivers, 150 benthic ecosystem types (Figure 1.1) and 13 pelagic ecosystem types have been defined, based on biotic and/or abiotic factors (SANBI, 2022). Ecosystem types are nested within 54 biogeographic ecotypes (previously called substratum types), 16 functional ecosystem groups, and four bathomes: shore, shelf, deep-sea benthic and pelagic (SANBI, 2022). Six ecoregions (four continental shelf and two deep-sea ecoregions) were previously recognised at the highest level of the classification, which were defined as large biologically distinct geographical regions containing characteristic species (Sink et al., 2019b; Sink et al., 2023).

Implementing data-driven approaches to marine bioregionalization which are more transparent and can incorporate measures of uncertainty has been identified as an area of priority research focus for South Africa (Sink et al., 2019a; Sink et al., 2023). This would allow quantitative datasets to inform boundaries, since past classifications have largely relied on expert input informed by occurrence records collected from multiple sampling methods (Lombard et al., 2004; Sink et al., 2012b; Sink et al., 2019b). Datasets collected by annual research trawl surveys conducted by the Department of Forestry, Fisheries and Environment (DFFE) have good potential for informing data-driven bioregionalizations in South Africa due to their systematic design and regular collection of quantitative data on epifaunal assemblages since 2011 for both west and south coasts. It is, however, unknown whether assemblage patterns detected by research trawling are similar to other epifaunal datasets used to inform the classification and map. The congruency of patterns between different sampling methods thus has implications for how quantitative datasets might be integrated or prioritised when informing data-driven approaches. If patterns are congruent between sampling methods it could imply that fewer datasets may be needed to inform bioregionalizations, as one dataset could be used as a surrogate for the other (Mellin et al., 2011).

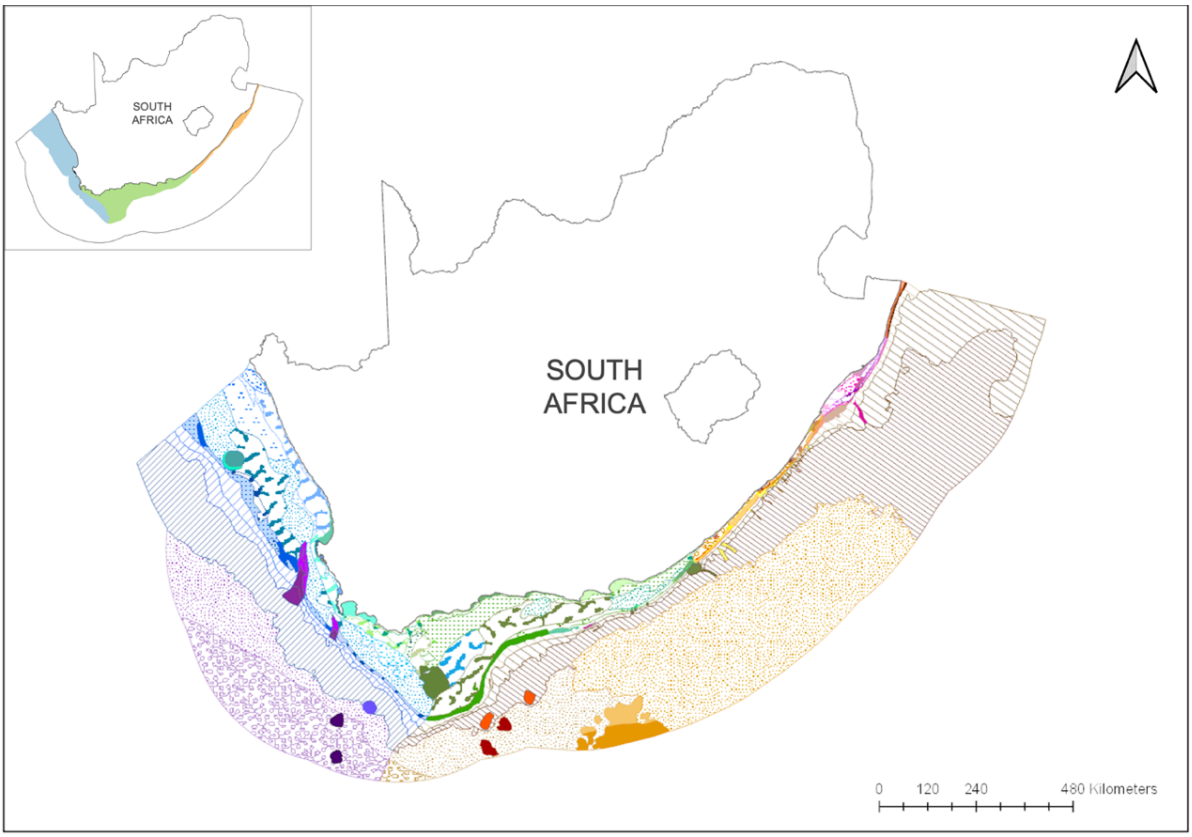

Figure 1.1 Map of 150 benthic ecosystem types for South Africa's Exclusive Economic Zone (EEZ). Map insert shows the ecoregions corresponding to the three coastal shelf biogeographic provinces. Key on following page (pg. 12). Source: Sink et al. (2019b:74-75).


Marine Ecoregions
Southern Benguela Ecoregion
Agulhas Ecoregion
Natal and Delgoa Ecoregions
Marine Ecosystem Types
Agulhas Basin Abyss
Agulhas Basin Complex Abyss
Agulhas Blues
Agulhas Boulder Shore
Agulhas Coarse Sediment Shelf Edge
Agulhas Dissipative Intermediate Sandy Shore
Agulhas Dissipative Sandy Shore
Agulhas Exposed Rocky Shore
Agulhas Exposed Stromatolite Rocky Shore
Agulhas Inner Shelf Mosaic
Agulhas Inner Shelf Reef
Agulhas Intermediate Sandy Shore
Agulhas Island
Agulhas Kelp Forest
Agulhas Lower Canyon
Agulhas Mid Shelf Mosaic
Agulhas Mid Shelf Reef Complex
Agulhas Mixed Shore
Agulhas Muddy Mid Shelf
Agulhas Muddy Outer Shelf
Agulhas Outer Shelf Reef Sand Mosaic
Agulhas Plateau
Agulhas Plateau Mosaic
Agulhas Reflective Sandy Shore
Agulhas Rocky Outer Shelf
Agulhas Rocky Plateau
Agulhas Sandy Inner Shelf
Agulhas Sandy Mid Shelf
Agulhas Sandy Outer Shelf
Agulhas Sheltered Rocky Shore
Agulhas Stromatolite Mixed Shore
Agulhas Upper Canyon
Agulhas Very Exposed Rocky Shore
Agulhas Very Exposed Stromatolite Rocky Shore
Aliwal Shoal Reef Complex
Alphard Bank
Amathole Hard Shelf Edge
Amathole Lace Corals
Browns Bank Rocky Shelf Edge
Cape Bay
Cape Basin Abyss
Cape Basin Complex Abyss
Cape Boulder Shore
Cape Exposed Rocky Shore
Cape Island
Cape Kelp Forest
Cape Lower Canyon
Cape Mixed Shore
Cape Rocky Inner Shelf
Cape Rocky Mid Shelf Mosaic
Cape Sandy Inner Shelf
Cape Sheltered Rocky Shore
Cape Upper Canyon
Cape Very Exposed Rocky Shore
Central Agulhas Outer Shelf Mosaic
Childs Bank Coral
Childs Bank Plateau
Delgoa Deep Shelf Edge
Delgoa Lower Canyon
Delgoa Lower Canyon
Delgoa Mixed Shore
Delgoa Rocky Mid Shelf
Delgoa Sandy Inner Shelf
Delgoa Sandy Mid Shelf
Delgoa Shelf Edge
Delgoa Upper Canyon
Delgoa Very Exposed Rocky Shore
Dumford Mid Shelf Reef Complex
Dumford Inner Shelf Reef Complex
Eastern Agulhas Bay
Eastern Agulhas Outer Shelf Mosaic
False and Walker Bay
Kei Fluvial Fan
Kei Reef Mosaic
Kingklip Koppies
Kingklip Ridge
Kosi Coral Community
KZN Bight Deep Shelf Edge
KZN Bight Mid Shelf Mosaic
KZN Bight Mid Shelf Reef Complex
KZN Bight Muddy Inner Shelf
KZN Bight Muddy Shelf Edge
KZN Bight Outer Shelf Mosaic
KZN Bight Sandy Inner Shelf
Leadsman Coral Community
Namaqua Exposed Rocky Shore
Namaqua Kelp Forest
Namaqua Mid Shelf Fossils
Namaqua Mixed Shore
Namaqua Muddy Sands
Namaqua Muddy Mid Shelf Mosaic
Namaqua Sandy Inner Shelf
Namaqua Sandy Mid Shelf
Namaqua Sandy Middle Shelf
Namaqua Sheltered Rocky Shore
Namaqua Very Exposed Rocky Shore
Natal Boulder Shore
Natal Deep Shelf Edge
Natal Delgoa Dissipative Intermediate Sandy Shore
Natal Delgoa Intermediate Sandy Shore
Natal Delgoa Dissipative Sandy Shore
Natal Delgoa Reflective Sandy Shore
Natal Exposed Rocky Shore
Natal Lower Canyon
Natal Mixed Shore
Natal Upper Canyon
Natal Very Exposed Rocky Shore
Orange Cone Inner Shelf Mud Reef Mosaic
Orange Cone Muddy Mid Shelf
Port St Johns Inner Shelf Mosaic
Port St Johns Muddy Shelf Edge
Port St Johns Muddy Mid Shelf
Protea Mid Shelf Reef Complex
Sodwana Coral Community
Southeast Atlantic Lower Slope
Southeast Atlantic Mid Slope
Southeast Atlantic Seamount
Southeast Atlantic Slope Seamount
Southeast Atlantic Upper Slope
Southern Benguela Dissipative Sandy Shore
Southern Benguela Dissipative Intermediate Sandy Shore
Southern Benguela Intermediate Sandy Shore
Southern Benguela Muddy Outer Shelf Mosaic
Southern Benguela Muddy Shelf Edge
Southern Benguela Outer Shelf Mosaic
Southern Benguela Reflective Sandy Shore
Southern Benguela Rocky Shelf Edge
Southern Benguela Sandy Outer Shelf
Southern Benguela Sandy Shelf Edge
Southern Benguela Shelf Edge Mosaic
Southern KZN Inner Shelf Mosaic
Southern KZN Mid Shelf Mosaic
Southern KZN Shelf Edge Mosaic
Southwest Indian Lower Slope
Southwest Indian Mid Slope
Southwest Indian Seamount
Southwest Indian Slope Seamount
Southwest Indian Upper Slope
St Helena Bay
St Lucia Mid Shelf Mosaic
St Lucia Sandy Inner Shelf
St Lucia Sandy Mid Shelf
Transkei Basin Abyss
Trafalgar Reef Complex
uThukela Canyon
uThukela Mid Shelf Mosaic
uThukela Mid Shelf Mud Coarse Sediment Mosaic
uThukela Outer Shelf Muddy Reef Mosaic
Western Agulhas Bays
Wild Coast Mid Shelf Mosaic
Wild Coast Inner Shelf Mosaic
Wild Coast Shelf Edge Mosaic

While epifaunal biogeographic patterns have been investigated using trawl data on the western margin (Lange & Griffiths, 2014; Shah, 2018), their patterns have not been compared to other epifaunal sampling methods. In addition to research trawling, towed camera surveys conducted by the DFFE (previously the Department of Environmental Affairs) and the South African Environmental Observation Network (SAEON) are regularly used to collect quantitative data on epifaunal assemblages and have already informed ecosystem type delineation in South Africa (Sink et al., 2019b).

This study is focused on benthic epifaunal assemblages which have been quantitatively sampled using research trawls and towed camera surveys on the Southern Benguela shelf, located on the western margin of South Africa. This was chosen as the study area since it has a relatively more comprehensive collection of research trawl and towed camera datasets suitable for comparison than the south coast.

Study area

Three biogeographic provinces have been acknowledged along the South African shelf (Figure 1.1): the cool temperate west coast (Southern Benguela ecoregion), the warm temperate south coast (Agulhas shelf ecoregion) and the warm subtropical east coast (Natal and Delagoa shelf ecoregions) (Emanuel et al., 1992; Sink et al., 2019b; Turpie et al., 2000). These patterns generally follow an increasing trend in biodiversity (e.g. species richness) and a decreasing trend in productivity (e.g. biomass) from west to east (Awad et al., 2002; Bustamante et al., 1995; Emanuel et al., 1992; Turpie et al., 2000). The western margin extends from the Namibian border to Cape Point along the coast and until approximately 21˚E offshore on the Agulhas Bank (Sink et al., 2019b) (**Error! Reference source not found.**). An area of overlap is recognised between the Southern Benguela and the Agulhas ecoregions from Cape Point to Cape Agulhas (Emanuel et al., 1992), with a high turnover in species composition (Awad et al., 2002). This oblique break between ecoregions is approximately where the Benguela and Agulhas Current Systems merge. The continental shelf is wide and gently sloping on the western margin, extending 240 km off the Orange River Mouth at the Namibian border, and is 50 km at its narrowest off Cape Point (de Wet & Compton, 2021). The shelf edge break is one of the deepest globally, occurring between 200–600 m (de Wet & Compton, 2021). The upper slope starts from just after the shelf edge until about 1000 m depth and was previously classified as part of the Southeast Atlantic Deep Ocean ecoregion (Sink et al., 2019b). There is limited knowledge of biodiversity patterns in deep ocean systems in South Africa (Sink et al., 2019b).

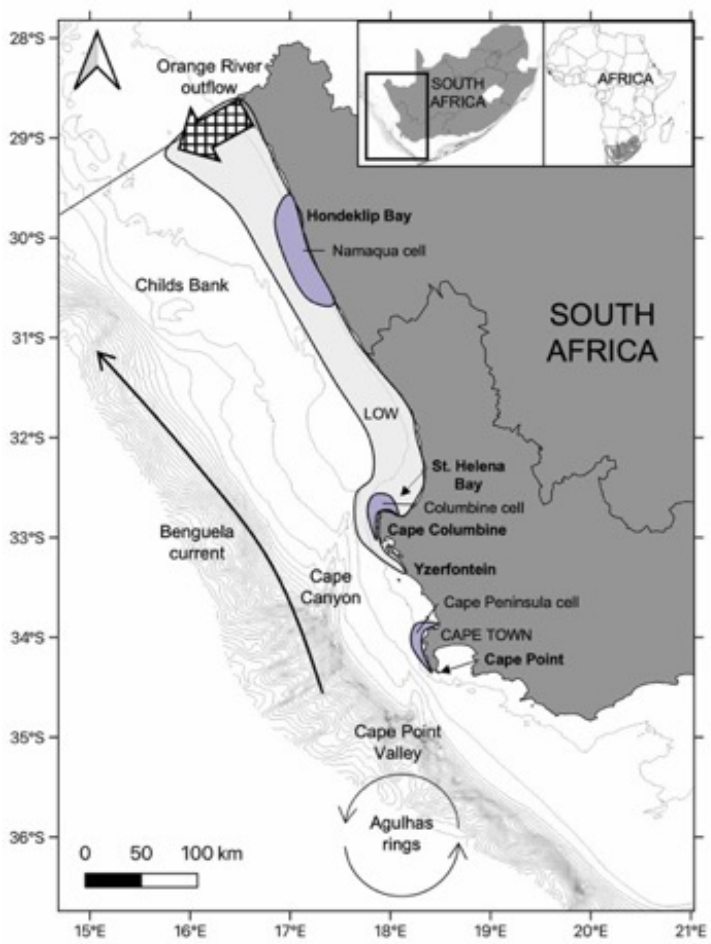

Figure 1.2 Study area located on the southern Benguela shelf of South Africa showing major physical and oceanographic features. Map inserts show location of study area on the western margin of South Africa. Purple areas demarcate distinct upwelling cells. The approximate region where Low Oxygen Waters (LOW) occur is indicated.

The functional ecosystem groups which occur within the study area include sandy shelves, muddy shelves, slopes and canyons (SANBI, 2022). The sediment across the shelf is mostly unconsolidated i.e. sand, muddy sand and gravel (Rogers & Bremner, 1991). Fine muddy sand is found along the shelf edge, and terrigenous muds rich in organic content are transported southwards along the coast from the Orange River mouth to Cape Columbine by a poleward undercurrent, forming an inner shelf mud belt (Rogers & Bremner, 1991). Diamond mining activities occur inshore near the Namibian border (Atkinson & Sink, 2008). Notable features along the shelf include Childs Bank plateau, southwest of Hondeklip Bay, and two major submarine canyons, namely the Cape Canyon off Cape Columbine and the Cape Point Valley off Cape Point (de Wet & Compton, 2021) (**Error! Reference source not found.**). The top of Childs Bank plateau occurs at about 180 m, with sandy substrate covering its flat top (de Wet & Compton, 2021). A diverse epifaunal community with dense ophiuroid beds and cold-water corals have been observed from video footage of Childs Bank (Sink et al., 2019b). Distinct and diverse epifaunal communities, including ophiuroid aggregations have been identified in the Cape Canyon (Filander et al., 2022a).

The cool, equatorward flowing Benguela Current characterises the western margin (Shannon, 1985) (**Error! Reference source not found.**). Dynamic wind-driven upwelling predominantly occurs over the shelf in the austral summer and spring, enriching the top layers with nutrients (Shannon & Nelson, 1996). Three upwelling cells, located off Hondeklip Bay, Cape Columbine and the Cape Peninsula are recognized along the west coast of South Africa where upwelling is intensified (**Error! Reference source not found.**). High productivity supports large species biomasses (Payne et al., 1989) and numerous important commercial fisheries, including demersal trawl, pelagic longline, small pelagic purse seine, line fishing and rock lobster fisheries (DEFF, 2020). Commercial trawling efforts, targeting mostly hakes, are concentrated on the shelf edge (Sink et al., 2012a). Persistent Low Oxygen Waters (LOW) result from decaying organic matter associated with high productivity (Jarre et al., 2015) are regular but variable features in the Namaqua subregion (north of Cape Columbine) and are most concentrated at depths shallower than 150 m (**Error! Reference source not found.**).

Study aims and chapter overview

The aims of this research are to 1) determine whether epifaunal abundance patterns are structured similarly between two regularly employed epifaunal sampling methods on the southern Benguela shelf (western margin) of South Africa and to 2) determine whether existing epifaunal abundance and environmental datasets collected by research trawling can delineate suitable bioregional patterns using an available data-driven approach to bioregionalization. These aims propose to assist with advancing methods required to inform a data-driven approach to marine bioregionalization and ecosystem classification, a national research priority in South Africa (Sink et al., 2023).

Chapter 2 addresses the first aim by quantifying and comparing epifaunal assemblage patterns detected by a towed camera and a research trawl so that their datasets can be appropriately prioritised or integrated when used in data-driven approaches. Various univariate and multivariate analyses, including an application of co-correspondence analyses (Co-CA), are used to compare species composition, diversity and assemblage structure between sampling methods. This is the first study to quantify epifaunal patterns between research trawls and towed camera surveys on the southern Benguela shelf of South Africa.

Chapter 3 addresses the second aim by classifying and predicting bioregions through the application of a data-driven approach using epifaunal abundance data collected by research trawling. This is achieved by applying a relatively recently developed modelling approach to bioregionalization, ‘Regions of common profile’ (RCP), which can utilize abundance data and perform classification and prediction simultaneously, thereby enabling diagnostic tests of models and maps of prediction uncertainty for estimated bioregions. This study represents the first attempt at predicting spatially continuous epifaunal bioregions on the southern Benguela shelf using a data-driven approach.

Chapter 4 discusses the implications of the main findings from chapter 2 and 3 towards monitoring and analysing patterns of biodiversity and makes recommendations towards informing a data-driven approach to marine bioregionalization in South Africa. Areas of further research and limitations of the study are identified.

CHAPTER 2: Comparing epifaunal assemblage patterns using a towed camera and a research trawl for the southern Benguela shelf of South Africa

Abstract

Quantifying abundance patterns and identifying sampling biases detected by various sampling methods is necessary for prioritizing and integrating datasets in data-driven approaches to bioregionalization. This chapter aims to determine the degree of similarity between patterns detected by a research trawl and a towed camera which routinely collect quantitative data on epifaunal assemblages on the southern Benguela shelf (western margin) of South Africa. Towed camera and research trawl sites were selected for comparison based on existing datasets using proximity of distance, depth and ecosystem type as selection criteria, identifying 18 pairs of sites. Univariate patterns of diversity amongst sites were assessed using linear correlations and patterns of species composition were graphically compared and assessed with Similarity of Percentages (SIMPER) analyses. To determine similarity in patterns of assemblage structure between sampling methods, a symmetric co-correspondence analysis (Co-CA) was used to quantify cross-taxa congruency (covariance in diversity patterns of different taxa). Co-CA maximizes the covariation between species and observations in the community abundance matrices, allowing assemblages from the same location to be compared that have been collected by different sampling methods. Some evidence of congruence between epifaunal patterns detected by the towed camera and research trawl was found, based on highly correlated important Co-CA ($r = 0.93, 0.93, 0.79, 0.80$), however, this was not significant ($p > 0.05$). No significant pattern in diversity was found between sampling methods. Sampling methods detected mostly different subsets of epifaunal assemblages. The towed camera detected small and patchily distributed taxa and sessile Anthozoans better, while the trawl detected patterns of larger bodied, highly motile Decapoda and cryptic Asteroidea better than the camera. Patterns were less similar at sites where the dominant species recorded by each sampling method was found in high abundance. These were the brittle star *Ophiura trimeni,* detected in high abundances by the towed camera and the hermit crab *Sympagurus dimorphus,* which dominated abundances detected by the research trawl. Both sampling methods provide different and complementary information about epifaunal assemblages and should ideally both be used when describing epifaunal distribution patterns. Findings suggest that congruency in patterns is context dependent, such as the habitat and species sampled and the spatial scale of interest, though further comparisons are recommended due to a low sample size possible for this study.

Introduction

Quantitative data for benthic epifaunal assemblages from unconsolidated sediments on the southern Benguela shelf (western margin) of South Africa are primarily collected using towed cameras and research trawl surveys. In recent years towed cameras have been used successfully in South African waters, as an affordable and less invasive method of sampling epifaunal assemblages (Adams, 2017; Haley et al., 2017; Nefdt, 2022; van der Heever et al., 2021; von der Meden et al., 2017). Towed camera surveys conducted on the west and south coasts by the Department of Fisheries, Forestry and Environment (DFFE) and the South African Environmental Observation Network (SAEON) have contributed valuable foundational knowledge of the outer shelf and slope (Sink et al., 2021). Annual research trawl surveys conducted by the DFFE systematically collect benthic data during the austral summer, covering the extent of both west and south coast shelves. While the main objective of these surveys has been the collection of data from commercially important demersal fish species to support management of fish-stocks, epifauna (as by-catch) have been routinely recorded and quantified since 2011 (Atkinson & Sink, 2018). This has contributed towards advancing knowledge of epifaunal species identifications and their distributions in the offshore environment (Atkinson & Sink, 2018). Species identified from research trawl surveys have also provided valuable baseline information from which to validate species observations from visual imagery. Due to considerable differences in sampling effort (area covered per site) and gear selectivity between sampling methods, they are proposed to target different subsets of the benthic epifauna. The congruency of epifaunal assemblage patterns detected by towed camera and research trawl sampling is, however, currently unknown. Several factors are likely to contribute towards detected patterns between sampling methods.

Visual sampling methods have a lower ecological impact compared to direct sampling methods (Cailliet et al., 1999; Lirman et al., 2007; McCormick & Choat, 1987; McIntyre et al., 2015; Spencer et al., 2005; Williams et al., 2015). With the advancement of technology, visual sampling methods have enabled the observation of new information which has not been achievable with direct sampling methods (Durden et al., 2016a; Solan et al., 2003). Species interactions, behaviour, habitat associations (Cailliet et al., 1999; de Mendonça & Metaxas, 2021; Spencer et al., 2005; Trenkel et al., 2004; Williams et al., 2015) and impacts from demersal trawling (Collie et al., 2000; Magorrian, 1997) are just some types of information which can be observed from imagery. Seabed images have become valuable datasets for informing ecosystem classifications by ground-truthing substratum types (Greene et al., 1999; Magorrian et al., 1995; Sink et al., 2019b). However, image quality can be hampered by factors such as speed of movement, sediment plumes and resolution (de Mendonça & Metaxas,

2021). Benthic imagery can be time consuming to process (Cailliet et al., 1999; Spencer et al., 2005) and can result in varying levels of species detection and identification, depending on the skill level of analysts (Durden et al., 2016b). A lack of physical specimens to confirm identifications from imagery has resulted in the use of operational taxonomic units (OTUs) or morphospecies types, which are not always standardised across research institutes or countries (Howell et al., 2019). Furthermore, some species simply cannot be identified by imagery alone, while others may be underestimated due to photonegative responses (McIntyre et al., 2015; Trenkel et al., 2004; Uzmann et al., 1977).

Direct sampling methods which collect physical specimens, such as trawls or dredges, provide more accurate species identifications and therefore may detect greater species richness compared to visual imagery (Williams et al., 2015). Physical specimens also provide better species' life-history information (e.g. age or size), and the collection of tissue samples necessary for genetic or taxonomic studies (Cailliet et al., 1999; Uzmann et al., 1977; Williams et al., 2015). Such collection of physical specimens is indispensable for establishing inventory lists during baseline or exploratory surveys (Przeslawski et al., 2018). Trawling and dredging, however, are known to underestimate epifaunal densities (Cailliet et al., 1999; Jamieson et al., 2013; McIntyre, 1956; Spencer et al., 2005; Uzmann et al., 1977; Williams et al., 2015). Trawls and dredges are limited by their net mesh sizes and therefore poorly detect species smaller than the net mesh size (de Mendonça & Metaxas, 2021; Trenkel et al., 2004). Sessile Anthozoans, such as Pennatulaceans, which can retract into the sediment, may also be poorly detected (de Mendonça & Metaxas, 2021). Trawls may have a greater vertical coverage above the seafloor, however, and are therefore better at detecting hyper-benthic species which occur just above the seabed (Trenkel et al., 2004).

Direct comparisons can be challenging when sampling efforts are at different scales, since standardizing effort across scales is not advisable (Lecours et al., 2015). Most studies which have explicitly compared a direct (either trawl or sled) and visual (either towed camera or ROV) benthic sampling method have found inconsistent patterns, acknowledging trade-offs between both approaches (Cailliet et al., 1999; de Mendonça & Metaxas, 2021; McIntyre et al., 2015; Spencer et al., 2005; Uzmann et al., 1977; Williams et al., 2015). Other studies which have compared assemblages across multiple spatial scales have found both inconsistent and consistent patterns in community structure, depending on the spatial scale of interest (Reiss et al., 2010; Silberberger et al., 2019). While some benthic sampling methods appear more likely to detect congruent ecological relationships (e.g. trawls/sleds and grabs/corers) compared to others (e.g. underwater visual census and grabs/corers), comparisons across sampling methods have been inconsistent, and the degree of congruency

is likely contextual (Przeslawski et al., 2018). Congruent spatial patterns between different assemblages (cross-taxa congruency) may indicate that different assemblages have similar responses to environmental conditions, trophic interactions or that they share bio-geographical or evolutionary histories, while incongruent patterns may indicate weak interactions or different responses (Gioria et al., 2011; Toranza & Arim, 2010).

Co-correspondence analysis (Co-CA) can be a useful approach to quantify patterns of cross-taxa congruency between assemblages directly (Alric et al., 2020; Gioria et al., 2011). Co-CA maximizes the covariation (common variance) between species and observations in the two community matrices being related, provided the assemblages are collected from the same location (or sampling unit) (ter Braak & Schaffers, 2004). Co-CA follows an eigenanalysis-based approach (weighted averaging) to assign species and site scores, such as in correspondence analysis (CA), with 'weight' denoting the species' abundance. Weighted averaging techniques assume a unimodal response and are appropriate for modelling species abundance data. Co-CA also appropriately handles the high dimensionality of multivariate data (greater number of species variables than site samples) and data with many rare species (many zeros) due to its use of the Chi-square distance (Alric et al., 2020; ter Braak & Schaffers, 2004). Since the data of each matrix being compared can be recorded on a different scale (ter Braak & Schaffers, 2004), this is a useful approach for directly quantifying patterns between different sampling methods which have been collected with various degrees of sampling effort.

This study presents the first quantitative comparison between a towed camera and research trawl on the southern Benguela shelf (western margin) of South Africa. The research in this chapter aims to determine the extent of congruency (alignment) in epifaunal assemblage patterns collected by a towed camera and a research trawl. The objectives are to quantify and compare patterns of diversity, species composition and assemblage structure between sampling methods using various univariate and multivariate techniques.

Methods

Site selection

Eighteen pairs of towed camera and research trawl sites were compared in this study (Figure 2.1). Available towed camera and research trawl sites were selected for comparison if they occurred at approximately the same location. A 25 nm^2 (~86 km^2) grid block was used as the maximum distance between pairs of sites, based on the size of a demersal research trawl survey grid block (Figure 2.1). Pairs of sites were only compared if they occurred within the same ecosystem type (as per Sink et al., 2019b) and differed by no more than 50 m in depth.

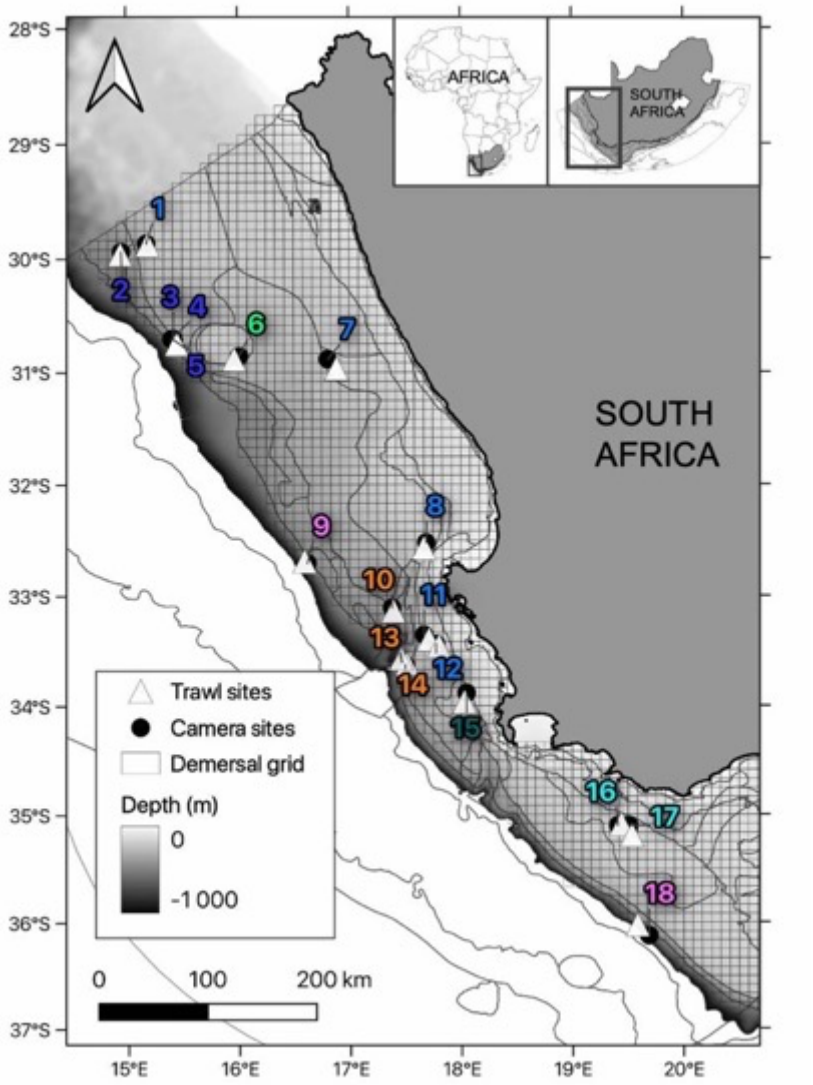

Figure 2.1 Research trawl (△) and towed camera (●) sites (1–18) collected on the southern Benguela shelf of South Africa which were compared in this study. Map inserts show location of study area on the western margin of South Africa. Demersal survey grid blocks (□) represent the area covered by the west coast research trawl survey. One grid block represents 25 nm^2. Ecosystem type boundaries are outlined in grey and sites are coloured by ecosystem type: ■Southern Benguela Sandy Shelf Edge (2, 3, 4, 5), ■Southern Benguela Sandy Outer Shelf (1, 7, 8, 11, 12), ■Southern Benguela Outer Shelf Mosaic (15), ■Southern Benguela Muddy Outer Shelf (16, 17), ■Childs Bank Plateau (6), ■Southeast Atlantic Upper Slope (9, 18), ■Cape Upper Canyon (10, 13, 14).

Towed camera and research trawl sites compared were an average distance of 4.9 ± 0.8 km away from one another and were furthest apart at site 18 (14.2 km) and closest at site 1 (1.5 km, Table 2.1). The selected sites covered a depth range of 154–703 m across the shelf and occurred across seven ecosystem types which encompassed sandy, muddy and mixed substratum types (Table 2.1). The greatest proportion of sites were located within sandy substratum ('Southern Benguela Sandy Outer Shelf' or 'Southern Benguela Sandy Shelf Edge', Table 2.1).

Table 2.1 Pairs of towed camera and research trawl sites (1–18) compared in this study, showing the distance between towed camera and research trawl sites (m), the depth range (m) and ecosystem type (coloured) of each site. Distances between pairs of sites are measured from each site's starting coordinates.

Site	Distance between towed camera & trawl sites (m)	Depth range (m)	Ecosystem type
1	1 500	250–266	Southern Benguela Sandy Outer Shelf
2	1 600	422–426	Southern Benguela Sandy Shelf Edge
3	1 900	373–381	Southern Benguela Sandy Shelf Edge
4	1 600	389–398	Southern Benguela Sandy Shelf Edge
5	6 300	383–385	Southern Benguela Sandy Shelf Edge
6	5 200	212–222	Childs Bank Plateau
7	11 100	216–227	Southern Benguela Sandy Outer Shelf
8	5 500	182–208	Southern Benguela Sandy Outer Shelf
9	3 000	568–608	Southeast Atlantic Upper Slope
10	3 400	398–391	Cape Upper Canyon
11	5 900	186–209	Southern Benguela Sandy Outer Shelf
12	3 100	174–183	Southern Benguela Sandy Outer Shelf
13	4 300	469–485	Cape Upper Canyon
14	1 800	378–421	Cape Upper Canyon
15	5 900	158–172	Southern Benguela Outer Shelf Mosaic
16	3 000	154–160	Southern Benguela Muddy Outer Shelf Mosaic
17	8 700	155–158	Southern Benguela Muddy Outer Shelf Mosaic
18	14 200	702–703	Southeast Atlantic Upper Slope

In total, sites were extracted from three research trawl surveys and five towed camera surveys collected between 2016 and 2020 and pairs of sites differed by no more than two years (Table 2.2). The discrepancy in sampling year was not considered a major limitation, since benthic epifaunal assemblages are known to remain relatively consistent over long periods of time (e.g. Lacharité & Metaxas, 2018).

Sampling effort differed substantially between the research trawl and towed camera, since the area of each trawl site was based on swept area, while the area of each towed camera site was based on the area analysed from 30 randomly selected images along a transect. With an average area sampled per site by the research trawl of 85731.14 ± 2345.47 m^2, compared to

21.27 ± 1.83 m^2 by the towed camera, the research trawl sampled an area that was on average 4000 times greater than that of the towed camera per site (Table 2.2).

Table 2.2 Site summaries for towed camera and research trawl sites selected for comparison. Mean ± SE values are shown in bold. Total areas (m^2) represent those before standardisation and were computed as swept area for the trawl and analysed area from images for the towed camera. Transect length and depth were rounded off to the nearest meter. A dash (–) indicates data unavailable. Surveys were collected by the *DFFE* or *SAEON* as indicated and were from the *Integrated Ecosystem Programme (IEP, Filander et al., 2022b),* a *Cape Canyon Survey (CCS),* the *Benthic Trawl Experiment (BTE) and a West Coast Visual Survey (WCVS). The trawl survey number represents the voyage number.*

Site	Survey	Year	Latitude (DD)	Longitude (DD)	Average depth (m)	Transect length (m)	Total area (m^2)
Towed camera					**327 ± 37**	**608 ± 78**	**21.27 ± 1.83**
1	IEP (DFFE)	2018	-29.8650	15.1798	266	–	20.16
2	IEP (DFFE)	2018	-29.9355	14.9541	422	–	17.33
3	BTE_18 (SAEON)	2018	-30.7002	15.4207	373	571	28.84
4	BTE_16 (SAEON)	2016	-30.7038	15.4020	398	1078	27.56
5	BTE_18 (SAEON)	2018	-30.7089	15.4230	383	337	17.85
6	IEP (DFFE)	2018	-30.8566	16.0111	212	–	35.30
7	CCS (DFFE)	2018	-30.8852	16.8072	227	522	34.13
8	CCS (DFFE)	2018	-32.5208	17.6884	182	432	15.62
9	IEP (DFFE)	2018	-32.7039	16.6201	568	–	21.42
10	CCS (DFFE)	2018	-33.1073	17.3789	398	636	34.86
11	CCS (DFFE)	2018	-33.3548	17.6671	209	788	16.36
12	CCS (DFFE)	2018	-33.4379	17.7743	183	212	15.28
13	WCVS (SAEON)	2019	-33.6035	17.4681	469	1308	15.49
14	WCVS (SAEON)	2019	-33.6278	17.4986	421	371	14.62
15	WCVS (SAEON)	2019	-33.8822	18.0474	158	604	15.58
16	WCVS (SAEON)	2019	-35.0995	19.4093	160	465	10.70
17	WCVS (SAEON)	2019	-35.1024	19.5095	155	484	16.79
18	WCVS (SAEON)	2019	-36.1247	19.6872	702	708	25.06
Research trawl					**327 ± 38**	**3123 ± 82**	**85731.14 ± 2345.47**
1	291	2017	-29.8747	15.1910	250	3278	89490.49
2	300	2020	-29.9579	14.9457	426	3239	88756.20
3	300	2020	-30.7428	15.4516	381	3434	95266.37
4	291	2017	-30.7453	15.4503	389	3241	90423.90
5	296	2019	-30.7552	15.4620	385	2185	60709.30
6	291	2017	-30.8840	15.9663	222	2426	64777.40
7	291	2017	-30.9668	16.8857	216	3260	88007.04
8	291	2017	-32.5675	17.6680	208	2574	70277.84
9	291	2017	-32.6872	16.5947	608	3222	91196.18
10	300	2020	-33.1363	17.3921	391	3157	88861.92
11	291	2017	-33.3937	17.7105	186	3222	87006.96
12	296	2019	-33.4559	17.8010	174	3297	86776.57
13	300	2020	-33.5667	17.4623	485	3364	92849.43
14	296	2019	-33.6182	17.5142	378	3334	93293.39
15	300	2020	-33.9619	18.0292	172	3242	88957.18
16	296	2019	-35.0887	19.4392	154	3241	86090.59
17	291	2017	-35.1900	19.5342	158	3260	85901.95
18	291	2017	-36.0248	19.5843	703	3241	94517.86

Data collection

Research trawl

Epifaunal abundance data obtained from research trawl surveys were collected over the western margin of South Africa during the years 2017, 2019 and 2020. Trawl surveys covered an area of operation from 20˚E to the South African-Namibian border and extended from the coast (minimum of 30 m) to the 800 m depth contour, although some isolated trawls have been conducted up to 1000 m. Surveys were conducted on board the research vessel FRS *Africana* during the austral summer (Jan–Feb) over a six-week period. Each survey had a target of 125 trawls of 30 minutes tow duration each, towed at a constant speed of 3.5 knots. A pseudo-random depth stratified survey design was applied, with the number of sites in each depth and longitude stratum being directly proportional to the area of each stratum (Atkinson et al., 2011b; Badenhorst & Smale, 1991; Yemane et al., 2008). Trawling occurred during daylight hours (30 minutes after sunrise and 30 minutes before sunset) to align with established protocol based on the daily behavioural cycle of the target species', the Cape hakes *Merluccius capensis* and *M. paradoxus*, (Pillar & Barange, 1997).

The trawl gear consisted of a four-panel 180 ft (55 m) German otter trawl net, with 9 m sweeps and 1.5 t Morgere multipurpose otter boards (Atkinson et al., 2011b; Yemane et al., 2008) (Figure 2.2). The 75 mm mesh cod-end was lined with a sleeve of pilchard netting (35 mm mesh, Yemane et al., 2008) for retaining large and small fish and consequently many of the invertebrates. For reasonable calculations of biomass and swept area estimates, door-spread and vertical mouth opening of the trawl net were recorded for each trawl. Approximate measures were a door spread of 60–75 m, a vertical mouth opening of 3–4 m and a horizontal mouth opening of 20–29 m (Atkinson et al., 2011b). Swept area was calculated using the following equation (Atkinson et al., 2011b):

$$Swept\ area\ (nm^2) = \left(speed\ (knots) \times\ duration\ {}^{mins}/_{60}\right) \times \left(mouth\ width \frac{m}{1852}\right)$$

All benthic invertebrates retained in the trawl net were recorded and sorted to lowest possible taxon, counted and weighed, yielding abundance and biomass for each species. Atkinson & Sink (2018) was referred to as a guide for identification and preservation of invertebrate species for surveys in 2019 and 2020 and to validate species observations from 2017. Species identifications were cross-referenced in the World Register of Marine Species (WoRMS Editorial Board, 2023).

Figure 2.2 Otter trawl gear used by the research trawl surveys in this study showing: A) Trawl net being hauled in with catch in-tact and net wings with headline and sweeps visible B) Close-up of headline with floats on deck C) Trawl door (Otter board) D) Landing catch on deck and E) Top view of trawl net and winch on aft deck. All photos taken on board FRS Africana. Source: L.J. Atkinson, 2011.

Towed camera

For this study, epifaunal abundance data were extracted from high-definition oblique images and videos of the seabed obtained from two similar models of the *Ski-Monkey* towed camera system [Sea Technology Services (Pty) Ltd, Cape Town] (Figure 2.3). Images were obtained from surveys collected between 2016 and 2019 by the *Ski-Monkey* III (SAEON) and the *Ski-Monkey* II (DFFE) systems. Both towed camera systems operated to depths of approximately 700 m, following the same standard operating procedures between surveys (von der Meden et al., 2021).

Figure 2.3 The Ski-Monkey II towed camera system. Source: L. Adams, 2018.

The *Ski-Monkey* towed camera system consisted of a custom-build waterproof camera housing fitted on a heavy steel frame (± 450 kgs) with skis (Figure 2.3), allowing it to be towed along the seabed. Two LED lamps were fitted to the housing to illuminate the seafloor. A Canon EOS 760D digital camera was mounted in the housing at a 45˚ angle relative to the horizontal plane, approximately 90 cm above the seafloor. The *Ski-Monkey* system was fitted with three lasers in a triangular configuration, enabling quantification of the processed seabed area in each image. At each towed camera site, the *Ski-Monkey* system was lowered off the stern of the ship until contacting the seafloor and towed behind the vessel at approximately 0.5–1 knot for 30 minutes, resulting in an average transect length of 608 ± 78 m in this study (Table 2.2). A stainless-steel electromechanical sea cable, incorporating two copper conducting cores allowed for live viewing of the seabed via the camera onto a computer screen onboard the vessel, where the camera shutter and settings were controlled. As many non-overlapping images and videos were taken as permitted by seabed conditions and visibility.

Images were analysed with SeaGIS Transect-Measure © (www.seagis.com.au/transect, user license owned by SAEON) software to extract epifaunal densities from images (Figure 2.4). All suitable, good quality images (in focus, with seabed and lasers visible) were identified for

each site and 30 images were analysed per site. Previous tests of epifaunal species-area accumulation have shown that 20–25 images (or a processed area of 8.3-11.5 m^2) sufficiently capture approximately 80 % of the species richness (Adams, 2017). The analysis of 20–30 images per station is currently a standard approach in South Africa (e.g. Haley et al., 2017; Nefdt, 2022; von der Meden et al., 2017). All epifauna within a defined area of good visibility within an image were identified and counted in this study (Figure 2.4).

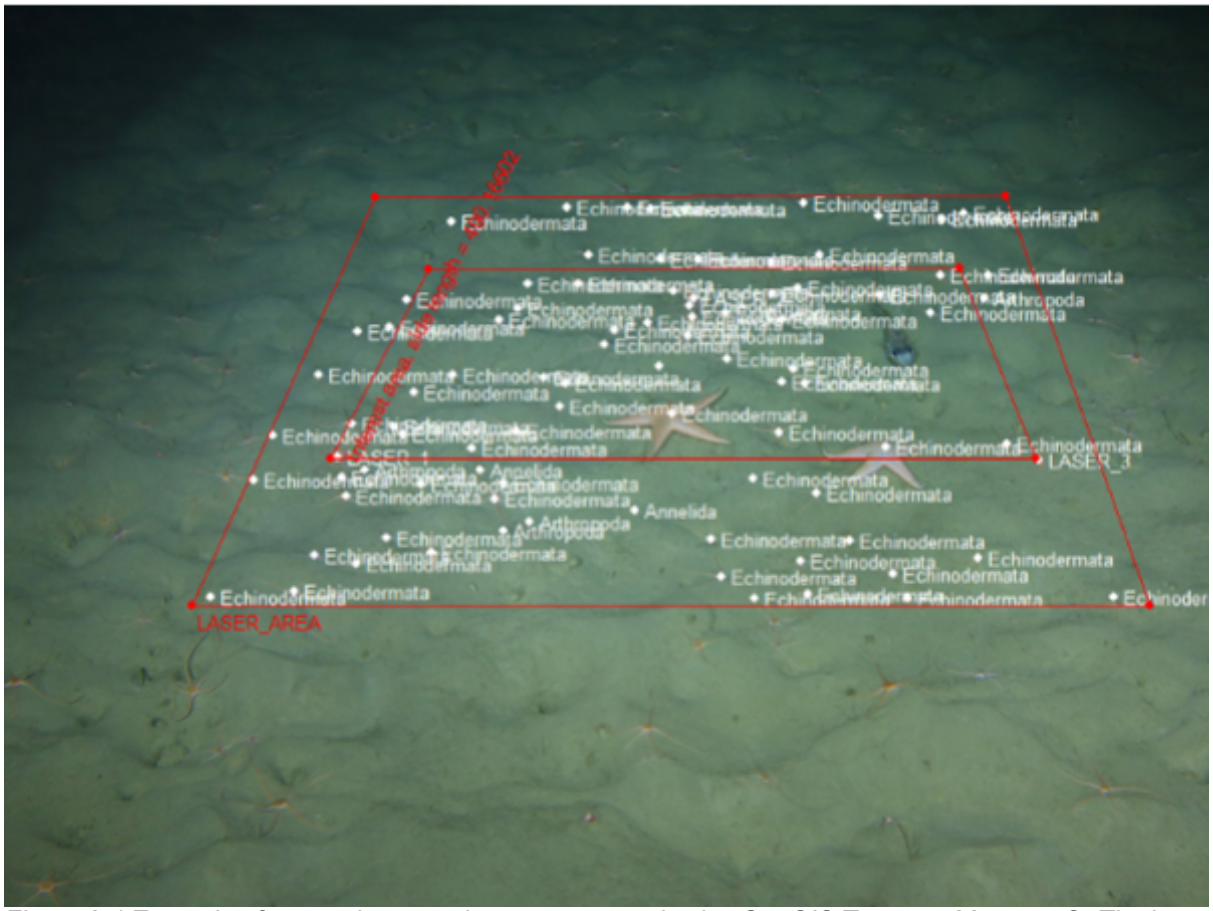

Figure 2.4 Example of a towed camera image processed using SeaGIS Transect-Measure ©. The inner quadrat represents the calibrated area of the image (based on the three laser points), and the outer quadrat represents the total area processed in the image, based on visibility. White labels (displaying phylum) show where a species was detected and counted.

Where sites had more than 30 suitable images for analysis, images were selected at random (Table 2.3). Where sites had fewer than 30 suitable images available, image stills extracted from video were additionally analysed (Table 2.3). Using the three-laser configuration and a customised Transect-Measure modelled calculation, either a 'laser calibration file' (when pre- or post-survey in-pool calibrations were available) or a 'generic calibration file' (when no pre- or post-survey in-pool calibrations were available and for all images extracted from video) were used to quantify the area of seabed processed per image (Table 2.3). Differences in calculated area between laser and generic calibrations files was deemed to be less than 5%,

with the laser calibration giving marginally more accurate scaling, hence being considered optimal when in-pool calibrations are available.

Table 2.3 Number of images and video stills analysed for each towed camera site, showing corresponding pixel size and whether a laser calibration file was used. Where no laser calibration file was available (N), a generic calibration was applied. An asterisk (*) denotes that at least one image in that site had pixel dimensions of 6000 x 3368. NA = Not Applicable (i.e. where no video footage was analysed).

Site	Images		Video stills		Laser calibration
	Number analysed	Pixel size	Number analysed	Pixel size	
1	11	6000 x 4000 *	19	1920 x 1080	N
2	30	6000 x 4000	0	NA	N
3	30	6000 x 4000	0	NA	Y
4	30	5184 x 3456	0	NA	N
5	30	6000 x 4000	0	NA	Y
6	30	6000 x 4000	0	NA	N
7	30	6000 x 4000	0	NA	N
8	19	6000 x 4000	11	1920 x 1080	N
9	10	6000 x 4000	20	1920 x 1080	N
10	30	6000 x 4000	0	NA	N
11	20	6000 x 4000 *	10	1920 x 1080	N
12	18	6000 x 4000 *	12	1920 x 1080	N
13	30	6000 x 4000	0	NA	Y
14	30	6000 x 4000	0	NA	Y
15	30	6000 x 4000	0	NA	Y
16	30	6000 x 4000	0	NA	Y
17	30	6000 x 4000	0	NA	Y
18	30	6000 x 4000	0	NA	Y

Data preparation

Pelagic species (jellyfish and salps) were excluded from this study, being poorly sampled by demersal trawl gear (Atkinson, 2009). Where identifications of benthic invertebrates from camera surveys could not be verified due to a lack of validation images, that record was also removed from the dataset. Estimating abundance for colonial species can be challenging, however, a similar approach was followed for counting colonial organisms in trawl surveys and in towed camera imagery. All species belonging to the phyla Porifera, Bryozoa, Ascidiacea and Cnidaria were intuitively counted as one individual if it was readily distinguishable from other colonies. For species which only had biomass recorded, biomass was converted to counts based on abundance estimates from previous surveys (nine occurrences of eight species, Appendix A). Since densities were not directly comparable between the two sampling

methods due to the inconsistent sampling effort and discrepancy in area sampled between methods, area was standardized within methods only. Densities collected by the towed camera were standardized to individuals.m^{-2} and densities collected by the research trawl were standardized to individuals.1000 m^{-2}.

Statistical analyses

Univariate comparisons

Number of species

The total number of species for the most abundant epifaunal groups detected by each method was calculated across sites. Epifaunal groups were represented at the Class level, except for Malacostraca which was represented at the Order level due to the relatively greater contribution to richness of this Class. Classes with fewer than four species detected across methods were grouped into an 'Other' category. To highlight compositional similarities and differences in species richness detected by sampling methods, a Venn diagram was used.

Relative density

Relative densities (%), represented by pie charts, of the most abundant epifaunal Classes and species were calculated for each sampling method. Relative densities were based on species averages across sites and then aggregated by Class. Classes which contributed less than 1 % to overall density detected by each method were grouped into an 'Other' category. Relative densities of the five most abundant species detected by each method on average were represented by pie charts. Stacked bar charts were used to highlight differences in species relative densities of the five most abundant species for selected sites.

Diversity indices

Diversity indices: number of species (S), number of individuals (N), Pielou's evenness (J') and Shannon diversity (H'), were calculated for each towed camera and trawl site in PRIMER v7 (Clarke & Gorley, 2015) using the recommended defaults. Shannon diversity was based on the natural log (to the base e). Due to inconsistent sampling effort between methods, diversity was only compared relatively, based on correlation between sites. To assess whether epifaunal diversity was significantly correlated between sampling methods scatterplots were used and a linear regression line (±SE) was added to plots using the 'ggpubr' package (Kassambara, 2020) in R (R Core Team, 2021), RStudio (RStudio Team, 2021). The regression coefficient, R, and associated p-value were calculated to assess the strength and

significance of relationships. The logarithmic scale was applied to better visualize the relationships of number of species (S) and individuals (N).

Multivariate comparisons

Species contributions to similarity

One-way similarity of percentages (SIMPER) analyses were performed in PRIMER v7 for each sampling method to highlight the species which contributed the most to the average similarity within each sampling method. A fourth-root transformation was applied to reduce the weight of highly abundant species (Field et al., 1982). The contribution (80 % cut-off) of the species responsible for the similarity within methods was calculated using the Bray-Curtis measure of similarity on the fourth root transformed species matrices (Clarke et al., 2014).

Co-correspondence of community patterns

To quantify and test for community concordance between sampling methods, a symmetric co-correspondence analysis (Co-CA, ter Braak & Schaffers, 2004) was performed in RStudio using the 'coca' function from the 'cocorresp' package (Simpson, 2009). The symmetric Co-CA differs from the predictive form in that neither of the community matrices plays the explanatory or the predictive role (ter Braak & Schaffers, 2004). Species abundances were log+1 transformed to downweigh the contributions of highly abundant species (ter Braak & Schaffers, 2004). Log transforming data has been advised when variables are strongly skewed, as with count data (Kenkel, 2006; ter Braak & Smilauer, 2015). Co-CA relates the two abundance matrices by assigning common site weights, defined here as the average of the row sums of each site x species matrix (ter Braak & Schaffers, 2004). The co-structure of the community matrices is quantified by maximising the covariation between the weighted average species scores between abundance matrices, thereby identifying patterns common to both communities being compared (ter Braak & Schaffers, 2004). Important axes explaining most of the co-structure were retained, using a scree-plot as a visual aid. The variance (%) explained for each abundance matrix by the important axes was then quantified. Pearson product-moment correlation coefficients were calculated for important axes and indicate the strength of the relationship between sample scores being compared. Correlations range from 0-1 and therefore do not indicate if relationships between sample scores were negatively correlated. A Monte-Carlo permutation test (n = 9999 repetitions) was performed to evaluate the significance of the association between communities using the 'randtest.coca' function developed by (Alric et al., 2020).

The ‘adegraphics’ R package (Siberchicot et al., 2017) was used to construct ordination biplots for the first two axes, plotting towed camera and trawl species and site scores based on code developed by Alric et al. (2020). Interpreting the biplots uses the centroid principle and biplot rule (ter Braak & Schaffers, 2004). Sites are plotted at the centre of the species they contain, and species are plotted in the centre of the sites they were recorded in (centroid rule). The origin (located at 0) indicates the mean co-variance and samples located further from the origin indicate stronger co-associations between them (biplot rule).

Results

Univariate comparisons

Number of species

A total of 104 species from 20 epifaunal groups were detected across the 18 sites sampled (Figure 2.5). The research trawl detected 83 species and the towed camera detected 61 species, with 40 species (38 %) detected by both sampling methods (Figure 2.5). The richest Class detected by the towed camera was Anthozoa (13 species), while the richest Class detected by the trawl was Decapoda (21 species, Figure 2.5). Asteroidea species were poorly detected by the towed camera compared to the trawl (Figure 2.5). A greater proportion of species were identified to species level by trawl sampling compared to towed camera sampling, at 81 % and 57 % respectively (Appendix B).

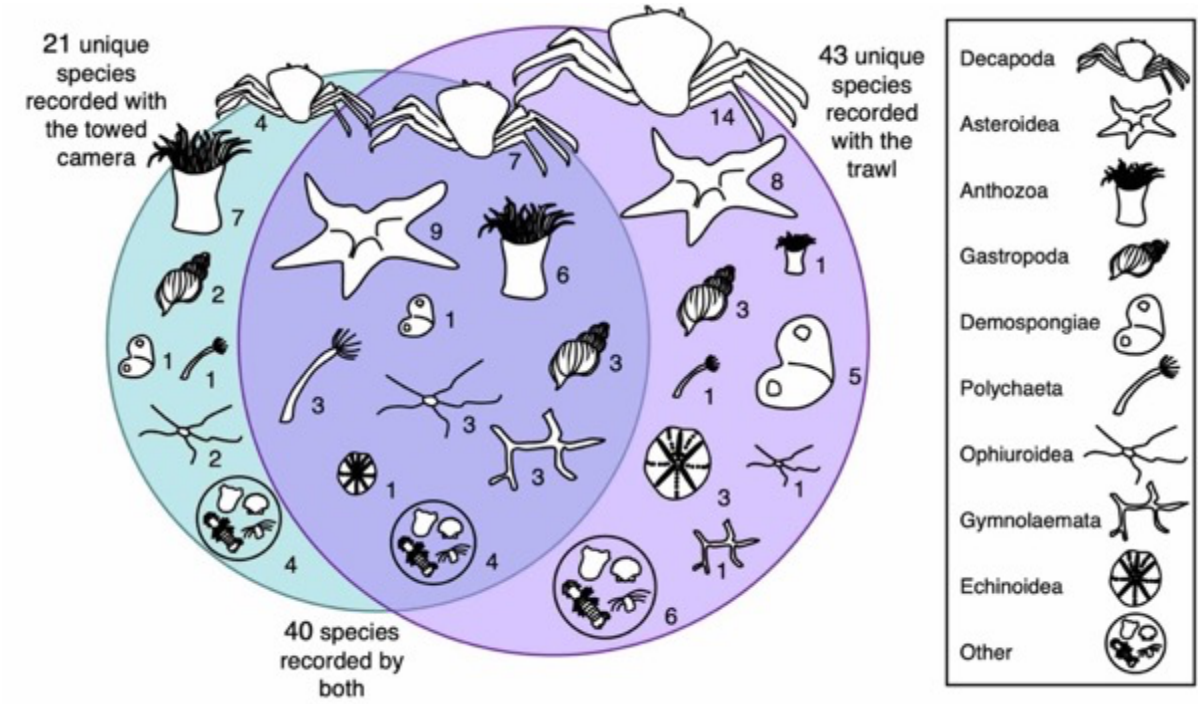

Figure 2.5 Venn diagram of the total number of epifaunal species recorded by the towed camera (blue) and research trawl (purple) across the 18 sites, showing the overlap in species sampled by both methods (blue/purple). Circles are scaled to present the total number of species recorded by methods. Numbers show counts of species for major taxa (species icons) and icons are scaled in size to represent that number. Major taxa are at the Class level, except for Malacostraca (Decapoda) – shown at the Order level due to its large contribution to composition. Classes with fewer than 4 species recorded across methods were grouped into an 'Other' category and details are shown in Appendix B.

Relative density

Epifaunal abundance detected by the towed camera was dominated by Ophiuroidea (89 %), while abundance detected by the trawl was dominated by Decapoda (82 %, Figure 2.6). Conversely, Decapoda and Ophiuroidea only represented 2 % of the densities detected on

average by the towed camera and trawl, respectively (Figure 2.6). While Asteroidea was the second most dominant Class detected by the trawl (6 %), it contributed very little to the density detected by the towed camera (< 2 %, Figure 2.6).

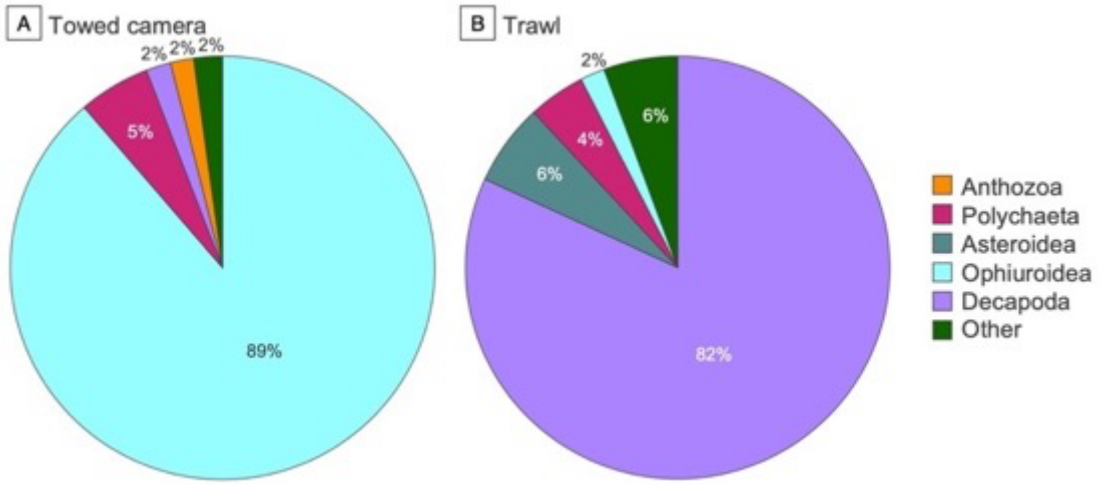

Figure 2.6 Relative densities (%) for the most abundant epifaunal groups detected by towed camera and research trawl sampling methods. Densities are based on species averages across sites which were then aggregated at the Class level. Classes contributing less than 1 % to density were grouped into an "Other" category. Based on densities standardised to individuals.m^{-2} for the towed camera and individuals.1000 m^{-2} for the trawl. Further details provided in Appendix C.

The sampling methods detected different dominant species (Figure 2.7). The five most abundant species detected by each sampling method accounted for 95 % and 83 % of the densities detected by the towed camera and trawl, respectively (Figure 2.7A and B). The small brittle star *Ophiura trimeni* dominated densities detected by the towed camera (88 %), and the hermit crab *Sympagurus dimorphus* was the most abundant species detected by the trawl (65 %, Figure 2.7A and B). These dominant species, *O. trimeni* and *S. dimorphus,* were abundant at different sites and ecosystem types (Figure 2.7C and D). The hermit crab *S. dimorphus* was the most abundant across the 'Southern Benguela Sandy Outer Shelf' (sites 7, 8 and 11) and the 'Southern Benguela Outer Shelf Mosaic' (site 15, Figure 2.7D). The brittle star *O. trimeni* was the most abundant across the 'Southern Benguela Sandy Shelf Edge' (sites 2, 3 and 5) and the 'Cape Upper Canyon' (sites 10, 13 and 14), where it contributed to > 50 % of the density at those sites (Figure 2.7C) and occurred in dense beds of aggregations (Appendix D).

Diversity indices

Diversity measures showed no significant linear relationships detected by the sampling methods (Figure 2.8). The strongest relationship in diversity patterns between sampling methods was for the log of the number of species (S) which exhibited a positive linear relationship amongst sites that was marginally significant (R = 0.47, p = 0.052, Figure 2.8A).

At site 1, a substantially higher number of 36 species was detected by the trawl compared to 11 species detected by the towed camera (Figure 2.8A). The log of the number of individuals (N) detected between sampling methods was slightly negatively correlated, though this was non-significant (R = -0.031, p = 0.9, Figure 2.8B). At sites 7 and 8 (dominated by *S. dimorphus)*, a relatively higher number of individuals was recorded by the trawl, while a relatively higher number of individuals was recorded by the towed camera at site 10 (dominated by *O. trimeni*, Figure 2.8B). Weak relationships between sampling methods were detected for Pielou's evenness (J') and Shannon diversity (H') and were therefore not shown.

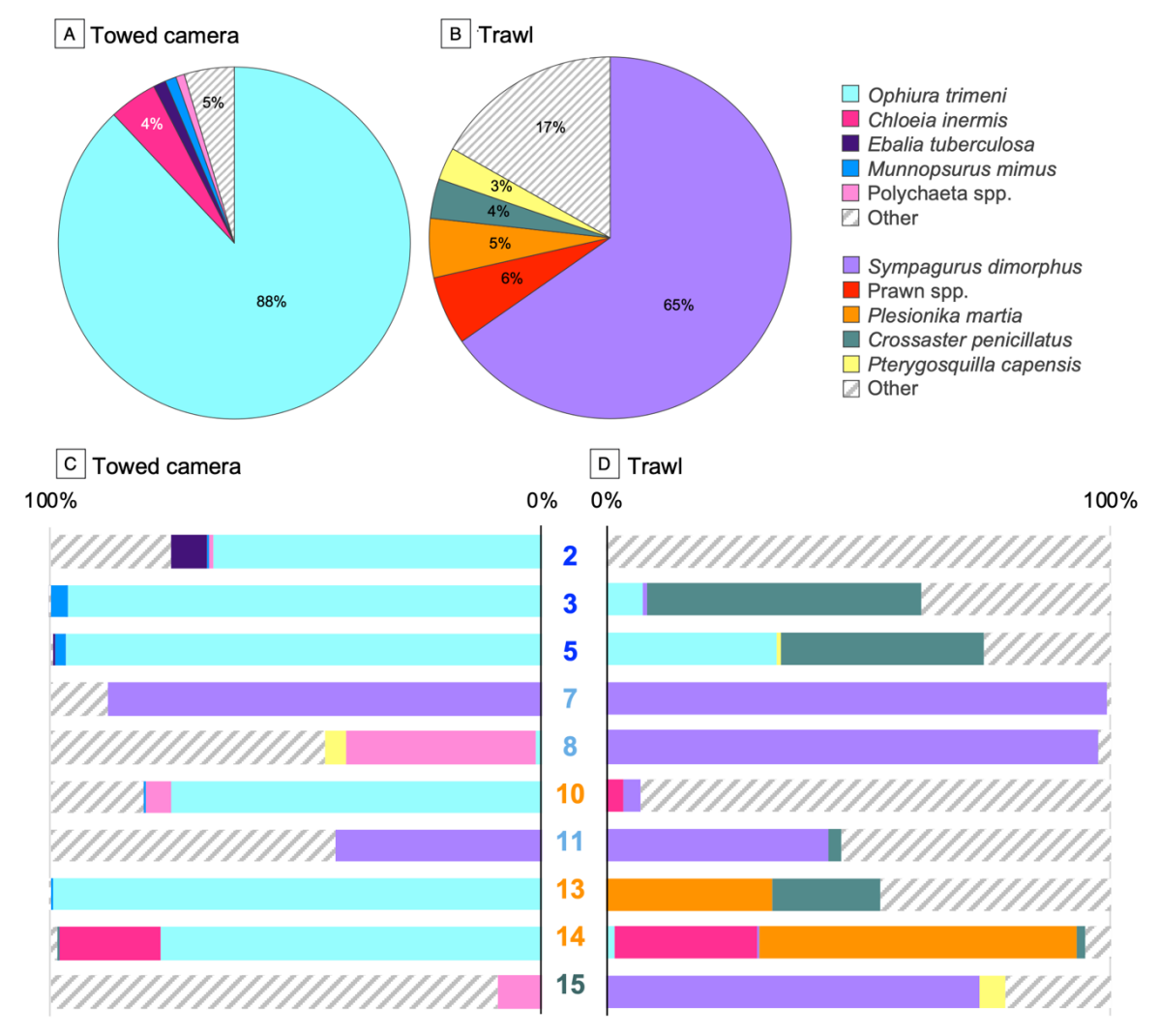

Figure 2.7 Relative densities (%) for the five most abundant epifaunal species on average detected by A) towed camera and B) research trawl sampling methods overall and by C) towed camera and D) research trawl sampling methods at selected sites. Only sites are shown where either Sympagurus dimorphus *(sites 7, 8, 11 and 15) or* Ophiura trimeni *(sites 2, 3, 5, 10, 13 and 14) were the most abundant. Sites numbers are coloured by ecosystem type: Southern Benguela Sandy Shelf Edge (2, 3, 5), Southern Benguela Sandy Outer Shelf (7, 8, 11), Southern Benguela Outer Shelf Mosaic (15), Cape Upper Canyon (10, 13, 14). Percentages not labelled in pie charts indicate a relative contribution to density of 1 %. Based on densities standardised to individuals.m^{-2} for the towed camera and individuals.1000 m^{-2} for the trawl. Further details provided in Appendix C.*

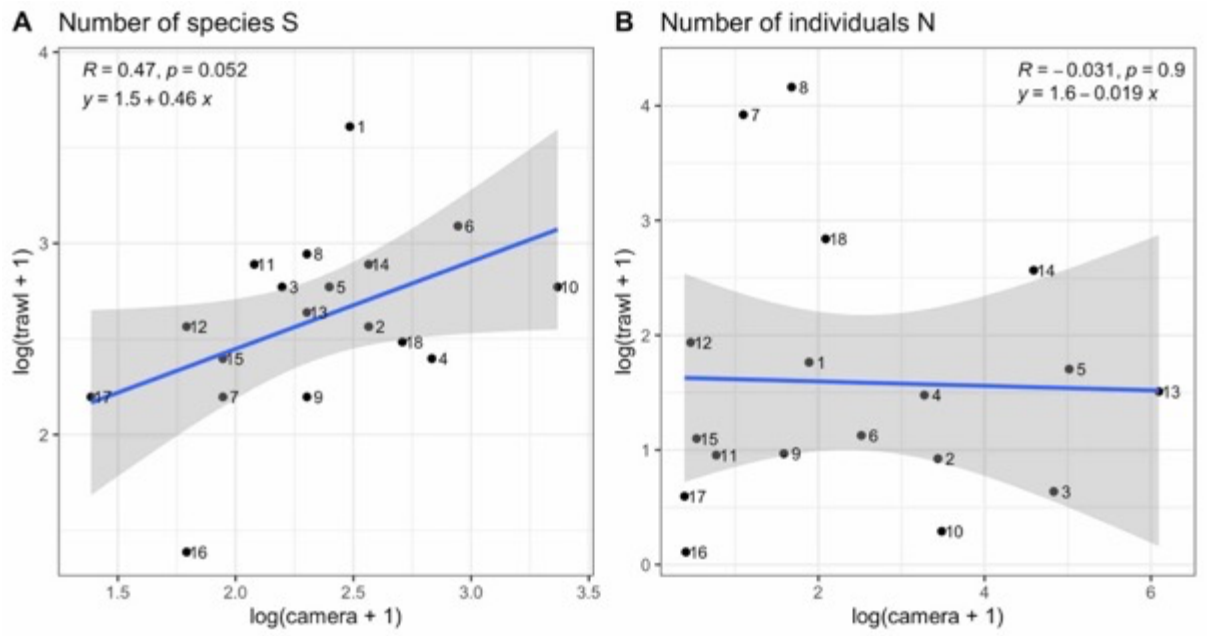

Figure 2.8 Correlation plots of diversity indices (A–B) between towed camera and research trawl sites (numbered 1–18). Line of linear regression (y) shown in blue ± SE in grey. Regression coefficients (R) and associated p-values (p) are shown. Diversity indices were calculated in PRIMER 7 using the recommended defaults. The log scale was used for easier visualization.

Multivariate comparisons

Species contributions to similarity

SIMPER analyses revealed comparable similarity among the 18 sites when sampled by the towed camera (22.66 %) and the trawl (20.44 %), although a greater number of species contributed to the average similarity within trawl samples in comparison (trawl = 14 species, towed camera = 9, Figure 2.9). Different species were responsible for the similarity within each sampling method, with the exception of the hermit crab *S. dimorphus*, the only species which contributed towards the average similarity within both sampling methods (Figure 2.9). An unidentified anemone species Actinaria spp. contributed the most to the average similarity among the 18 sites sampled by the towed camera (4.54 ± 1.18, Figure 2.9). While the brittle star *O. trimeni* contributed the most to the relative density sampled by the towed camera (Figure 2.7A), it did not contribute the most to average similarity within sites sampled by the towed camera (3.59 ± 1.80, Figure 2.9). *S. dimorphus* was the highest contributing species to average similarity within trawl sites (3.43 ± 1.09, Figure 2.9).

The eight species contributing the most to average similarity within sampling methods were on average smaller when detected by the towed camera (5.8 cm) compared to the trawl (12.3 cm, Figure 2.10). These species ranged in size between 2–10 cm when detected by the towed camera and between 7–18 cm when detected by the trawl (Figure 2.10).

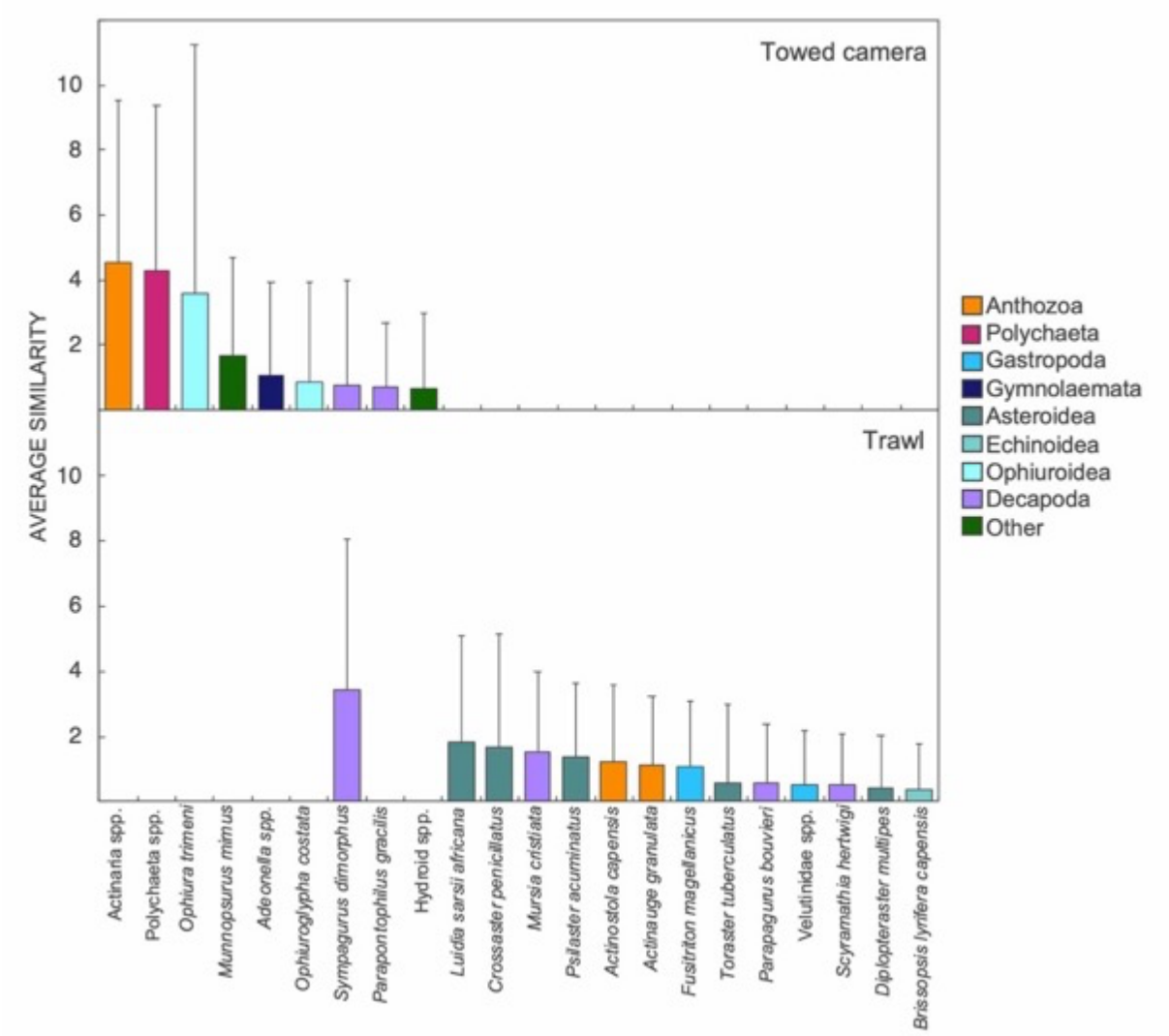

Figure 2.9 SIMPER results for towed camera and research trawl sampling methods representing epifaunal species contributions to average similarity (up to 80% Bray-Curtis similarity) within each sampling method (+ SE), based on 4th-root transformed abundance data. Average similarity within towed camera and trawl sites was 22.66 and 20.44 respectively. Colours represent Classes.

Co-correspondence analysis

The fitted symmetric co-correspondence (Co-CA) model (with all axes) explained 97.81 % of the total inertia sampled by the towed camera and 97.97 % of the total inertia sampled by the trawl (Table 2.4). Most of the covariation between towed camera and trawl samples (73.31 %) was explained by the first four axes (Axis 1: 26.24 %, Axis 2: 20.50 %, Axis 3: 15.29 %, Axis 4: 11.28 %, Table 2.4) and as indicated by the scree-plot showing the decomposition of eigenvalues along the axes (Figure 2.11). With the first four axes retained, the model explained a substantial proportion of the total towed camera and trawl sample variances, 51.75 % and 42.71 % respectively (Table 2.4). Covariation between towed camera and trawl sample scores were strongly correlated on the first two axes (r = 0.93, 0.93, Table 2.4). The third and fourth axes were correlated, but not as strongly (r = 0.79, 0.80, Table 2.4). Monte-

Carlo permutation tests performed on all Co-CA axes indicated covariation between sample scores were not significant (p = 0.386, Table 2.4).

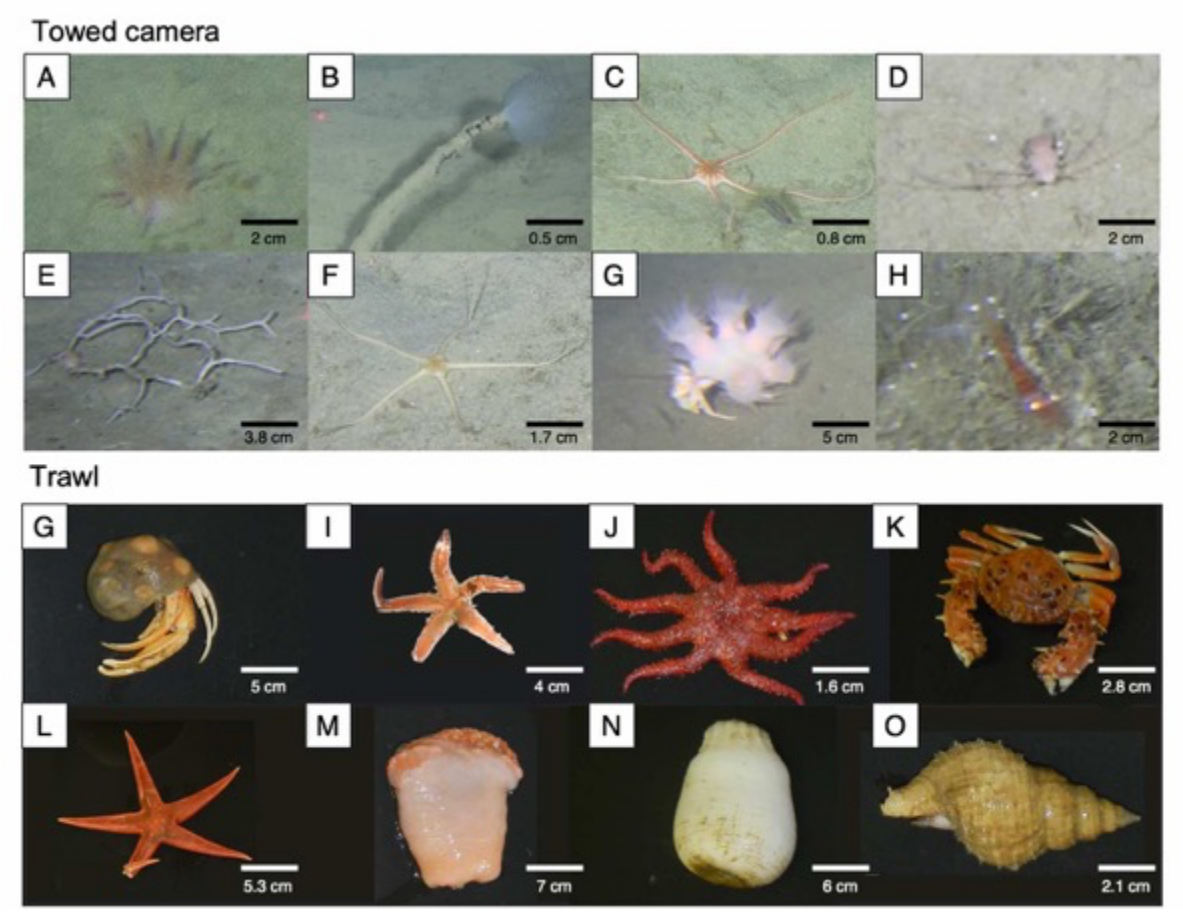

Figure 2.10 Representative images of the top eight species contributing the most to the 80 % Bray-Curtis similarity within sampling methods, based on SIMPER results. ***A.*** *Actinaria spp.* ***B****. Polychaeta spp.* ***C.*** Ophiura trimeni ***D.*** Munnopsurus mimus ***E.*** Adeonella *spp.* ***F.*** Ophiuroglypha costata ***G.*** Sympagurus dimorphus ***H.*** Parapontophilus gracilis ***I.*** Luidia sarsii africana ***J.*** Crossaster penicillatus ***K.*** Mursia cristiata ***L.*** Psilaster acuminatus ***M.*** Actinostola capensis ***N.*** Actinauge granulata ***O.*** Fusitriton magellanicus*. Source: SAEON and DFFE.*

Ordination biplots plotted for the first two axes represented 46.74 % of the covariance between methods and accounted for 33.80 % and 17.30 % of the variance in the towed camera and trawl datasets, respectively (Figure 2.12). Sites from the same ecosystem type and depth occupied similar positions in the plots for both methods (Figure 2.12). Sites from the 'Childs Bank Plateau' (site 6), the 'Southern Benguela Muddy Outer Shelf' (sites 16 and 17), the 'Southern Benguela Outer Shelf Mosaic' (site 15) and the 'Southeast Atlantic Upper Slope' (sites 9 and 18) were similarly located on the plots for trawl and towed camera. While environmental drivers were not investigated here, the shallower sites separated out to the left of the origin, and the deeper sites separated out to the right of the origin for both towed camera and trawl samples (Figure 2.12). However, sites from the 'Southern Benguela Sandy Shelf Edge' (sites 2, 3, 4 and 5) and the 'Cape Upper Canyon' (sites 10, 13 and 14) clustered closer to the origin (i.e. were more similar to the mean co-variance) when detected by the towed

camera compared to the trawl (Figure 2.12). Conversely, sites from the 'Southern Benguela Sandy Outer Shelf' (sites 1, 7, 8, 11 and 12) were closer to the origin when sampled by the trawl (Figure 2.12).

Table 2.4 Summary of symmetric co-correspondence analysis (Co-CA) of epifaunal towed camera and research trawl abundances. Pearson product-moment correlation coefficients indicate correlation between sample scores for each axes. Covariation explained (%) is the percent of co-structure between towed camera and trawl species tables explained by each axes of the Co-CA. Cumulative variance explained (%) is the total amount of variance explained for towed camera and trawl species tables by the Co-CA with each additional axes. Monte-Carlo permutation test with all axes was non-significant, p = 0.386.

CoCA Axes	Eigenvalue	Correlation coefficient	Co-variation explained (%)	Cummulative variance explained (%)	
				Towed camera	Trawl
Axis 1	0.668	0.93	26.24	18.67	7.50
Axis 2	0.522	0.93	20.50	33.80	17.30
Axis 3	0.389	0.79	15.29	43.86	30.20
Axis 4	0.287	0.80	11.28	51.75	42.71
Axis 5	0.226	0.82	8.90	56.94	55.00
Axis 6	0.128	0.71	5.04	62.53	64.84
Axis 7	0.081	0.73	3.19	65.36	73.36
Axis 8	0.073	0.88	2.89	70.65	76.99
Axis 9	0.065	0.84	2.57	75.69	81.02
Axis 10	0.027	0.84	1.04	77.88	84.58
Axis 11	0.026	0.84	1.02	87.17	86.47
Axis 12	0.017	0.90	0.65	90.46	87.93
Axis 13	0.015	0.72	0.59	92.67	91.11
Axis 14	0.012	0.88	0.47	95.32	92.88
Axis 15	0.005	0.97	0.18	96.16	94.41
Axis 16	0.002	0.61	0.08	97.60	95.95
Axis 17	0.001	0.90	0.05	97.81	97.97

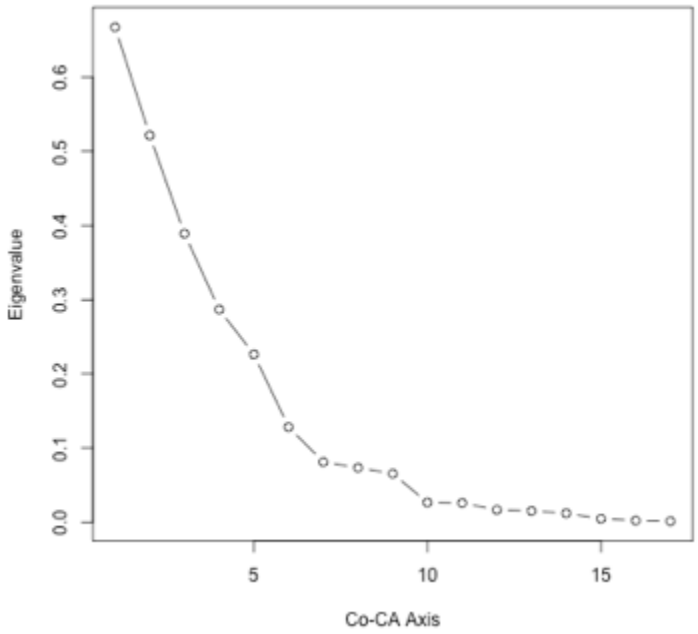

Figure 2.11 Scree plot showing decomposition of eigenvalues across axes, based on symmetric co-correspondence analysis (Co-CA) of towed camera and research trawl epifaunal abundances.

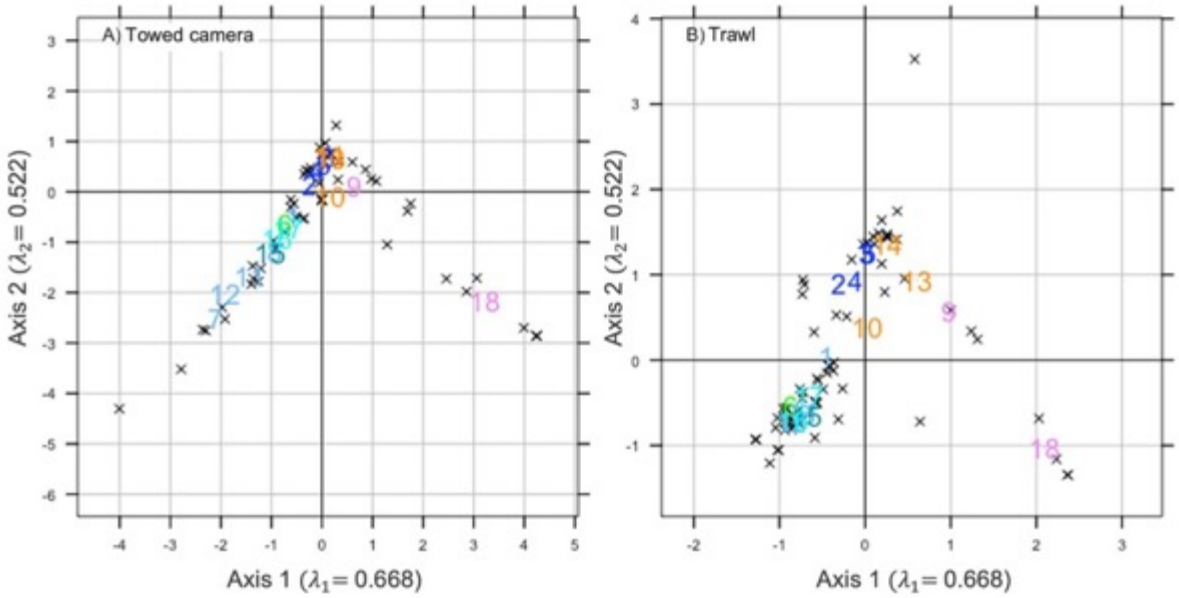

Figure 2.12 Ordination biplots for the first two axes, based on symmetric co-correspondence analysis (Co-CA) of epifaunal towed camera and research trawl abundances across 18 sites. Site scores (1–18) are coloured by ecosystem type: Southern Benguela Sandy Shelf Edge (2, 3, 4, 5), Southern Benguela Sandy Outer Shelf (1, 7, 8, 11, 12), Southern Benguela Outer Shelf Mosaic (15), Southern Benguela Muddy Outer Shelf (16, 17), Childs Bank Plateau (6), Southeast Atlantic Upper Slope (9, 18), Cape Upper Canyon (10, 13, 14). Species scores are represented by black crosses (×).

Discussion

This study was the first to quantitatively compare and test for congruence in epifaunal assemblage patterns between towed camera and demersal research trawl surveys on the southern Benguela shelf (western margin) of South Africa. Comparisons highlighted notable differences in composition and diversity detected by the towed camera and research trawl. Both sampling methods should ideally be utilised where possible to gain a broader view of benthic epifaunal assemblages (Jørgensen et al., 2011; Williams et al., 2015). Limited availability of sites which were close enough for comparison may have contributed towards inconclusive Co-CA findings. However, similarities and differences in assemblage patterns were noted between sampling methods. These were dependent on the dominant species detected and the ecosystem type sampled. While further testing is recommended, it is likely that congruence in assemblage structure between sampling methods depends on multiple factors (Mellin et al., 2011). This study shows comparisons are necessary to understand the advantages and limitations between different sampling methods so that they may be effectively applied to meet management objectives (Przeslawski et al., 2018).

The towed camera and research trawl sampling methods compared in this study recorded mostly different subsets of benthic epifaunal assemblages. Size, motility, behaviour and spatial dispersion patterns of species appeared to be the most influential factors which explained differences in species' selectivity between sampling methods. Characteristic species varied in size within each sampling method but were smaller on average when observed with the towed camera. Species smaller than the trawl's net mesh size (35–75 mm in this study) e.g. the isopod *Munnopsurus mimus* (< 2 cm) were poorly recorded by the trawl compared to the towed camera. Other studies have reported similar net mesh sizes (de Mendonça & Metaxas, 2021; Trenkel et al., 2004), and failure to detect individuals smaller than the net's mesh is a well-known limitation of trawl sampling (Costello et al., 2017; de Mendonça & Metaxas, 2021; Jamieson et al., 2013; Nybakken et al., 1998; Spencer et al., 2005; Trenkel et al., 2004).

Species with different motility and behavioural characteristics were contrastingly detected between the towed camera and trawl sampling methods. Specifically, a species' attachment and behaviour within the sediment, speed of movement, potential sensitivity to light and location above the seabed influenced detection between sampling methods. The trawl recorded higher richness and relative densities of Decapods (crustaceans) compared to the towed camera. Of the benthic epifauna recorded in this study, Decapoda were the most motile, and may have been fast enough to move out of the towed camera's path, which requires

slower tow speeds compared to trawling (McIntyre et al., 2015; Trenkel et al., 2004; Uzmann et al., 1977). Highly motile species can also be under-sampled by towed cameras due to photonegative responses (Cailliet et al., 1999; McIntyre et al., 2015). The towed camera had a limited field of view above the seafloor of approximately 90 cm, compared to the trawl, which had a vertical mouth opening of 3–4 m in this study. As a result, hyperbenthic species which hover just above the seafloor, such as prawns, can be poorly detected by the towed camera.

Higher richness and relative densities of Asteroidea were detected by the trawl compared to the towed camera. Burying behaviours of Asteroidea, as observed in this study, hampered identification to species level for most Asteroidea encountered in towed camera images. Cryptic species, such as those which can burrow just below the sediment, are generally poorly detected by benthic imagery methods (McIntyre et al., 2015; Nybakken et al., 1998). On the other hand, Anthozoans which were able to retract into the sediment and escape capture from trawling e.g. Cerianthidae (burrowing anemones) were more readily detected by the towed camera. This has similarly been observed for several Pennatulacea (sea pen) species (Chimienti et al., 2018; de Mendonça & Metaxas, 2021). Anthozoans which may be firmly attached to the sediment or flexible enough to bend underneath the trawl net e.g. Antipatharia (black corals) and Alcyonacea (soft corals) were also better detected by the towed camera, as noted by Williams et al. (2015) for a benthic sled. These characteristics of Anthozoans contributed to the greater richness and relative densities of Anthozoans detected by the towed camera compared to the trawl.

The trawl detected more species than the towed camera across the 18 sites sampled, recording 22 more species than the towed camera. Other studies have also found a direct epibenthic sampling method to detect higher taxonomic richness than a visual sampling method (Bowden, 2011; Williams et al., 2015), which was expected given the considerably larger area sampled by the trawl in this study. Additionally, physical specimens collected by the trawl allowed easier identification of species to a lower taxonomic resolution (Bowden, 2011; Cailliet et al., 1999; Jørgensen et al., 2011; Williams et al., 2015), further contributing to the greater richness detected. Species identifications from imagery were sometimes hampered due to the low resolution of video stills which were processed for some sites, reducing species richness (de Mendonça & Metaxas, 2021; McIntyre, 1956; McIntyre et al., 2015; Spencer et al., 2005; Uzmann et al., 1977). Limited knowledge of some epifaunal species observed by imagery which have not been recorded by trawling, also hampered species' identifications from imagery. As such, unidentifiable species were sometimes grouped into higher taxa, further reducing richness detected by the towed camera (Durden et al., 2016a; Howell et al., 2019; McIntyre et al., 2015).

Although the towed camera observed higher total densities across sites compared to the trawl, densities were not compared directly due to discrepancies in sampling area between the two methods (Ellingsen et al., 2007; McIntyre, 1956). While previous studies have observed higher densities detected with towed cameras (Cailliet et al., 1999; McIntyre et al., 2015; Nybakken et al., 1998; Spencer et al., 2005; Uzmann et al., 1977; Williams et al., 2015), it is unknown to what extent the towed camera detected higher densities than the trawl, since species detected differed substantially in abundances between sampling methods.

Diversity was not significantly correlated between the towed camera and research trawl. While richness exhibited a moderately positive linear relationship (although not significant), density was weakly negatively correlated. This can be explained by different spatial distribution patterns between the dominant species detected by each sampling method. The dominant species detected by the towed camera, the brittle star *Ophiura trimeni,* occurred in dense aggregations (Appendix D) but was poorly detected by the trawl due to its small size (< 1 cm disk diameter). Conversely, the hermit crab *Sympagurus dimorphus* dominated trawl detected abundances and was not as well detected by the towed camera. This could be due to *S. dimorphus* being motile enough to move out of the towed camera's field of view. The brittle star *O. trimeni* was most abundant at sites along the shelf edge, including sites in the upper canyon, while the hermit crab *S. dimorphus* was most abundant at sites across the sandy outer shelf, similarly observed by Lange & Griffiths (2014) and Shah (2018). At sites where *O. trimeni* was present in high densities, richness and density of other species was low. Though *O. trimeni* aggregations have been poorly recorded in the literature, high density aggregations for the genus have been observed with a visual sampling method for *O. ljungmani* (Gage & Tyler, 1982; Tyler & Gage, 1980)*, O. bathybia* (Rybakova et al., 2020) and *O. sarsi* (Fujita & Ohta, 1989). These studies similarity noted an absence of megafauna amongst the brittle star beds, with low diversity being characteristic of dense ophiuroid beds in general (Rex, 1983).

Other studies have also found visual sampling methods were better at observing species which formed high density and patchy aggregations compared to trawling (Cailliet et al., 1999; de Mendonça & Metaxas, 2021; McIntyre, 1956; Trenkel et al., 2004). A study by McIntyre (1956) compared an Agassiz beam trawl, towed camera and Van Veen grab and noted that the trawl method was least efficient at sampling the dominant species, the brittle star *Ophiothrix fragilis,* which formed high density aggregations in patches, as observed by the towed camera. Since trawls aggregate species across larger distances, information on finer scale distribution patterns is lost (Basford et al., 1990). These findings suggest that species dispersion patterns at local scales are important explanatory variables for patterns detected

by towed camera and trawl sampling methods on the southern Benguela shelf of South Africa and should be considered when sampling (Trenkel et al., 2004).

Overall congruence between assemblage structures detected by each sampling method was not significantly similar (Monte-Carlo permutation test). This could suggest that assemblage patterns differed between the towed camera and research trawl, however, similarities were observed in broad patterns. Although Co-CA axes were not significantly correlated, high correlations were found between important Co-CA axes (1–4), and a notable proportion of each dataset's variance was explained by these axes. Sites were similarly separated along gradients of depth and ecosystem type between sampling methods (Co-CA biplots) which suggests at least some similarity in patterns between sampling methods at broad spatial scales. However, further investigation into whether sampling methods exhibited similar ecological patterns to these (and other) environmental drivers may be warranted to test this. Patterns of epifaunal assemblages are often well described by depth (Basford et al., 1990; Buhl-Mortensen et al., 2012; Ganesh & Raman, 2007; González-Irusta et al., 2015; Howell, 2010; Leathwick et al., 2012; Snelder et al., 2007), so it is likely that both sampling methods were able to detect similar broad patterns of epifaunal communities reflecting changes in depth (or variables correlated with depth). Depth was similarly found to explain the most variation in epifaunal patterns detected by a research trawl survey on the western margin of South Africa (Lange & Griffiths, 2014).

The different patterns of the dominant species, *O. trimeni* and *S. dimorphus,* likely explained the non-congruence in patterns detected between sampling methods, since these species were highly abundant at different sites. Weak congruence between assemblage patterns may imply that assemblages have different environmental (or species) responses, requirements or evolutionary histories (Gioria et al., 2011; Toranza & Arim, 2010). Differences in patterns of distribution between the dominant species detected in this study could suggest that factors such as intraspecific behaviour amongst *O. trimeni* (e.g. reproduction) or responses to food availability could be driving their patterns independently of other faunal taxa. However, it is possible that their predatory avoidance behaviour (Fujita & Ohta, 1989) may be somewhat congruent with other taxa (though negatively correlated). It is worth noting that Co-CA does not detect a negative correlation (Hanson et al., 2015), so even the strong correlations between axes scores in this study may have been negative.

Previous studies comparing congruence between benthic communities have found similarities in broad scale (100s of kms) patterns between epifaunal and infaunal assemblages, explained by hydrodynamic variables, while patterns at meso (10s of kms) and fine (< 1km) scales were

inconsistent with one another (Reiss et al., 2010; Silberberger et al., 2019). Epifaunal patterns compared between a trawling or dredging method and a visual imaging method have yielded inconsistent patterns of diversity, composition and assemblage structure (de Mendonça & Metaxas, 2021; McIntyre, 1956; Williams et al., 2015), though patterns in relative abundance have been found to be highly similar when only taxa sampled by both methods are compared (Nybakken et al., 1998). Interestingly, patterns of assemblage structure were found to be significantly similar on the western margin of South Africa between the same research trawl compared in this study and a grab sampling method for infauna (Brandt, 2022). However, not all taxa respond similarly to environmental variables and may exhibit different patterns even when sampled with the same sampling method. This was noted in a study by Ellingsen et al. (2007) that found more consistent patterns in species distributions between Polychaeta and Isopoda compared to Bivalvia, despite Polychaeta being sampled with a different sampling method to the other two faunal taxa. Whether different sampling methods detect similar patterns or not appears dependent on the context, including the type of habitat, taxa or location being sampled (Flannery & Przeslawski, 2015), which has implications for biological surrogacy (Mellin et al., 2011). As a result, the similar and different patterns observed in this study may be indicative of different responses exhibited across epifaunal taxa, giving rise to potentially varying degrees of congruency between towed camera and trawl sampling methods, depending on the taxa or habitat sampled.

Limitations

While a non-significant result may indicate that patterns were different between sampling methods, a low sample size of 18 sites available for comparison may have prevented a significant result from being detected, if there was one. While comparing sites post-hoc is a valid option in areas where surveys have not specifically deployed multiple sampling methods, further comparisons are recommended between sampling methods. This study was limited by the availability of previously collected data from towed camera and trawl sites, and as a result, paired sites may not have compared truly co-occurring assemblages (spatially and temporally). Although care was taken to compare sites that were from approximately the same location, limited ecosystem type validation (particularly at finer scales) prevented certainty of knowing whether towed camera and research trawl sites were collected from the same substratum or habitat types.

As an example, the number of species detected at site 1 by the towed camera and research trawl differed substantially (36 by the trawl compared to 11 by the towed camera), suggesting that the trawl may have detected a more diverse community associated with a different

substratum or ecosystem type at that site. It is acknowledged that many ecosystem types are not homogenous at very fine spatial scales and more realistically resemble “mosaic” ecosystem types, highlighting the need to ground-truth ecosystem types offshore (Sink et al., 2019b). It should however be noted, that while the large distances between sites compared may have hindered direct comparisons from being made, co-correspondence analysis is acknowledged to be robust enough to detect the congruence of broad ecological patterns between sampling methods across the shelf. This is because even though the sites compared differed in distances between them, their sampling units were relatively isolated i.e. sites compared were closer to each other than to any other site pair that was compared. More than likely, a greater number of samples may be needed to adequately detect patterns. As an example, a study by Reiss et al. (2010) similarly compared communities from different surveys with paired sites being up to 21 nm apart (a greater distance than used in this study), however, they were able to obtain a greater sample size of 130 sites.

All sites compared were collected in the same season, however, most comparisons were made between sites collected in different years. Although sites compared differed by no more than two years, and epifauna are assumed to be relatively stable across short temporal scales (Lacharité & Metaxas, 2018), the dominant species observed by the towed camera suggests this was not necessarily the case in this study. Aggregations of the brittle star *O. trimeni* have not been studied on the South African shelf, however, studies of other *Ophiura* species, and indeed of many Echinoderms in general, suggest that high density aggregations, as observed in this study, are not necessarily stable features over long periods of time (Uthicke et al., 2009). The density of *O. lyungmani* aggregations has been thought to be related to reproduction, being synchronous spawners, with recruitment undergoing highly variable annual cycles in early spring (Gage & Tyler, 1982). It has been hypothesised that variable amounts of particulate organic matter reaching the seafloor from the surface may be driving the strong variability observed in recruitment (Tyler & Gage, 1980). *Ophiura* feeding aggregations are also known to occur around carcasses (Warner 1982), and high densities have been observed feeding on damaged fauna in areas after trawling activity has ceased (Ramsay et al. 1998).

In this study, the highest densities of *O. trimeni* were observed along the shelf edge, where commercial trawling on the west coast is concentrated (Sink et al., 2012a). Notable increases in *O. trimeni* abundances have been observed after trawling has ceased along the western shelf edge of South Africa (Atkinson et al., 2022). These potential drivers imply that high variability in density over annual scales can be expected for *O. trimeni* and may therefore have affected differences detected between sampling methods. This is not to say that the trawl might have detected higher densities of *O. trimeni* if sites were better paired, since the trawl

is clearly not selective for this species. However, *O. trimeni* aggregations have been observed to exclude other species or physically avoid them (Fujita & Ohta, 1989), and species associated with these aggregations can therefore be assumed to be different to periods when aggregations are not present in such high densities. This would affect detected assemblage patterns between sampling methods if towed camera and research trawl methods were not sampling similar densities of aggregations between years.

Recommendations

Both research trawl and towed camera sampling methods compared in this study detected different subsets of epifauna and provide different measures of biodiversity which offer complementary information about the epifaunal benthos. Studies should consider their specific requirements when using a certain sampling method or dataset. Trawl sampling was found to provide higher estimates of species richness at higher species resolutions. Species which were more readily detected by trawling were highly motile species (e.g. Decapoda), cryptic species (e.g. Asteroidea) and hyperbenthic species (e.g. prawns). The towed camera was better at detecting smaller species (e.g. *Ophiura trimeni*), flexible bodied or fragile species (e.g. Antipatharia) and sessile Anthozoans which can retract into the sediment (e.g. Cerianthidae). Other considerations include that substratum type, species interactions and behaviours are observable from imagery, while the collection of physical specimens is possible with trawling (e.g. Cailliet et al., 1999; Uzmann et al., 1977; Williams et al., 2015). While towed cameras have a lower ecological impact (e.g. Durden et al., 2016a), trawling more effectively surveys wider spatial extents (e.g. McIntyre, 1956; Rees et al., 1999).

Marine ecosystem classifications and maps should ideally be informed by various sampling methods collected at multiple scales, since no one sampling method effectively detects all ecosystem components (Buhl-Mortensen et al., 2012; Cailliet et al., 1999; Clark & Rowden, 2004; Colquhoun et al., 2007; Jørgensen et al., 2011; Silberberger et al., 2019; Uzmann et al., 1977; Williams et al., 2015), as shown in this study. Deploying multiple sampling platforms is most applicable during baseline or exploratory surveys, whereafter fewer sampling methods may be more effective for monitoring purposes (Przeslawski et al., 2018). As an example, a towed imaging system combined with either a beam trawl or benthic sled (prioritising the sled only in rocky substrata) was found to be the most effective combination of sampling methods for epifaunal assemblages to inform habitat characterisation and mapping in New Zealand (Bowden, 2011).

Due to the smaller spatial extent over which towed camera surveys have been conducted across the western margin of South Africa, these datasets alone lack the spatial coverage to

inform a data-driven bioregionalization over the entire continental shelf. On the western and southern margins of South Africa, the greater spatial and temporal coverage of trawl surveys compared to towed camera surveys is more applicable for informing data-driven bioregionalizations or predictions of species distributions (Murillo et al., 2016; Pitcher et al., 2012; Woolley et al., 2019). Direct sampling methods also provide useful baseline information required to establish species inventory lists (Przeslawski et al., 2018). However, where data have been collected by towed cameras, they provide better information about substratum and habitat types (e.g. Bowden, 2011; Buhl-Mortensen et al., 2012; Spencer et al., 2005) or finer scale "patchy" distributions which the trawl does not detect well (e.g. de Mendonça & Metaxas, 2021; Trenkel et al., 2004), as seen in this study. Since imagery provides a true reflection of the seabed, visual sampling methods are more sensitive to detecting change and may therefore be more appropriate for monitoring purposes once baseline studies have been conducted (Przeslawski et al., 2018). However, the use of consistent sampling approaches across monitoring surveys should be emphasised to ensure reproducibility (Przeslawski et al., 2019).

This study highlights quantitative comparisons are necessary to understand advantages and limitations between sampling methods so that datasets collected inform appropriate context. Co-correspondence analysis (Co-CA) has been shown to be a useful analytical tool for assessing patterns of cross-taxa congruency between datasets (Alric et al., 2020; Gioria et al., 2011; Hanson et al., 2015) and offers a novel way of directly quantifying congruence between datasets on different scales (area surveyed at a site, in this study), since the only requirement for this analysis is that datasets compared were collected at the same location. Further investigation into the congruence of patterns between towed camera and trawl sampling methods is advised, though differences detected have shown the trawl to be ineffective at capturing finer scale patterns (e.g. *Ophiura trimeni* aggregations) compared to the towed camera. Where possible, deployment of multiple sampling methods in the same locations is recommended to provide a more comprehensive overview of assemblages and would enable better opportunities for comparing patterns between different datasets.

Conclusion

This study presented the first quantitative comparison of epifaunal biodiversity patterns between a towed camera system and a demersal research trawl on the southern Benguela shelf (western margin) of South Africa. Patterns were compared to assess the relevance of each dataset when informing data-driven marine bioregionalizations. Notable differences in composition and diversity were found between sampling methods. However, limited

availability of towed camera and research trawl sites from the same location prevented a conclusive assessment of whether assemblage structures were congruent between sampling methods. Different distribution patterns between the dominant species detected between sampling methods, the brittle star *O. trimeni* and the hermit crab *S. dimorphus*, suggest that congruency in assemblage structure may be highly contextual and could vary depending on the habitat or species being sampled. Ultimately, both sampling methods offer different but complementary information about benthic epifaunal patterns on the southern Benguela shelf of South Africa and should be used simultaneously, where possible, to describe the epifaunal benthos. This study highlights the necessity of comparisons to understand the advantages and limitations of each sampling method and identify the contexts under which they are best suited. The importance of long-term monitoring is emphasised, sampling with both methods at the same location where possible, so that more robust comparisons may be quantified in the future.

CHAPTER 3: Applying a data-driven approach to ecosystem classification and mapping for the southern Benguela shelf of South Africa

Abstract

Data-driven approaches to bioregionalization have the benefit of being able to predict bioregions in biologically poorly sampled regions by relating them to more expansively collected and readily available environmental variables. On the southern Benguela shelf (western margin) of South Africa, quantitative data systematically collected by research trawl surveys offer powerful information for management. This study aimed to determine whether existing epifaunal abundance and environmental datasets collected by research trawling can delineate suitable bioregional patterns using an available data-driven approach to bioregionalization. Regions of Common Profile (RCPs) models, implemented using the 'ecomix' R Package, were used to statistically determine bioregions, based on epifaunal abundance and environmental data from three years of research trawl surveys. After removal of rare species and highly correlated covariates, the final model used 46 species from 325 sites and three environmental predictor variables (bottom temperature, dissolved oxygen and slope). The best model defined five epifaunal bioregions along a depth gradient, with varying degrees of confidence. RCP 5 along the inner shelf (<150 m) and RCP 1 along the upper slope (>500 m) were predicted with the highest degrees of confidence. RCP 5 responded strongly to low oxygen and RCP 1 responded strongly to low temperatures. RCP 2, 3 and 4 which occurred at intermediate depths across the study area (~150 – 500 m) where the greatest species richness was found, were predicted with the highest uncertainty, suggesting that additional environmental predictors are required to improve predictions across these bioregions. Bioregions broadly aligned with known patterns for the southern Benguela shelf of South Africa, highlighting the usefulness of research trawl survey data to produce data-driven bioregionalizations at broad spatial scales. The RCP approach is advantageous in that uncertainty can be generated throughout, allowing mapped outputs to be interpreted easily and meaningfully.

Introduction

Various approaches and statistical techniques are available for classifying and predicting species distributions in response to their environment (Ferrier & Guisan, 2006). These can be applied to produce numerically derived bioregionalizations by mapping modelled outputs against continuous environmental data layers. Just as sampling methods have biases in how they collect data, different statistical techniques do not perform equally well and are appropriate under different contexts (Guisan & Zimmermann, 2000; Norberg et al., 2019). Methods for modelling species distributions can either predict species responses individually, referred to as species distribution models (SDMs) and habitat suitability models (HSMs, Rowden et al., 2017), or they can consider multiple species ('community-level modelling', Ferrier & Guisan, 2006). While single-species distribution maps have important ecological and conservation applications, they are not technically considered bioregionalizations as used in this study. Here, the term 'bioregionalization' is used to describe regions which are relatively homogenous in species' assemblage structure and environmental characteristics, therefore excluding single-species distributions maps (Rowden et al., 2018). Bioregionalizations must also be explicitly informed by biological and environmental data and therefore do not include mapped outputs, such as seascapes, which use environmental variables as proxies for biological assemblages (Woolley et al., 2019).

At the community-level, Ferrier & Guisan (2006) defined three commonly used approaches for predicting and classifying responses of multi-species assemblages, based on the order that prediction and classification occur. The "predict first, then group" approach applies multiple SDMs to predict species distributions individually, whereafter their combined outputs are clustered into groups based on species' similar predicted responses to environmental gradients (Ferrier & Guisan, 2006). Maximum Entropy ('MaxEnt', Phillips et al., 2004) is a commonly used distribution modelling technique since it can handle presence-only data, which often characterizes freely available species occurrence record databases e.g. Ocean Biodiversity Information System (OBIS). O'Hara et al. (2011) used MaxEnt to model the distributions of 267 Ophiuroid species in the Indian, Pacific and Southern Oceans, whereafter a two-stage clustering process (non-hierarchical k-means and hierarchical agglomerative clustering) was used to define similar groups.

Woolley et al. (2019) defined an additional sub-group in this approach, whereby species can be modelled simultaneously, using joint SDMs (JSDMs, Ovaskainen & Abrego, 2020), thereby identifying common patterns in species responses. Hierarchical Modelling of Species Communities (HMSC, Ovaskainen & Soininen, 2011; Ovaskainen et al., 2017) is a hierarchical

JSDM technique which uses a Bayesian approach to provide information at multiple levels (community or species). Occurrence or abundance data can be handled and information on species traits or phylogenies can be considered. Stephenson et al. (2021) developed a bioregionalization for New Zealand by applying HMSC to jointly predict the distribution of 66 benthic taxa, after which k-means clustering was applied to define groupings. A particular advantage of modelling multiple species simultaneously is that more rare species can be retained, since "strength is borrowed" from more common or abundant species (Ferrier & Guisan, 2006; Hui et al., 2013; Leathwick et al., 2006a; Ovaskainen & Soininen, 2011). Simultaneously predicting species distributions in a single model also allows uncertainty in parameter estimates to be retained throughout the modelling procedure, thereby giving more of a realistic sense of the uncertainty associated with classified bioregions (Woolley et al., 2019).

A "group first, then predict" approach clusters species together first, based on a similarity metric or similar response to environmental variables, after which SDMs are used to predict each group against selected environmental variables (Ferrier & Guisan, 2006). Since fewer models are required, this approach can be easier to implement (Woolley et al., 2019). In the Barents Sea, Buhl-Mortensen et al. (2020) first applied a hierarchical ordination of species and sites using a two-way indicator species analysis (TWINSPAN, Hill, 1979) to hierarchically classify sites and identify key indicator taxa. Random Forest (RF, Breiman, 2001) models were then used to predict relationships of clustered groups against 15 environmental predictors. TWINSPAN is a similar multivariate technique to Detrended Correspondence Analysis (DCA, Hill & Gauch, 1980), which identifies important gradients and can be used to cluster assemblages. RF is a popular machine-learning algorithm due to its flexible nature and ability to be applied in classification (presence-absence) or regression (abundance). Machine learning techniques, such as RF or Boosted Regression Trees (BRT, Elith et al., 2008) can be more flexible since they do not make assumptions about the underlying distribution of the response variable, however, this can make them sensitive to overfitting (Norberg et al., 2019).

An alternative approach to performing classification and prediction as separate steps, is that species may be classified and predicted simultaneously within a single model (Ferrier & Guisan, 2006). The use of a single model for classification and prediction can easily provide estimates of uncertainty that are more reliable, which is helpful in communicating to managers and for determining areas which require further data (Woolley et al., 2019). Simultaneous classification and prediction of multi-species assemblages allows model diagnostics to be performed, thereby assessing how well groupings explain variation in the data (Woolley et al., 2019). There are fewer methods in this approach, as most are relatively recent, with methods

including Species Archetype Models (SAMs, Dunstan et al., 2011; Hui et al., 2013), Regions of Common Profiles (RCPs, Foster et al., 2013) and Bayesian model-based cluster analysis (ter Braak et al., 2003). Hill et al. (2017) applied RCP models to map bioregions on the Kerguelen Plateau in the southern Indian Ocean, classifying and predicting seven demersal fish assemblages using three environmental predictors. RCP models can utilise both presence-absence and abundance data to identify similar sites based on their environmental response profiles and species catch profiles (mean expectation or abundance of all species belonging to an RCP) by explicitly incorporating information about species locations (Foster et al., 2013; Foster et al., 2017). RCP models have been applied successfully in the marine environment and have been recommended for deriving data-driven bioregionalizations (Hill et al., 2020; Woolley et al., 2019).

Formally, RCP models follow a multivariate adaptation of a mixture-of-experts modelling framework (Jacobs et al., 1991), whereby the 'mixing proportions' (i.e. species' catch profiles or the expected probability of occurrence or abundance of species belonging to an RCP bioregion) may vary across sites but not on the conditional distribution. Setting it apart from standard mixture models is that these mixing proportions vary with covariates as well (Foster et al., 2013). The site groupings (RCPs or bioregions) are treated as latent variables in the model, since they cannot be observed, and sites are classified as belonging to one of a finite number of RCP groups. All sites within the same RCP group are assumed to share a constant species profile (expected abundance of each species per bioregion), defined by model coefficients. The occurrence of each RCP bioregion is predicted probabilistically across the study area as a function of the environmental covariates. This use of latent factors to relate variation in the biological data to environmental and spatial data mitigates the need to perform a two-stage analysis, thereby allowing uncertainty to be quantified and mapped.

The use of systematically collected survey data have been recommended over presence-only data when informing predictive models, since they are less spatially biased and provide more robust information about species absences and environmental conditions (Austin, 1998). While occurrence datasets (presence-only or presence-absence) are more common and easily combined, abundance data offers useful information for management and conservation of species and ecosystems. Models informed by abundance data reveal greater detail into species-environment relationships and can predict not only where species are likely to occur, but where they are likely to thrive (where their abundances are highest) or be most vulnerable, offering more information for management applications (Stephenson et al., 2021). Trawl collected survey data monitor both the west and south coast continental shelves of South Africa and have the potential to be a valuable dataset for predictive modelling of bioregions,

due to their systematic design (absences can be inferred), good spatial and temporal coverage and their collection of quantitative (abundance and biomass) data on demersal fish and invertebrate (epifaunal) distribution patterns. Environmental variables measured at the seafloor are also simultaneously monitored across trawl sites, resulting in biological and environmental datasets obtained at the same temporal and spatial scale. As such, species-environment relationships inferred can be more ecologically meaningful.

The research in this chapter aims to apply a data-driven approach to bioregionalization to assist with advancing data-driven methodologies for marine bioregionalization in South Africa. The objectives are to predict bioregions and estimate their uncertainty, associated species profiles and environmental responses using epifaunal abundance data collected by research trawl surveys on the southern Benguela shelf (western margin) of South Africa.

Methods

Biological data

Research trawl datasets were used due to their better systematic survey design across the shelf compared to other sampling methods e.g. towed cameras. Epifaunal abundance (counts) data obtained from demersal research trawl surveys conducted over the southern Benguela shelf (western margin) of South Africa (approximately 118 000 km^2) from ~ 70–800 m were used for this study (Figure 3.1). Data were obtained from three years (2017, 2019 and 2020) of austral summer surveys following the research trawl sampling protocols described in Chapter 2: Data collection methods (Research trawl, pg. 24). Each survey sampled between 110–120 x 30-minute trawl sites. Prior to data cleaning, the raw biological dataset consisted of a total of 535 691 individuals from 274 taxa recorded at 358 sites during the three years of trawl surveys.

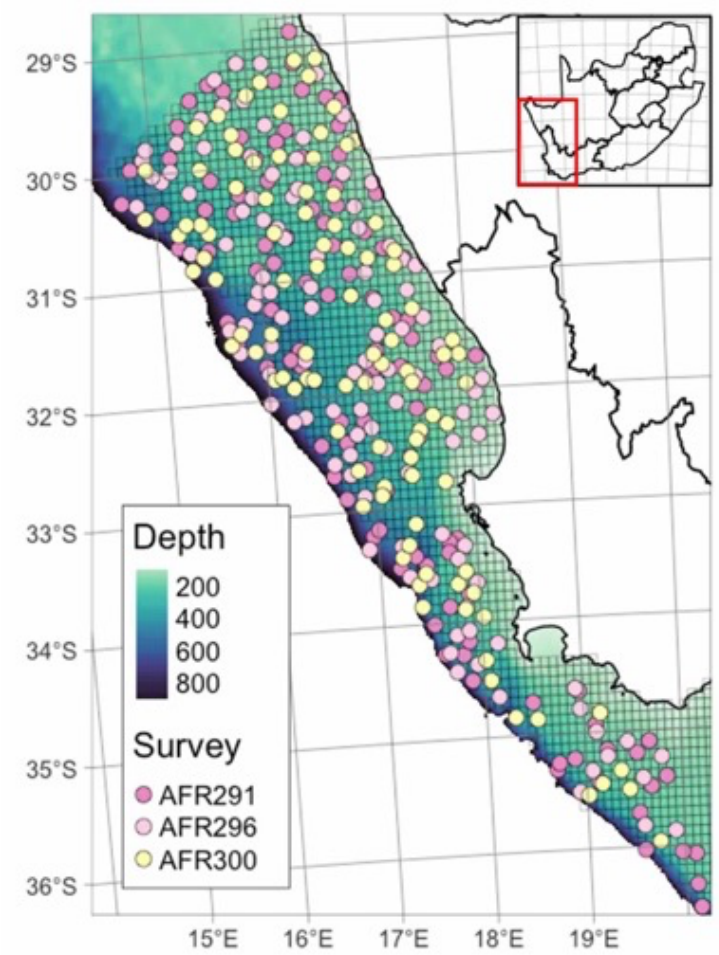

Figure 3.1 Map of the southern Benguela shelf of South Africa, shaded by depth (m). Map insert shows the location of the study area on the western margin of South Africa. Grid blocks (□, 5 x 5 nm) map the extent of the west coast demersal research trawl surveys. Trawl sites, at which epifaunal counts and environmental variables used in the analysis were collected, are shown, and coloured by survey (year). Location of trawl sites are based on start position of 30-minute trawl site.

Rare species were excluded from the analysis to remove data noise, and since they do not necessarily add important information for bioregionalization (Foster et al., 2017; Hui et al., 2013). While the threshold for defining rarity is contextual and somewhat arbitrary, species have been considered rare if they occurred at fewer than 1–5 % of sites (Foster et al., 2017; Hill et al., 2017; Lyons et al., 2017; Woolley et al., 2019). Since this was a first attempt at modelling epifaunal bioregions based on abundance in the region, species were arbitrarily considered rare if they occurred at fewer than 6 % of sites, due to the large number of rare species in the dataset (20 % of species occurred at one site only). Sites with fewer than three species recorded were removed. Taxa which could not be reliably identified to Genus or species level were excluded. After filtering, a total of 303 289 individuals from 46 epifaunal species recorded at 325 sites were used to inform the final model.

Environmental predictor data

Covariate selection is an important step in model development; selecting appropriate predictor variables that are both ecologically meaningful and explain a significant proportion of the biological variation (Austin, 2002). Since easily accessible offshore environmental bottom data for South Africa are generally available at coarse resolutions, limited timescales, and lack *in-situ* validation e.g. Bio-Oracle (Assis et al., 2017; Tyberghein et al., 2012), only variables from oceanographic measurements *in-situ* and slope derived from bathymetry were used as predictors for this study (Table 3.1).

Table 3.1 Environmental predictor variables (continuous) considered for modelling epifaunal bioregions. Range values based on in-situ measurements at the seafloor. Environmental covariates used in the final model are indicated by an asterisk (*).

Variable	Unit	Range	Data Source	Reference
Temperature*	°C	3.8 – 10.4	Fisheries independent survey (CTD)	DFFE 2017, 2019, 2020
Pressure	*db*	71.1 – 864.4	*as above*	*as above*
Salinity	PSU	34.2 – 35.0	*as above*	*as above*
Oxygen*	*ml/l*	0.1 – 5.1	*as above*	*as above*
Turbidity	NTU	0.9 – 5.3	*as above*	*as above*
Depth	*m*	70.6 – 856.7	*as above*	*as above*
Slope*	*Degrees*	0.0 – 8.4	Bathymetry raster (derived from digital single-beam echo-sounding data)	de Wet & Compton, 2021

Oceanographic variables, including temperature, pressure, salinity, oxygen, turbidity and depth were collected by the research trawl surveys over the same years as the biological data (Figure 3.1). Data were collected *in-situ* via an *SBE 19plus V2 SeaCAT Profiler CTD* (Sea-Bird Scientific, 2022) attached to the headline of the trawl net. Oceanographic data were

continuously measured along the 30-minute trawl transect at 4 scans per minute. *Seasoft V2: SBE Data Processing* software (Sea-Bird Electronics Inc., 2017) was used to correct for misalignment in the data, derive variables (e.g. salinity) and convert the raw CTD data, following the *Recommended SBE 19plus V2 profiling CTD Data Processing Steps* outlined in Sea-Bird Scientific (2017). Recommended default parameter values were retained. After processing, mean (± SD) values for each variable were calculated for all trawl sites after isolating the bottom data of the CTD profile (Appendix E). The "Slope" tool from the "Spatial Analyst Toolbox" in ArcGIS Pro version 2.9.0 (ESRI) was used to derive slope values from a recent bathymetry layer, compiled from digital single-beam echo-sounding data (de Wet & Compton, 2021). Slope values were assigned to each trawl site using the location of the trawl start point (as were latitude and longitude values).

Strong correlations between predictor variables can confound modelling. For this reason, highly correlated covariates (Pearson correlation coefficient of $r > 0.7$) were excluded from the analysis. Pressure, salinity, temperature, and depth were highly correlated ($r > 0.8$) across the study area (Figure 3.3). The most proximal variable to the distribution of benthic epifauna was retained to improve model robustness and relevance (Austin, 2002; Kenchington et al., 2019). Temperature was retained over pressure, salinity and depth since it has been considered the most proximal (of the correlated variables) to the distribution of marine ectotherms (Schmidt-Nielsen, 1990 as cited by Tyberghein et al., 2012). Temperature was also slightly less correlated with oxygen ($r = 0.67$) compared to that of pressure, salinity and depth ($r = 0.7$, Figure 3.3). Turbidity measures were very low across the study area (mean = 1.24 ± 0.49 NTU, Appendix E), and the effect thereof on the benthos at meso scales was considered negligible. For this reason, turbidity was excluded. The only environmental covariates therefore included as predictors for modelling epifaunal bioregions were bottom temperature (˚C), bottom dissolved oxygen (ml/l) and slope (˚).

To predict estimated bioregions spatially, gridded raster layers were produced (Figure 3.2). Universal kriging was used to interpolate the site wide CTD derived variables (temperature and oxygen) with the `'gstat'` R package (Pebesma, 2004) in RStudio v. 4.10. Rasters were interpolated to a resolution of 0.004˚ (approximately 400 m x 400 m). The `'raster'` R package (Hijmans et al., 2022) was used to combine the raster layers into a multidimensional (or stacked) raster layer for spatial prediction.

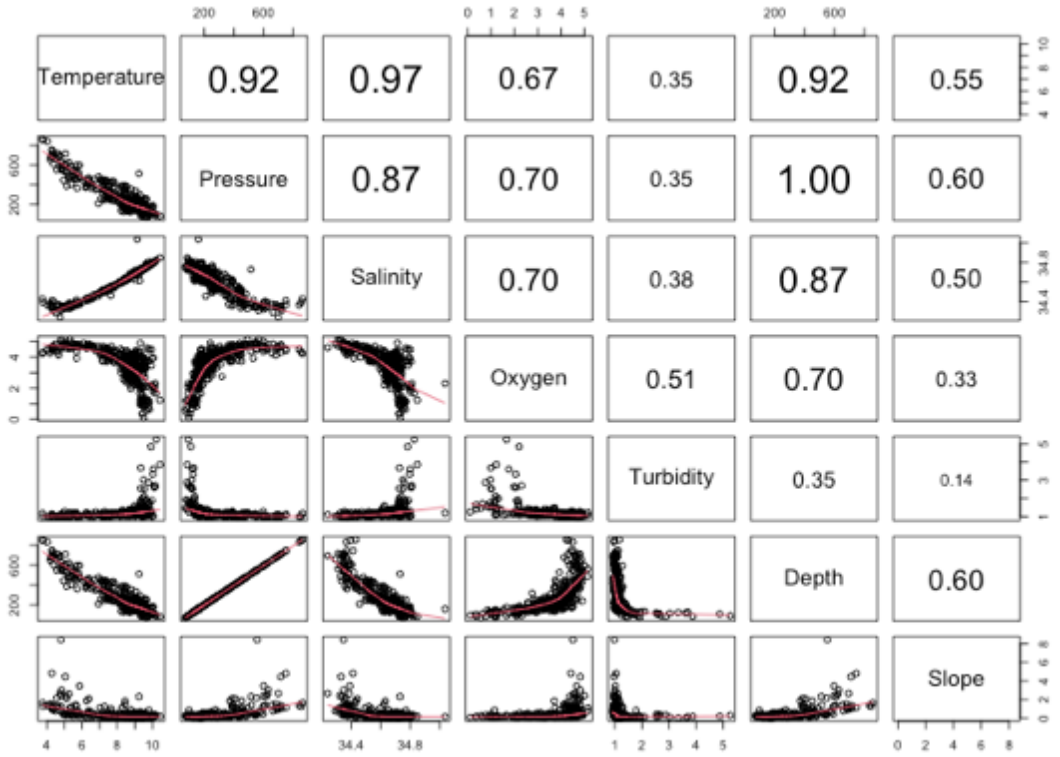

Figure 3.3 Pairs plots and Pearson correlation coefficients (r) for environmental covariates considered for modelling.

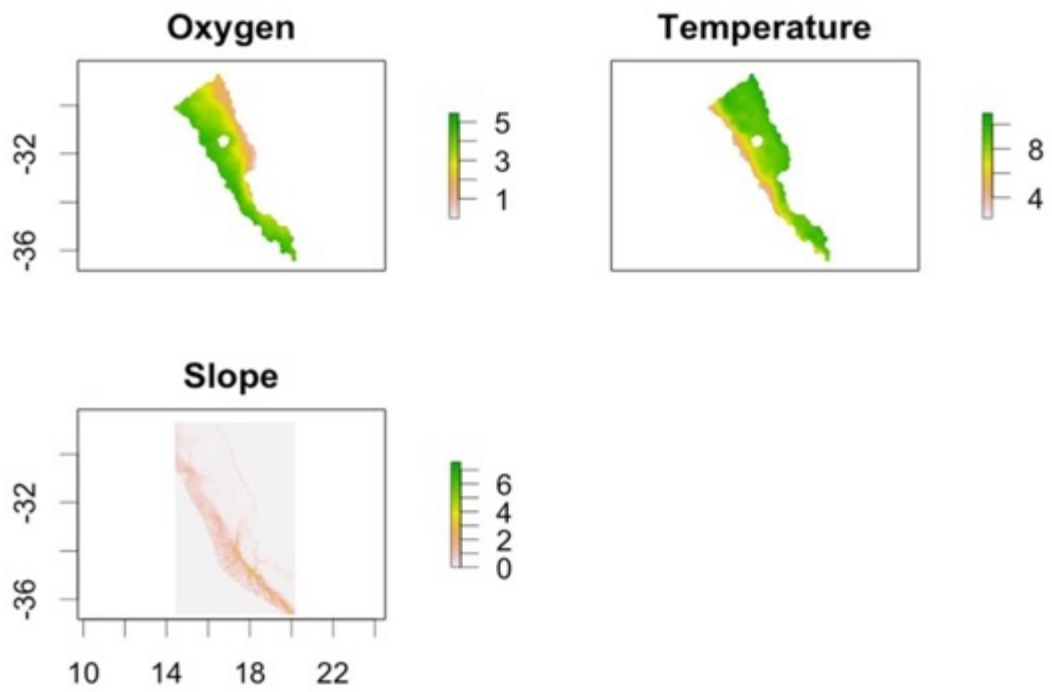

Figure 3.2 Environmental space used for predicting RCPs. Oxygen (ml/l) and temperature (˚C) raster layers were based on in-situ CTD collected data from research trawl surveys and kriged across the study area. The blank space in kriged layers represents an area where limited samples were available for kriging. Slope was derived from bathymetry (de Wet & Compton, 2021) in ArcGIS Pro (ESRI).

Regions of Common Profile (RCP) model

Taking into account the available data, the Region of Common Profile (RCP) modelling framework was identified as a suitable approach to statistically determine bioregions and estimate their associated species profiles and environmental responses. The detailed modelling framework is outlined in Foster et al. (2013) and Foster et al. (2017), where the model for the expectation of each species' observations resembles a generalized linear equation described as:

Equation 1:

$$g\left[\mathbb{E}\left(y_{ij}\middle|z_{ik}\right)\right] = g\left(\mu_{ij}\right) = \alpha_j + Z_i^{\mathrm{T}}\tau_j + v_i$$

where $g(\cdot)$ is a link function (log-link or identity link) and y_{ij} is the species datum for species $j, j = 1, \dots, S$ at site $i, i = 1, \dots, n$. Each site's catch profile (mean expectation for all species at a site) is described by the vector u_i. Sites with an approximately equal u_i can be thought to belong to the same RCP group $k, k = 1, \dots, K$, such that each RCP can be described by a constant species profile u_k. α_j is a species-specific intercept for the j_{th} species; τ_j is a $K \times 1$ vector of species parameters containing step changes for each RCP and v_i is a model constant added as an offset term for site i. $f\left(y_{ij}\middle|z_i\right)$ denotes the sampling distribution for $y_{ij}|z_i$ whose mean is given by equation 1. In this study, the negative binomial sampling distribution was chosen for over-dispersed abundance data.

z_i is a $K \times 1$ indicator vector for the i_{th} site, denoting which RCP each site belongs to. Since z_i is unobserved, it is treated as a latent factor in the model, such that the model resembles a mixture-of-experts model (Jacobs et al., 1991) for defining the RCP type. z_i is assumed to be the result of a multinomial sampling process with one trial and $k \times 1$ probability vector π_i which is allowed to vary depending on the site's location. This is defined as $\pi_i = h(X_i)$, where X_i is a design matrix containing the spatial and environmental covariate data for site i and $h(\cdot)$ is the additive logistic function (Aitchison, 1982) whose k_{th} element is:

Equation 2:

$$\pi_{ik} \triangleq h(X_i, k) = \begin{cases} \dfrac{\exp\left(X_i^T \beta_k\right)}{1 + \sum_{m=1}^{k-1} \exp X_i^T \beta_{k'}}, & if\ 1 \le k \le K-1 \\ 1 + \sum_{m=1}^{k-1} \pi_{ik'}, & if\ k = K \end{cases}$$

Where β_k are the parameter values for the k_{th} linear combination $(k = 1, \dots, K-1)$.

Modelling steps in R

The 'ecomix' package (Woolley, 2022) was used to fit the RCP models in RStudio version 4.1.0 (RStudio Team, 2021). The 'ecomix' package builds on previous packages 'RCPmod' (Foster et al., 2013) and 'Species-Mix' (Dunstan et al., 2011) and is the latest development for executing both RCP and SAMs models. Computation steps for fitting RCP models included 1) performing multiple fits to estimate the best model, 2) estimating uncertainty for making predictions 3) and performing diagnostics of the best model. The source code used for the analyses were adapted from Woolley (2021) and are freely available from GitHub (https://github.com/eco4cast/Statistical-Methods-Seminar-Series/tree/main/woolley_ecomix).

1) Model fitting and group selection

To fit the models, the continuous environmental covariates (temperature, oxygen and slope) were centred and standardised into 2nd degree orthogonal polynomials by adding a quadratic term for each variable. Epifaunal abundances were modelled with a negative binomial error distribution. Model parameters were estimated using penalized maximum likelihood (Foster et al., 2013). To maximise the log-likelihood and guard against finding local maxima, multiple fits were performed. For the likelihood to optimise, a reasonable number of starts should be chosen (Foster et al., 2013). Therefore, 100 multiple fits were performed per model in this study. The number of RCP groups over which multiple fits were performed was also set beforehand. In this case, 2–8 groups were chosen to reasonably cover the range of likely groupings. A control was added to help smooth the log-likelihood by setting several mild penalties on the estimated parameters, retaining the recommended default penalties from Foster et al. (2017).

To determine the number of RCP groups, Bayesian Information Criterion (BIC) was used to select the best model by selecting the model that minimized BIC (Foster et al., 2013), appropriate for mixture models (Keribin, 2000). To avoid selecting a model with RCP groups that have low site affinity (low number of sites assigned to them), site memberships of RCP groups (sum of posterior probabilities) were inspected for all models to ensure no groups were poorly represented and that all sites had indeed been classified into an RCP.

2) Estimating uncertainty and prediction

Bayesian bootstrapping (Rubin, 1981) as applied in Foster et al. (2017) was used to estimate uncertainty in parameter estimates and predictions. Confidence intervals around the point predictions were taken as a symmetric 95 % interval from a bootstrap distribution of 100

iterations. RCP predictions were generated with the 'predict' function. To predict expected abundances (number of individuals) of species at an average site for each RCP (including upper and lower confidence intervals), species catch profiles were calculated directly from model coefficients.

Probabilistic maps of the spatial distribution of each of the RCPs (including upper and lower confidence intervals around point estimates) were predicted in environmental space across the study area. A hard classification (non-probabilistic) was produced by fixing an RCP type in space, based on the most likely RCP at each point in space. Species catch profiles were estimated for each bioregion, represented by the mean ± standard deviation (SD) of species abundances for an average site. Plotted species catch profiles were represented on the log scale (by defining a "link" response) for easier visual inspection of the group contents for each RCP. Environmental responses of each RCP were quantified from model coefficients and assessed with partial plots. For partial response plots, the value of each environmental covariate was kept at the mean value, except for the variable of interest. Code and additional functions used to plot the partial responses were adapted from Hill et al. (2020) and are freely available on GitHub (https://github.com/Hillna-IMAS/Bioregion_Methods).

3) Model diagnostics

The best model was assessed through various diagnostic tests, as outlined in Foster et al. (2017). To check whether the model reasonably captured the variation in the data, random quantile residuals (RQR, Dunn & Smyth, 1996) adapted for mixture models (Dunstan et al., 2013) were inspected. The distribution of the RQR should be standard normal if the model performs well. To visually inspect homogeneity of variance in residuals, RQR were plotted against fitted values. Quantile-Quantile (QQ) plots were used to check for normality of residuals. Dispersion represents the variability associated with each species' mean expectations, due to the mean-variance relationship varying between species as a function of the mean (μ) and dispersion parameter (ϕ) (Warton et al., 2012). Since species with large means tend to be associated with higher variances (and larger values of the dispersion parameter) than species with small means, the dispersion parameter (estimated for each species) was inspected to check for large values and identify which species were associated with the most variability in abundance estimates.

Since RCP groups are latent (unobserved), traditional validation of how well the RCP groups represent the data is difficult to perform. However, the robustness and stability of RCP groups and log-likelihoods can be assessed by removing subsets of the data of increasing size. The Cook's distance metric (Cook, 1979) was used to assess the stability of RCP groups, as

adapted by Foster et al. (2017). Plots indicate how much predicted RCP membership probabilities (on average) change after a certain subset of data is removed, with larger values indicating a greater instability of RCP groups. The predictive log-likelihood was also plotted against hold-out sample size (i.e. number of sites removed) as an additional visual check of model stability. A notable drop or variability in the predictive log-likelihood as subsets of the data are removed indicates an unstable model, one that will be poor at predicting new observations (Foster et al., 2017).

Results

RCP group selection

The Bayesian Information Criterion (BIC) was minimized at five groups (32617.91), after 100 random starts were performed (Figure 3.4). The relationship between BIC and number of groups was approximately concave (Figure 3.4), an indication that enough groups were tested (Lyons et al., 2017). The final model interpreted consisted of five RCP groups (Appendix F). Sites were reasonably represented within each bioregion, as indicated by the sum of posterior probabilities (Table 3.2).

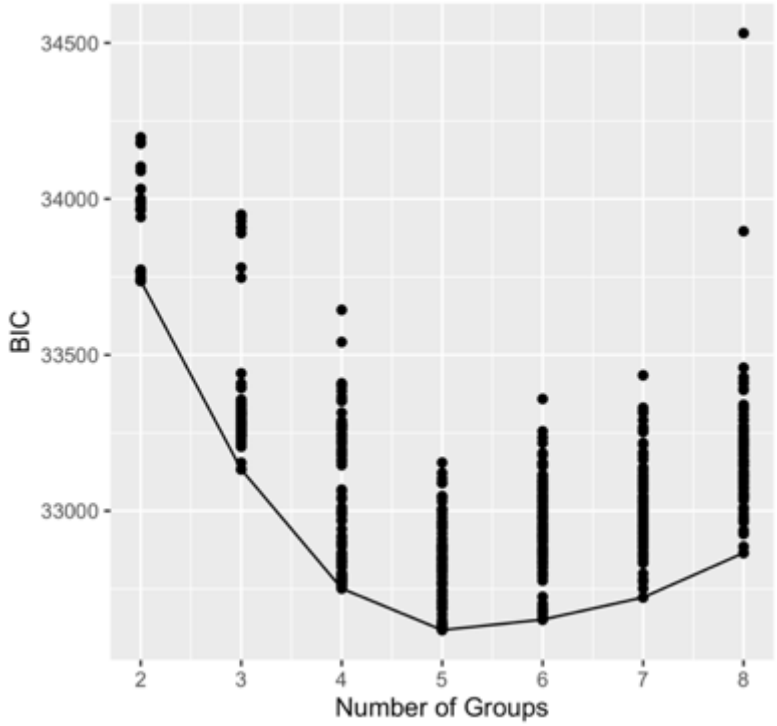

Figure 3.4 BIC values for models with 2–8 RCP groups, run with 100 random starts, using temperature + oxygen + slope as environmental predictor variables. Values are based on a model using 46 epifaunal species from 325 sites. The best model minimizes BIC (5 groups).

Table 3.2 Predicted number of sites (sum of posterior probabilities over sites) in each RCP bioregion. Sites are probabilistically classified into RCPs based on environmental covariates and species. Numbers of site probabilities are based on a model with five groups, using 46 epifaunal species from 325 sites and three predictor variables.

	1	2	3	4	5
Predicted number of sites in each RCP (sum of posterior probabilities)	56.77	97.95	50.69	66.52	53.07

Predicting spatial patterns and RCP bioregion contents

The five RCPs (also referred to as bioregions) followed a depth gradient across the shelf (Figure 3.5). Since depth was not included as a predictor, exact depth ranges are not known, hence bathymetry contours were mapped over predicted RCPs to indicate approximate depth

ranges (Figure 3.5). RCP 5 was closest to the coast (light green), followed by RCP 2 (orange), 4 (pink) and 3 (purple), with RCP 1 (dark green) being the deepest bioregion (Figure 3.5).

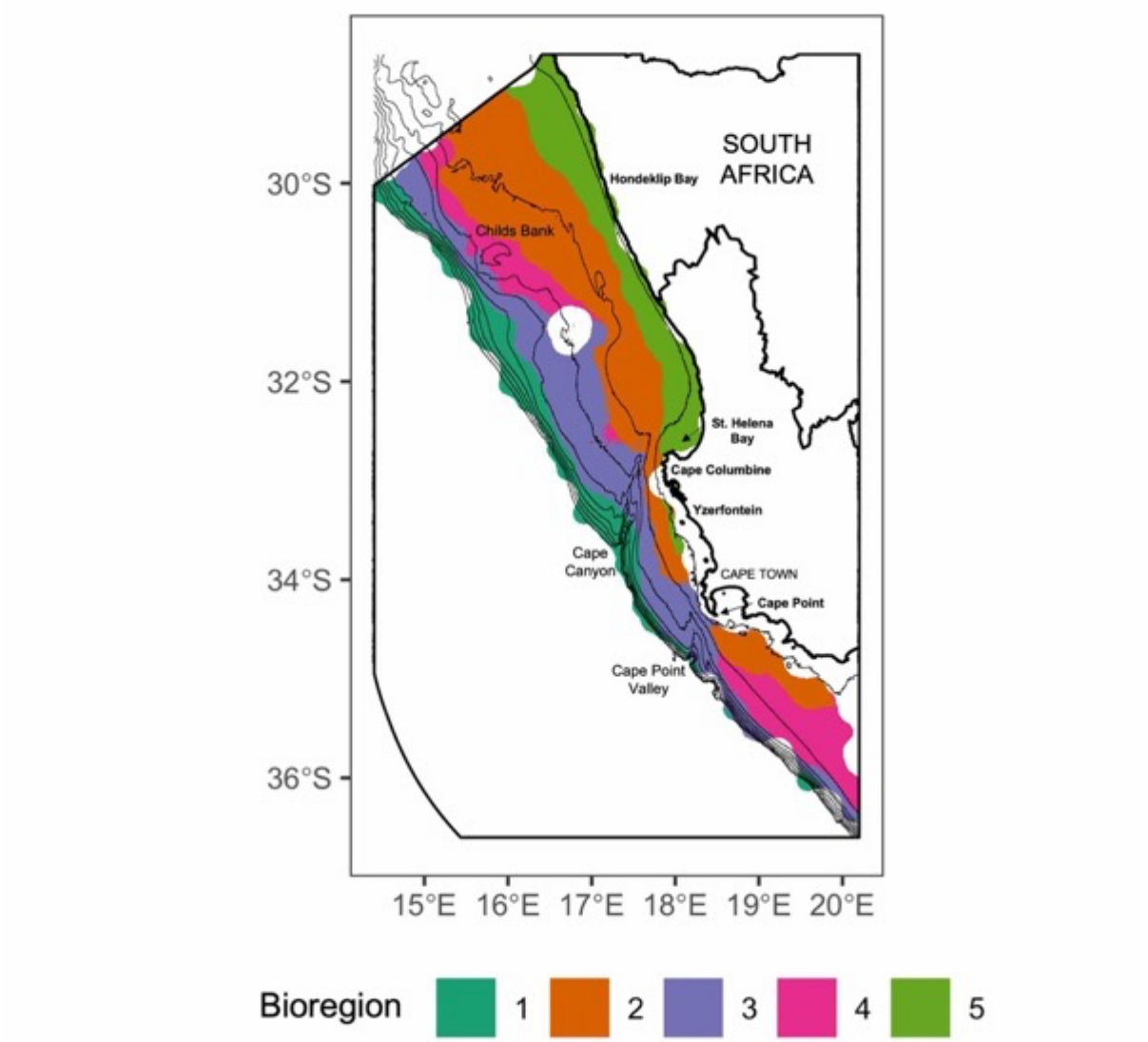

Figure 3.5 Predicted spatial distributions of RCP groups to produce a hard (non-probabilistic) classification across the environmental space of the study area. Bathymetry contours are shown in 100 m intervals from 100–1000 m depth. Bioregions (RCP 1–5) are separated by colour and based on a model using 46 epifaunal species from 325 sites and three covariates.

The deepest (RCP 1) and shallowest (RCP 5) bioregions were predicted across the shelf with a high degree a certainty, as indicated by probability values close to 1 (dark red) in both the upper (right) and lower (left) confidence interval (CI) panels (Figure 3.6). Bioregions (RCP 2, 4 and 3) over intermediate depths (~150–500 m) were associated with lower degrees of certainty (wider CIs) as indicated by light red colours in the lower CI panels and darker red colours in the upper CI panels (Figure 3.6). RCP 4 overlapped substantially in space with RCP 2 and 3, and was predicted with the least amount of certainty, with lower probabilities (light red colours) of prediction (Figure 3.6). All bioregions were least certain around their boundaries, as seen by the lightest red colours occurring towards the edges of bioregions

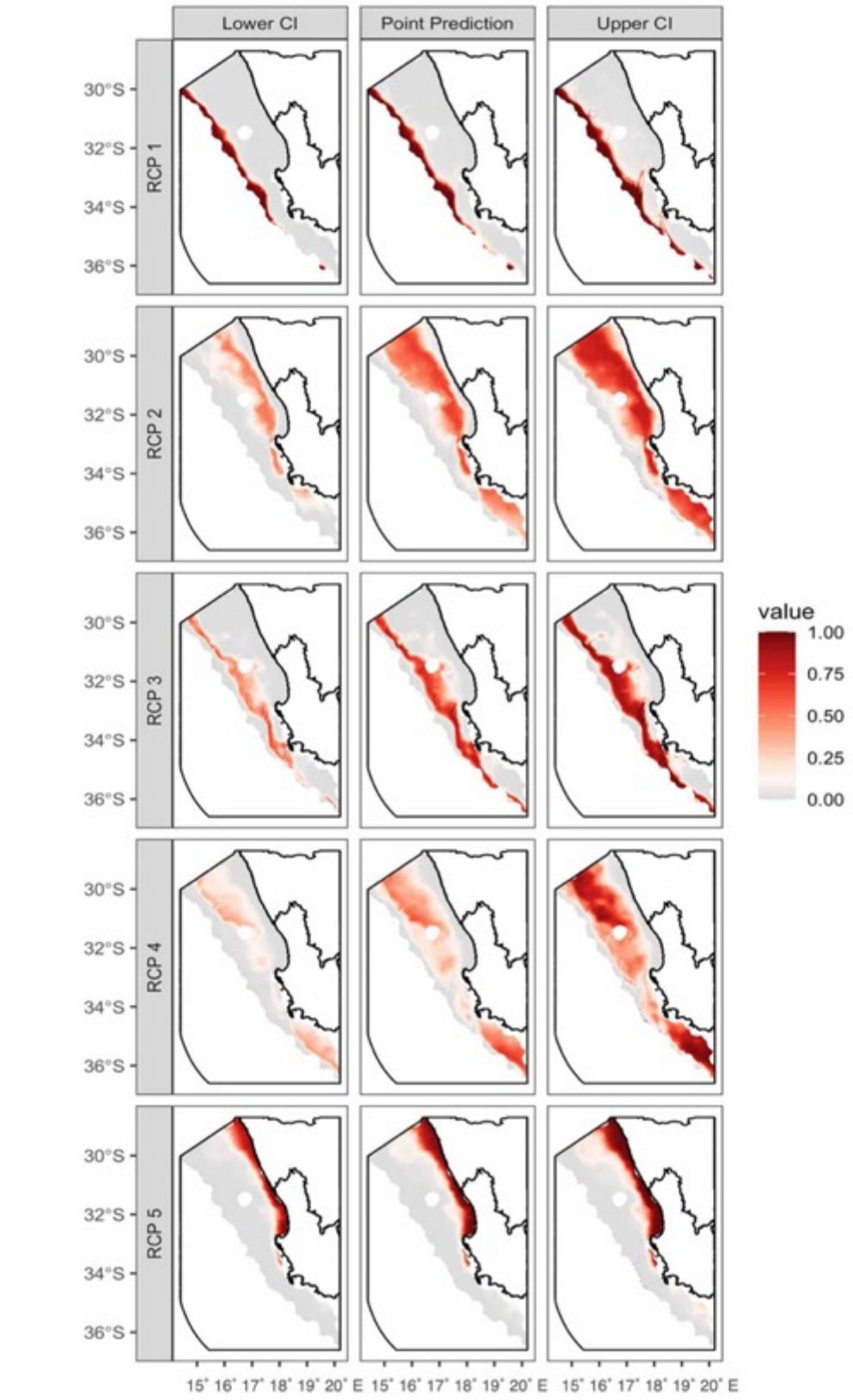

Figure 3.6 Predicted spatial distributions (± SE) of RCP bioregions across the environmental space of the study area. RCPs (1–5) are separated by rows. Middle panels represent the spatial distribution of the point predictions (mean) for each RCP, while uncertainty is represented by bootstrapped 95 % confidence intervals (right and left panels). RCPs are based on a model using 46 epifaunal species from 325 sites and three covariates. RCP probabilities are shaded from low (grey) to high (dark red).

All RCP bioregions responded strongly to at least one of the environmental predictors tested. Temperature varied across the shelf from 3.76–10.44 ˚C, dissolved oxygen varied from 0.11–5.14 ml/l and slope varied from 0.002–8.448 ˚ (Figure 3.7). The deepest bioregions (RCP 1 and 3) had the strongest responses to temperature and the shallowest bioregion (RCP 5) responded most strongly to oxygen (Figure 3.7). RCP 3 was the only bioregion with a strong response to slope (Figure 3.7).

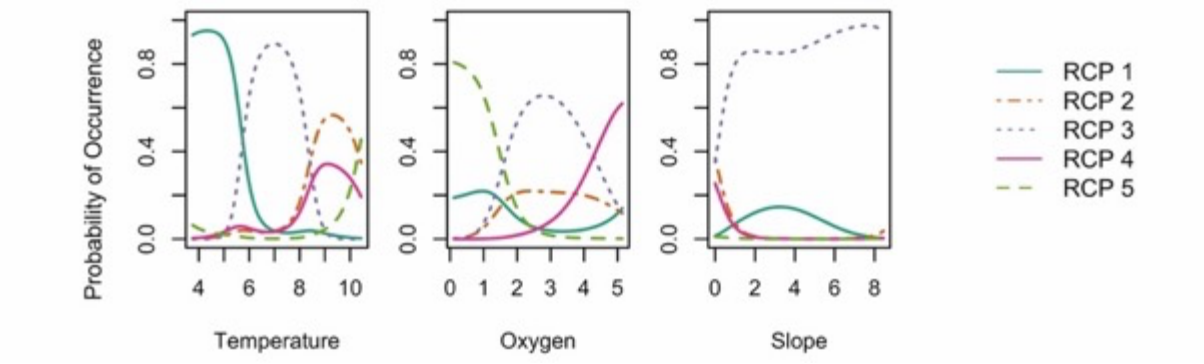

Figure 3.7 Partial effects plots for the effect of each of the continuous environmental variables: temperature (˚C), oxygen (ml/l) and slope (˚), on the probability of occurrence of the five epifaunal RCP bioregions across the study area. RCPs are based on a model using 46 epifaunal species from 325 sites and three covariates. Covariates were held at their mean values to make the predictions.

Species turnover between the bioregions followed a strong depth gradient, with all bioregions sharing some species in common with adjacent bioregions (Figure 3.8). Species with the highest predicted abundances in RCP 5 and RCP 1 tended to have low predicted abundances at intermediate bioregions e.g. *Plesionika martia* and *Sergia spp.* in RCP 1, and *Cavernularia spp.* and *Pasiphae sp. 1* in RCP 5 (Figure 3.8). The dimorphic hermit crab *Sympagurus dimorphus* was estimated to be the most abundant species (based on mean abundance) in bioregions of intermediate depths, RCP 2–4 (Figure 3.8). Both hermit crabs *S. dimorphous* and *Parapagurus bouvieri* were estimated to peak in abundance in RCP 3, however, *S. dimorphous* was more abundant than *P. bouvieri* in shallower bioregions, while *P. bouvieri* was more abundant than *S. dimorphous* in the deeper bioregion, RCP 1 (Figure 3.8). RCP 4 and 3 were the most species rich, with 22 and 21 species respectively, predicted to occur with mean abundances greater than 1 (Figure 3.8). The shallowest bioregion, RCP 5 was the least species rich, with 9 species predicted to occur with mean abundances greater than 1 (Figure 3.8).

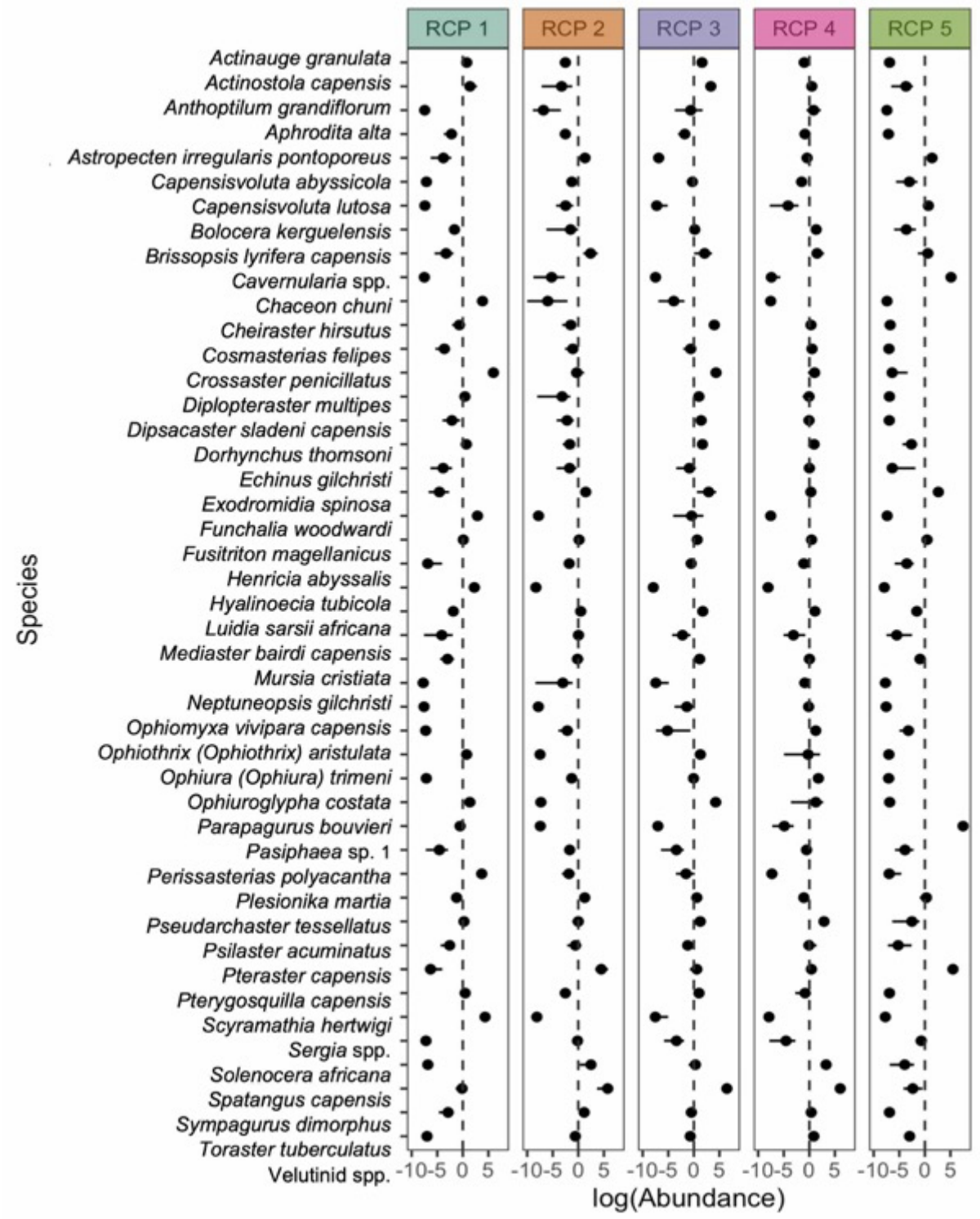

Figure 3.8 Average species catch profiles, the estimated mean abundances of species predicted at a site in each bioregion (RCP 1–5). Abundances are represented on the link scale (log abundance) ± lower and upper confidence intervals (CI) for easier visualization. Predicted abundances are based on a model using 46 epifaunal species and three environmental predictor variables (temperature, oxygen, and slope) from 325 sites. Note that species associated with negative log(abundance) values indicate estimated abundances of less than 1 individual per site, but greater than 0 (Appendix G).

RCP 5 was predicted to occur with a high probability north of St. Helena Bay to the South African-Namibian border at approximate depths of 100–150 m (Figure 3.5). RCP 5 responded most strongly to oxygen, with a high probability (> 0.8) of occurring in low oxygen (< 0.3 ml/l) waters (Figure 3.7). This bioregion was associated with the warmest temperatures (> 10 ˚C), but only moderately (0.45 probability occurring at maximum temperature 10.44 ˚C) and had no response to slope (Figure 3.7). The glass shrimp *Pasiphae* sp.1 was the most abundant species predicted to occur in this bioregion, albeit with high variability in SD of the mean (1906.28 ± 788.50 ind., Figure 3.8). This was followed by the Cape mantis shrimp *Pterygosquilla capensis* (246.23 ± 43.05 ind.) and the small sea pen *Cavernularia* spp. (183.81 ± 85.63 ind., Figure 3.8). Predicted abundances of *Pasiphae* sp.1 and *Cavernularia* spp. were low (less than 1 ind. per site) for other bioregions (Figure 3.8).

RCP 2 covered the greatest area across the shelf (Figure 3.5), with the highest certainty of occurring near the boundary of RCP 5 (Figure 3.6). This bioregion responded most strongly to temperature, with a probability > 0.5 of occurring in relatively warm bottom waters of 8.82–9.96 ˚C (Figure 3.7). It had a low response to oxygen and slope (Figure 3.7). The most abundant species predicted for this bioregion were the hermit crab *S. dimorphus* (363.27 ± 156.16 ind.), the Cape mantis shrimp *P. capensis* (110.62 ± 100.92 ind.) and the heart urchin *Brissopsis lyrifera capensis* (14.76 ± 13.51 ind., Figure 3.8).

RCP 4 had the highest certainty of occurring southeast of Cape Point and northwest of (and including) Childs Bank (Figure 3.6). This bioregion responded strongly to oxygen, with a > 0.5 probability of occurring in waters with a bottom oxygen concentration of 4.68–5.14 ml/l (Figure 3.7). The most abundant species for RCP 4 were the hermit crab *S. dimorphus* (466.32 ± 204.96 ind.), the purple sea urchin *Spatangus capensis* (27.47 ± 7.67 ind.) and the starfish *Psilaster acuminatus* (18.37 ± 5.61 ind., Figure 3.8).

RCP 3 was the second deepest bioregion, with a wide predicted distribution across the middle of the shelf (Figure 3.5). This bioregion responded strongly to slope and temperature. RCP 3 had a high probability (> 0.8) of occurring in bottom temperatures of 6.32–7.67 ˚C and at all slope values greater than 1 (Figure 3.7). RCP 3 was most likely to occur (> 0.5) in bottom waters with an oxygen concentration of 1.94–3,87 ml/l (Figure 3.7). The hermit crab *S. dimorphous* peaked in abundance in this bioregion (695.54 ± 249.69 ind.), followed by the starfish *Crossaster penicillatus* (83.81 ± 36.01 ind.) and the hermit crab *Parapagurus bouvieri* (79.03 ± 38.79 ind., Figure 3.8).

RCP 1 was predicted with a high certainty along the deepest area of the shelf (Figure 3.6). This bioregion responded most strongly to temperature, with a high probability (> 0.8) of

occurring in the lowest bottom temperatures (3.76–5.24 ˚C, Figure 3.7). It had a low predicted response to oxygen and slope, however, was more likely to occur in low oxygen waters than oxygenated waters, with a 0.22 probability of occurring in bottom oxygen of 0.98 ml/l (Figure 3.7). The starfish *Crossaster penicillatus* (413.24 ± 114.00 ind.) was the most abundant species in this bioregion, followed by the prawns *Sergia* spp. (81.13 ± 23.77 ind.) and *Plesionika martia* (43.88 ± 18.76 ind., Figure 3.8). The red crab *Chaceon chuni* (48.30 ± 12.05 ind.) and prawn species *P. martia, Sergia* spp. and *Funchalia woodwardi* (18.13 ± 4.94 ind.) were distinguishing species for this bioregion, since their estimated abundances were low for other bioregions (Figure 3.8).

Model diagnostics

Random quantile residuals (RQR) were approximately normally distributed for the best model fitted and variation was reasonably well captured in the model (Figure 3.9). Hold-out tests (removing subsamples of sites) assessing the robustness of RCPs indicated an adequate performance, as indicated by the relatively small changes in the predictive log-likelihood (black line, Figure 3.11). The deepest (RCP 1) and shallowest (RCP 5) bioregions were most stable with respect to removing subsets of the data (Figure 3.11). Although the predictive log-likelihood initially decreased, it remained relatively stable and did not fluctuate much, indicating acceptable stability with respect to removing subsets of the data (Figure 3.11).

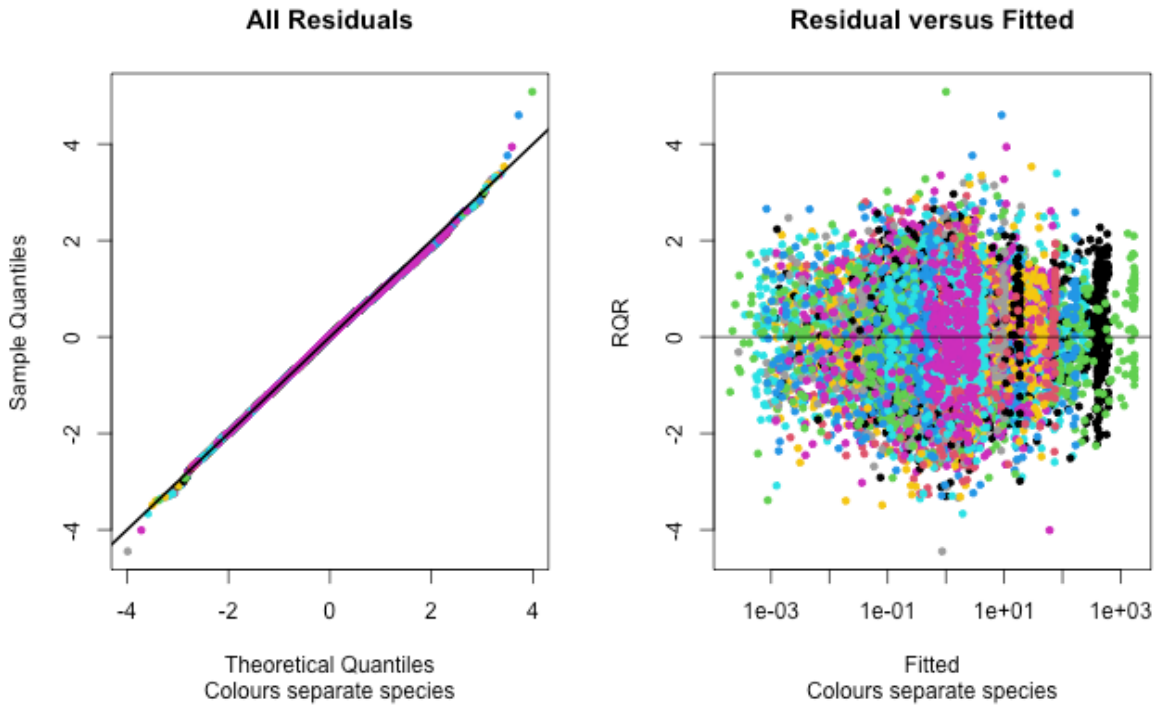

Figure 3.9 Randomised quantile residual (RQR) diagnostic plots (calculated using Smyth-Dunn residuals). Left: quantile-quantile (QQ) plot testing for normality and Right: RQR against fitted values testing for homogeneity of variance in residuals. Colours are reused between the 46 species.

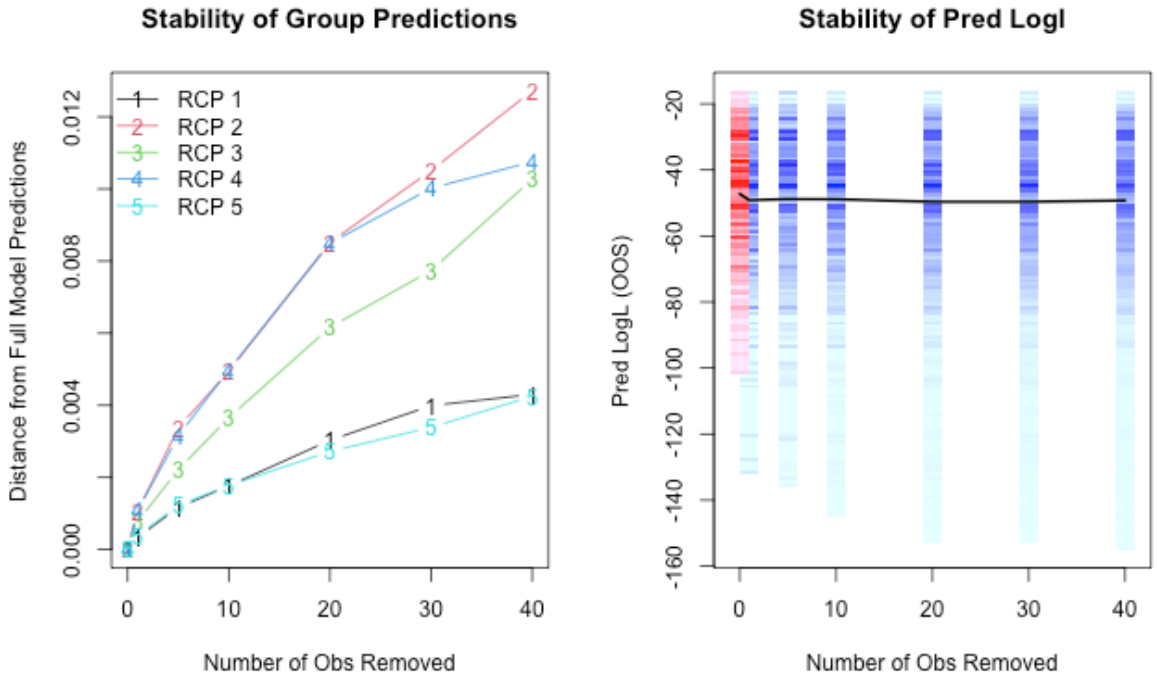

Figure 3.11 Diagnostic plots assessing stability of RCP groups, based on Cook's distance (left) and predictive log-likelihood (right), against hold-out sample size. The predictive log-likelihood of the final model is indicated in red colours and with samples removed in blue colours.

Variability in estimated abundances was high for some species, as captured by large values (greater than 10) of the dispersion parameter for nine species (Figure 3.10). These were the brittle star *Ophiura trimeni,* the glass shrimp *Pasiphaea sp. 1,* the large sea pen *Anthoptilum grandiflorum,* the African mud shrimp *Solenocera africana,* the anemone *Bolocera kerguelensis,* the cushion starfish *Pteraster capensis,* the prawn *Sergia spp.,* the hermit crab *Parapagurus bouvieri* and the small sea pen *Cavernularia spp.* (Appendix F).

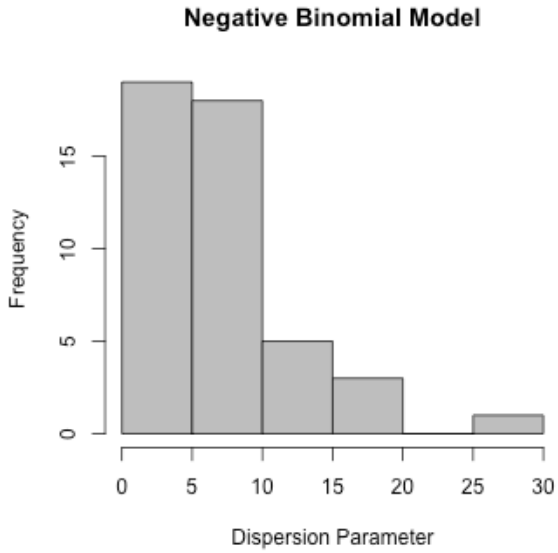

Figure 3.10 Frequency distribution of dispersion parameter values estimated for all species by the RCP model with a specified negative binomial sampling distribution.

Discussion

This study produced the first data-driven bioregionalization, based on epifaunal abundance data from demersal research trawl surveys, for the southern Benguela shelf (western margin) of South Africa. Five bioregions with varying environmental responses and expected species abundances (species' catch profiles) were defined by applying a Region of Common Profile modelling approach. The deepest and shallowest bioregions were spatially predicted with the highest certainty. These bioregions had the clearest responses to environmental predictors and were associated with more distinguishing species (species predicted with low abundances in other bioregions). The greatest uncertainty in spatial predictions was estimated for bioregions at intermediate depths, which were occupied by both shallow and deep species and were dominated by the same hermit crab species (*S. dimorphus*). These bioregions responded less clearly to environmental predictors used in this study, and a lack of relevant environmental predictors may have resulted in higher uncertainty of estimated bioregions across intermediate depths.

Alignment of bioregions with previously described patterns

Previously classified 'habitat' and 'ecosystem' types for the southern Benguela shelf of South Africa were mapped at finer scales than what was defined here, with 42 habitat types and 43 ecosystem types classified by Sink et al. (2012b) and Sink et al. (2019b) at the lowest level of the classification for the southern Benguela shelf, respectively. However, close alignment with these classifications at the regional scale was observed, with Sink et al. (2012b) defining 6 'ecozones' for the southern Benguela shelf, while a synonymous level of the classification was not defined by Sink et al. (2019b). Both classifications followed an expert-derived hierarchical approach to classification, with substantially greater datasets informing the most recent classification (SANBI, 2022; Sink et al., 2019b; Sink et al., 2023). Key environmental and biological drivers of offshore patterns considered by Sink et al. (2012b) were substrate categories, depth and slope, geology and grain size, and biogeography (Sink et al., 2012b). Building on the previous classification, Sink et al. (2019b) incorporated improved bathymetric and biogeographic information to refine the classification and map. Such additional environmental datasets included satellite imagery, single-beam and multi-beam bathymetric datasets, recent and historical sediment datasets, and oceanographic data (temperature, oxygen, and salinity) (Sink et al., 2019b). Biological datasets used to refine the classification included data from visual surveys, grabs, historical dredges, recently defined infaunal and epifaunal biotopes and vulnerable marine ecosystems (Sink et al., 2019b).

The deepest and shallowest bioregions (RCP 1 and 5) were predicted with the highest certainty across the study area. These bioregions aligned more closely with previously defined ecosystem classifications and maps for the western margin of South Africa compared to the bioregions predicted across intermediate depths. RCP 5 occurred from St. Helena Bay to the South Africa-Namibian border, from about 70–150 m which aligned most closely with the 'Namaqua Inner Shelf' ecoregion (Sink et al., 2012b) and the 'Namaqua Muddy Mid Shelf Mosaic' ecosystem type (Sink et al., 2019b). The spatial extent of RCP 5 corresponded to similarly observed changes in communities at approximately 150 m on the western margin (Karenyi, 2014; Lange & Griffiths, 2014; Shah, 2018; Smale et al., 1993).

RCP 1 was the deepest bioregion and corresponded most closely to what has previously been defined as the 'South Atlantic Upper Bathyal' ecoregion and the 'Southeast Atlantic Upper Slope' ecosystem type (Sink et al., 2012b; Sink et al., 2019b). The upper slope occurs just after the shelf edge break (Howell 2010), which has been reported to feature at approximately 400–500 m on the western margin (de Wet & Compton, 2021; Emery et al., 1992). Distinct changes in cephalopod (Roeleveld et al., 1992), demersal fish (Atkinson et al., 2011b; Roel, 1987), macrofauna (Karenyi, 2014) and epifauna (Lange & Griffiths, 2014; Shah, 2018) have been observed at approximately 400–500 m where the shelf edge and upper slope intersect.

RCP 1 and 5 were defined by clearer responses to environmental predictors compared to the other bioregions. Low temperatures (3.76–5.24 ˚C) distinguished RCP 1, and low oxygen concentrations (< 0.3 ml/l) distinguished RCP 5 (Figure 3.7). Low oxygen bottom waters (< 2 ml/l) are a variable but permanent feature known to occur on the Namaqua Inner Shelf (shallower than 150 m), which form due to upwelling (Jarre et al., 2015). Productivity and related variables, such as hypoxia, were found to be particularly influential for this area when defining a seascape classification for the west coast and shelf (Karenyi et al., 2016a). A sharp decrease in bottom temperatures with a steep increase in depth at the shelf edge break (Dingle & Nelson, 1993) has been thought to influence changes in communities associated with the upper slope in South Africa (Roeleveld et al., 1992; Smale et al., 1993). Temperature, as well as other collinear variables such as salinity are properties associated with different water masses, with which epifaunal biogeographical patterns are known to align (Buhl-Mortensen et al., 2020; Limongi et al., 2023; Neumann et al., 2017; Snelder et al., 2007). On the western continental slopes of South Africa, cephalopods as an example, have been found to be associated with different water masses, such as the cold Antarctic Intermediate Waters (AIW) in the order of 3–4 ˚C (Roeleveld et al., 1992). While RCP 1 had a small probability of occurring in low oxygenated waters, it is unclear why. Limited knowledge about the seafloor

below 500 m in South Africa (Griffiths et al., 2010) suggests this feature requires further investigation.

While species abundances can be associated with multiple RCPs, each RCP should be defined by a distinct species' catch profile, or the expected abundances of each species (Foster et al., 2013). None of the bioregions in this study had the same species' catch profiles, however, more similarities were found between catch profiles at intermediate depths (RCP 2, 3 and 4). Species catch profiles defining RCP 1 and 5 were distinctly different and associated with more distinguishing species (species that were not expected in other bioregions). The most abundant species predicted to occur in RCP 1 was the starfish *Crossaster penicillatus* (Figure 3.8), also identified by (Lange & Griffiths, 2014) as the most abundant species of their deepest community defined along the shelf edge and upper slope (identified only to family as Solasteridae). Lange & Griffiths (2014) also found *Plesionka martia* and *Chaceon chuni* (identified as *Chaceon quinquedens)* as highly abundant species along the shelf break, as found in this study. *P. martia* similarly occurs along the shelf edge and upper slopes in the Mediterranean and has been observed to peak in abundance at similar depth ranges, between 400–600 m, in the eastern-central Mediterranean (Maiorano et al., 2002). Prawn species, *P. martia, Sergia* spp. and *Funchalia woodwardi*, and the red crab *C. chuni* were distinguishing species for this bioregion, being predicted with negligible abundances across the other bioregions. Zooplankton food sources have been thought to influence distributions of prawns e.g. *P. martia* (Cartes et al., 2021) and *Sergia lucens* (Omori & Ohta, 1981), while some species of the genus *Crossaster* are known to occur in low temperature and mixed waters on the shelf break in the North-East Atlantic e.g. *C. squamatus* (Ringvold & Moum, 2020).

The most abundant species predicted to occur in the shallowest bioregion, RCP 5, was the prawn *Pasiphaea sp. 1.* Although not identified to species level for this study, *Pasiphaea semispinosa* has been described to have a similar distribution and has been documented alongshore north of Cape Columbine up to depths of 200 m (Gibbons et al., 1994; Kensley, 2006). While this species is regarded as pelagic (Kensley, 1981), noting the close coupling of the benthic-pelagic realms, particularly in shallower waters (Sink et al., 2012b; Sink et al., 2019b), this distribution likely reflects benthic patterns too. The mantis shrimp *Pterygosquilla capensis* was predicted with high abundance in RCP 5 which aligns with what is known about this species' distribution off the west coast of South Africa, occurring in waters shallower than 150–200 m (Griffiths & Blaine, 1988) and in low oxygen (< 1 ml/l) waters with temperatures > 10–11 ˚C (Abelló & Macpherson, 1990). *Cavernularia* spp. was predicted to occur at high abundance in RCP 5 and with low abundances across all other bioregions. *Cavernularia* is a known shallow water genera which favours soft sediments associated with coral reef

(Williams, 2011). RCP 5 was predicted with the lowest species richness, which aligns with what is hypothesised about oxygen minimum zones (OMZs), as diversity is thought to be less due to higher physical stress (Levin, 2003).

RCP 2, 3 and 4 (~150–500 m) did not align as closely with previously defined ecosystem classifications and maps as RCP 1 and 5 did, though there were some consistencies at a broad level. RCP 3 broadly corresponded to a previously defined 'Southern Benguela Shelf Edge' ecoregion (Sink et al., 2012b) and encompassed the 'Southern Benguela Muddy and Sandy Shelf Edge' and 'Southern Benguela Shelf Edge Mosaic' ecosystem types (Sink et al., 2019b). RCP 3 also overlapped somewhat with the 'Southern Benguela Outer Shelf Mosaic' ecosystem type (Sink et al., 2019b) in the middle of its predicted distribution where hard rocky ground is known to occur (Karenyi, 2014; Sink et al., 2012b; Sink et al., 2019b). Since substrate type was not used as a predictor in this study, it is possible that including this variable as a predictor may refine the boundaries of RCP 2, 3 and 4. However, trawling mostly avoids hard ground and would therefore be unable to provide the data for species associated with hard ground.

RCP 2 and 4 covered a spatial extent similar to the 'Southern Benguela Outer Shelf' ecoregion defined by Sink et al. 2012, however, there was not much agreement at finer scales. RCP 2 covered a large area of the shelf and encompassed parts of several previously defined ecosystem types (Sink et al., 2019b). Northwest of Cape Point these were: the 'Southern Benguela Sandy Outer Shelf', 'Southern Benguela Outer Shelf Mosaic' and 'Namaqua Muddy Sands', while southeast of Cape Point RCP 2 had closer alignment with the 'Southern Benguela Muddy Outer Shelf Mosaic'. Closer agreement to the previous classification was similarly found southeast of Cape Point for RCP 4, which mostly encompassed the 'Southern Benguela Sandy Outer Shelf' ecosystem type (Sink et al., 2019b). Northwest of Cape Point the spatial extent of RCP 4 included the 'Southern Benguela Sandy Outer Shelf', 'Southern Benguela Outer Shelf Mosaic' and 'Childs Bank Plateau' (Sink et al., 2019b).

Childs Bank is a limestone plateau (de Wet & Compton, 2021) and is classified as a submarine bank and unique ecosystem type (Sink et al., 2012b; Sink et al., 2019b). Such features are thought to support distinctive biological communities (Howell, 2010). While changes in bioregional patterns around the area of Childs Bank were detected in this study, they were moderate, and it's unlikely that assemblages on the plateau and to the southeast of Cape Point are the same. RCP 4 had the strongest response to high oxygen, which could explain why the areas classified as RCP 4 to the north and south of Cape Point were grouped together, even though expected assemblages are likely different in reality. Additional relevant

environmental predictors would be needed to more appropriately differentiate between sites classified as RCP 4.

While the intermediate bioregions responded somewhat differently to environmental predictors, they did not have as clearly defined responses as RCP 1 and 5. RCP 2 and 4 differed mostly from one another in terms of responses to oxygen, with RCP 4 on the outer shelf having a higher probability of occurring where dissolved oxygen was higher. Although RCP 3 had a strong response to temperature (6.32–7.67 ˚C, Figure 3.7) and the strongest response to slope, it had a high probability of occurring where slope values were > 1 ˚, which may not be the best predictor to discriminate finer patterns. While slope has been acknowledged as an important predictor for epifaunal distributions (Bouchet et al., 2015; Davies et al., 2009; Durden et al., 2015; Mohn & Beckmann, 2002; Wilson et al., 2007; Yesson et al., 2012) and for western margin seascapes (Karenyi et al., 2016a), trawl sampling tends to avoid strongly sloping terrain, and therefore the fauna sampled by trawls may not be as affected (and therefore well predicted) by slope. The detection of weak and indistinct environmental response for these bioregions, as well as the higher uncertainty in predictions found, suggests that important environmental predictors for these bioregions were missing from this study, e.g. substrate type. A similar observation was made by Hill et al. (2017) when they too found greater uncertainty associated with RCPs at intermediate depths (~400–700 m) of their study area (100–1200 m). In addition, they mentioned the greater challenges of defining assemblages at intermediate depths, since both shallow and deep species are often found together, therefore being characterised by a wider range of environmental responses, as noted by Leaper et al. (2014).

The ecosystem types which broadly aligned with RCP 2, 3 and 4 (discussed above) were characterized by different sediment types (Sink et al., 2019b) and may correspond to different epifaunal assemblages. Substrate type is often used as a predictor when classifying spatial units associated with different benthic assemblages (Buhl-Mortensen et al., 2012; Connor et al., 2004; Howell, 2010; Lombard et al., 2004; Sink et al., 2012b; Sink et al., 2019b; Vasquez et al., 2021). Contrary to what was found in this study, different epifaunal communities and biotopes to the southeast and northwest of Cape Point have been defined with hierarchical cluster analysis based on trawl data (Lange & Griffiths, 2014; Shah, 2018). However, the same species, *S. dimorphus,* dominated estimated abundances at these bioregions (RCP 2, 3 and 4) and could explain the similarities found between these bioregions in this study. This anemone hermit crab was previously found across a similarly wide distribution and was also the most abundant species over the continental shelf (Lange & Griffiths, 2014). *S. dimorphus* has a wide depth range globally (91–1995 m, Lemaitre, 2004), and peaks in abundance

between 200–300 m on the western margin have been detected with trawl sampling (Wright et al., 2020). RCP 2, 3 and 4 were all partly distributed over this observed depth range.

Although there was only broad alignment to previous classifications, many other biological and environmental data sources were considered to define the previous ecosystem classification and map (Sink et al., 2019b; Sink et al., 2023), which could explain some of the differences detected between the previous classification and this study's findings. However, the authors of previous classifications have noted the limitations of the expert driven approach, specifically calling for more data driven approaches to iteratively improve ecosystem type maps (Sink et al., 2023). In addition, noting the dominance in abundance of *S. dimorphus* detected across the shelf in this study, it's plausible that bioregional patterns of epifauna detected by research trawls may not be that diverse over the western margin. A similar number (six) of epifaunal communities were detected over the western margin using research trawls (Lange & Griffiths, 2014). These could be due to strong environmental drivers, such as depth, % organic carbon, maximum chlorophyll concentration and sediment characteristics, which were important predictors in defining a similar number (five) of seascapes across the middle–outer shelves (40–400 m) over the western margin (Karenyi et al., 2016b). It is therefore likely that the number of epifaunal bioregional patterns defined in this study is a fairly realistic representation of patterns detected by research trawl sampling.

Other similarities to previously observed species abundance patterns were also detected in RCP 2, 3 and 4. Both dominant hermit crabs *S. dimorphus* and *Parapagurus bouvieri* have been found to peak in abundance at different depth ranges over the western margin, between 201–300 m and 401–450 m, respectively (Wright et al., 2020). *S. dimorphus* has also been noted to be more abundant and occupy a wider distribution than *P. bouvieri* (Wright et al., 2020). In this study, both species of hermit crabs peaked in abundance in RCP 3, which occurred between 200–500 m at variable parts across the shelf, encompassing the ideal depth range for both these species. *S. dimorphus* was not only more abundant than *P. bouvieri,* but it was also distributed across shallower bioregions (RCP 2 and 4), while *P. bouvieri* was more abundant than *S. dimorphus* in the deeper bioregion, RCP 1, aligning with previously observed patterns (Wright et al., 2020).

Limitations and recommendations for improving the bioregionalization

This study was limited by the number, type and suitability of available environmental predictors. In South Africa, freely available, comprehensive and validated environmental layers for key abiotic seabed variables are not always at the necessary resolution required for finer scales, and may be interpolated from limited samples or satellite data e.g. Bio-ORACLE

(Assis et al., 2017; Tyberghein et al., 2012) which can lead to spurious results. This study found bottom dissolved oxygen and bottom temperature to be useful predictors for the inner shelf and upper slope bioregions respectively, when informed by research trawl data, though any number of predictors correlated with them may also be responsible for driving distributions of epifauna. Slope was not as applicable for predicting bioregions based on trawl data, given the limited changes in gradient in the study area and that the trawl tended to avoid sampling over steep seafloor. However, slope may be more relevant for other datasets which have been collected over steeper slopes (e.g. dredges in canyons).

Additional and relevant environmental predictors are likely necessary to define boundaries between bioregions at intermediate depths more appropriately (i.e. middle–outer shelves) e.g. substrate type, POC flux or seafloor current. Higher values of total organic carbon (TOC) have been found around Childs Bank (Atkinson et al., 2011a) and may be a potential predictor for epifaunal assemblages on the southern Benguela shelf, since organic carbon and nutrient inputs to the seafloor have been acknowledged as important drivers of benthic communities (Levin et al., 2001; O'Hara et al., 2020; Rex, 1981; Woolley et al., 2016). Current speeds, which affect food availability, have been found to predict fine scale distributions of epifaunal assemblages (Stephenson et al., 2022) and may be particularly relevant across the shelf edge and canyons where currents are intensified (Leathwick et al., 2012; Levin et al., 2001; Rubidge et al., 2016). Trawling pressure or frequency may also be a relevant predictor of benthic epifaunal distributions on the western margin, since trawling has been found to affect epifaunal distributions on the western margin of South Africa (Atkinson et al., 2011a).

The limited number of environmental predictors considered in this study (three) may have resulted in a low number of bioregions (five) being defined. Previous studies using RCPs determined nine bioregions with seven predictors for central western New South Wales, Australia (Lyons et al., 2017), and seven bioregions were defined with three predictors for demersal fish assemblages on the Kerguelen Plateau in the southern Indian Ocean (Hill et al., 2017). While it is expected that a greater number of bioregions would be defined with increasing environmental predictors, without having tested this, it is unclear whether including more predictors would substantially increase the number of bioregions defined using RCP models, since previous studies were conducted over larger areas of approximately 387 000 km^2 (Hill et al., 2017) and 220 000 km^2 (Lyons et al., 2017) in comparison to this study (~118 000 km^2). It is important to note that including more variables will only improve model accuracy and predictions up to a point, whereafter the inclusion of many variables does not provide much improvement and may further complicate the interpretation (Leathwick et al., 2006b).

Variable selection itself is not a straightforward process and is a limitation of data-driven bioregionalization approaches in general (Rowden et al., 2018). Some methods can incorporate variable selection into the modelling process, while others are less sensitive to collinearity between variables. Forward selection of environmental variables may be implemented within the RCP modelling process to simultaneously select the most appropriate number of bioregions and their predictors, based on a measure such as BIC (Hill et al., 2017). Other methods may select environmental variables prior to modelling using multivariate analyses to identify changes in communities along important gradient e.g. DCA or TWINSPAN (Buhl-Mortensen et al., 2015; Buhl-Mortensen et al., 2020). Separate Generalized Additive Models (GAMs) may be fitted to each species prior to modelling to assess which covariates explain the most variation, selecting the predictors relevant for the most species (Hui et al., 2013). Gradient Forest (GF, Ellis et al., 2012) is a machine learning method which incorporates environmental variable selection into the modelling process by identifying how much biological variation is explained by the most important variables (ranking) as well as identifying species compositional turnover along gradients and is less sensitive than regression methods to the inclusion of collinear variables (Pitcher et al., 2012).

This study was a preliminary analysis of only epifauna data from the most recent and validated research surveys and was therefore limited by the quantity of biological datasets considered. While the model was able to capture the over-dispersed nature of the data due to the natural variability exhibited by some species across sites, high uncertainties in estimated abundances for those species were noted. For improved accuracy and certainty of abundance estimates, more samples could be included (thereby decreasing variability) and/or better predictor variables which can explain the distribution of highly variable species could be considered.

It is noted that the threshold used to define rarity of species in this study was somewhat arbitrary. While this is not necessarily a limitation of the study, it is recommended that future studies test a wide range of thresholds for rarity to identify the optimal number of species for modelling, without losing too much information about rarer species, which may be of particular concern for conservation (Ovaskainen & Soininen, 2011). While multi-species models can estimate patterns of rare species more successfully than single-species models (Hui et al., 2013; Leathwick et al., 2006a; Ovaskainen & Soininen, 2011), extremely rare species are generally excluded since they can add noise to the model without offering much additional information for modelling (Foster et al., 2017; Hui et al., 2013). The cut off values used in other studies have also been somewhat arbitrary, considering a species rare if it occurred at fewer than 1–5 % of sites (Foster et al., 2017; Hill et al., 2017; Lyons et al., 2017) or based on the number of parameters, where species with occurrences less than the number of parameters

(or less than a third of the number of parameters) are considered rare (Hui et al., 2013). Rarity is most likely context dependant, and various thresholds should be tested for optimal performance.

Although model diagnostics were performed to check if model performance was reasonable, without validation using an independent dataset (i.e. data not used for modelling), it's impossible to evaluate how well bioregions approximated 'real' assemblages (other than crude comparisons to previously determined classifications and maps). Ironically, one of the motivations for using predictive models in the first place is to enable making the most out of often sparse biological datasets, so validating them against *more* data often requires *more* sampling (Stephenson et al., 2021). Validation with independent data, such as applied in Hill et al. (2017) was beyond the scope of this study, having limited access to additional validated surveys. However, the temporal regularity of which demersal research trawls are conducted on the west (and south) coasts certainly provide a good opportunity for validating models in the future.

Implications for data-driven marine bioregionalization in South Africa in the future

The bioregions defined in this study were clearly associated with specific assemblages and environmental responses. Together with the uncertainty estimates of the classified bioregions, these factors have the potential to provide valuable information for various stakeholders and applications (Rowden et al., 2018; Woolley et al., 2019), such as for marine spatial planning and effective decision making in South Africa (Sink et al., 2023). Since the development of RCP models to assist with bioregionalizations (Foster et al., 2013), they have been modified to include sampling artefacts (Foster et al., 2017) and a spatiotemporal component (Vanhatalo et al., 2021). Due to their relatively recent development and higher computational time required for large datasets, testing RCPs on a wide range of datasets has been limited (Hill et al., 2017), though studies have shown promise when producing bioregionalizations using RCPs (Hill et al., 2017; Hill et al., 2020; Lyons et al., 2017). The ability to directly quantify and assess the uncertainty associated with classified bioregions is more beneficial than two-stage methods which cannot propagate uncertainty throughout the bioregionalization process (Hill et al., 2020; Woolley et al., 2019).

Various other types of uncertainty can be estimated from other predictive methods, however, depending on the intended applications of the maps and need for uncertainty in bioregions, RCP models may be more or less applicable. Uncertainty of sampling coverage and model variability (represented by standard deviation of the mean compositional turnover averaged across each variable) have been estimated from GF models for a bioregionalization of New

Zealand's territorial seas (Stephenson et al., 2022). GF may be more applicable in contexts where flexibility is required, such as when species-environment relationships are not well defined, or when many covariates (which can be highly correlated) need to be assessed. HMSC is a similar method to RCPs, except that it uses a Bayesian approach, so specifying appropriate priors (i.e. prior distributions for model parameters) can be a bit more complicated (Hui et al., 2013). However, HMSC can incorporate information on species traits and phylogenies (Ovaskainen et al., 2017), which may be applicable if functional ecosystem units (e.g. IUCN) are preferred. It should also be noted that while estimating uncertainty in classifications is advantageous, various types of error are produced throughout the entire classification and mapping process which one ought to be mindful of (Strong, 2020). Ultimately, mapped outputs of data-driven classifications will only be as reliable as the input data used for prediction, with the quality and quantity of the biological and environmental datasets impacting predictive performance more than the specific modelling approach used (Bowden et al., 2021).

Conclusion

This study applied a potential approach which could be used for producing data-driven marine bioregionalizations in South Africa in the future, by predicting epifaunal bioregions on the southern Benguela shelf (western margin) of South Africa based on abundance data, using RCP models. Data-driven classification methods attempt to define bioregions which are less reliant on expert opinion and can predict bioregions that are most likely (given the data available) at unsampled locations. As deeper (and further offshore) frontiers are explored and sampling becomes more challenging, it is imperative to rely on data-driven methods to predict expected assemblages in the deep-sea (Jetz et al., 2019). This study applied a simultaneous approach to classification *viz.* Regions of Common Profile which can quantify uncertainty in predictions directly, producing probabilistic maps of bioregions. Since model diagnostics could be performed, assessing how well the predicted classification represented the data was possible. The bioregions of highest prediction certainty, the middle shelf (RCP 5) and shelf edge (RCP 1), also hosted the most distinct communities and were closely aligned with previously derived classifications based on hierarchical clustering. Temperature and oxygen were important predictors for different bioregions across the shelf, though it is recommended that future efforts should source and test a wider range of environmental covariates, such as sediment characteristics, organic carbon, current speeds, or trawling effects, particularly to discern differences in middle–outer shelf assemblages. Ultimately, different methods for classification and prediction are applicable under different contexts and testing a variety of

data-driven methods with different strengths and limitations is advised, validating models with independent datasets wherever possible.

CHAPTER 4: Synthesis

Marine bioregional, ecosystem and habitat classifications and maps are applicable for a wide variety of management applications and ecological studies (Diaz et al., 2004). Data-driven approaches to bioregionalizations can provide benefits and overcome challenges associated with expert-derived classification approaches, making the most out of sparse biological data by relating them to environmental predictors (Rowden et al., 2018; Woolley et al., 2019). However, many different approaches (Ferrier & Guisan, 2006) and statistical techniques (e.g. Hill et al., 2020; Reiss et al., 2014) for classification and prediction exist. Careful consideration should be given to the benefits and limitations of different approaches applied, as well as the biological and environmental data types used to inform bioregionalizations at various spatial scales (spatial extent and resolution). This is the first study to quantify benthic epifaunal abundance patterns on the southern Benguela shelf (western margin) of South Africa comparing between research trawl and towed camera sampling methods and to produce a data-driven bioregionalization using research trawl datasets. This study has contributed knowledge towards informing a data-driven approach to marine bioregionalization for South Africa by quantifying similarities and differences between two epifaunal datasets collected using different sampling methods. The data-driven approach to bioregionalization applied here can inform future bioregionalizations and has revealed insights gained from testing a data-driven approach to bioregionalization (Sink et al., 2023).

Main findings

The main findings of chapter 2 highlighted that the towed camera and research trawl detected largely different subsets of epifaunal assemblages. These differences in species detected could be explained by the sampling method's selectivity on species' size, motility, behaviour and spatial dispersion patterns. While patterns of species richness were similar between sampling methods (though not significantly), patterns of density were not comparable or correlated for all paired sites. Sites located along the shelf edge, where the small brittle star *Ophiura trimeni* was found, and sites located across the sandy outer shelf, where the hermit crab *Sympagurus dimorphus* was found, differed in patterns of density, as neither species was adequately detected by both sampling methods. However, patterns between sites where neither of these dominant species was found, appeared to be more congruent. As a result, this study was not conclusive in determining whether patterns of abundance (density) were congruent between sampling methods across the southern Benguela shelf of South Africa. However, these findings do suggest that congruence is highly contextual, depending on the species or habitat being sampled.

Chapter 3 determined five bioregions for the southern Benguela shelf of South Africa by applying Regions of Common Profile (RCP, Foster et al., 2013; Foster et al., 2017) models. This method shows promise for producing data-driven bioregions, though comparisons with other data-driven methods are advised. Alignment with previously detected bioregional patterns was found, with the best agreement for the inner shelf (RCP 5) and upper slope (RCP 1) bioregions. These bioregions were associated with the highest degree of certainty in spatial predictions, while the bioregions located at intermediate depths (RCPs 2, 3 and 4) were associated with greater spatial prediction uncertainty and differed the most compared to other bioregional patterns. High uncertainties across intermediate bioregions could be explained by: 1) a lack of suitable environmental covariates to predict distributions for a higher diversity of species (shallow and deep) which are expected to have wider gradients of responses to the environment (Hill et al., 2017) or by 2) patterns of epifaunal assemblages (and therefore bioregions) not being as strongly defined across the outer shelf, suggested by the dominance of *S. dimorphus* across the middle and outer shelves. While low oxygen and temperature appeared to sufficiently explain the spatial patterns of RCP 1 and 5, additional environmental variables are likely to greatly improve defining bioregions at intermediate depth ranges. Dispersion parameters were high for some species (and therefore abundance estimates were variable) suggesting a greater number of sites are required to reduce observed variability or more suitable environmental predictors are required to explain their highly variable distributions.

Implications for data-driven bioregionalizations and epifaunal monitoring

Both trawl and towed camera sampling methods were found to detect different subsets of epifaunal assemblages, resulting in the recommendation that both be used simultaneously, where possible, when describing benthic epifaunal patterns (Buhl-Mortensen et al., 2012; Jørgensen et al., 2011; Uzmann et al., 1977; Williams et al., 2015). Since offshore benthic biodiversity patterns in South Africa are not fully understood (Griffiths et al., 2010), with many epifaunal species still being newly discovered (Atkinson & Sink, 2018), utilising multiple sampling methods will lead to a more holistic understanding of the epibenthos than is possible with only one of the sampling methods. However, the type of sampling method used will depend on the aims and applications of the study (Uzmann et al., 1977; Williams et al., 2015). The towed camera was more effective for detecting small species with patchy distributions and Anthozoans which were firmly attached to or within the sediment, while the trawl better detected highly motile Decapoda and cryptic species which cannot be identified from imagery (e.g. burying Asteroidea). Studies focusing on one of these groups or species should consider analysing data obtained from the sampling method which best detects that taxon or taxa.

Towed cameras additionally provide information about species' behaviours e.g. interactions and associations (Cailliet et al., 1999; de Mendonça & Metaxas, 2021), while trawls provide physical specimens necessary for genetic or taxonomic studies and species' life histories (Chimienti et al., 2018; Uzmann et al., 1977; Williams et al., 2015).

Overall, the towed camera detected greater epifaunal densities than the trawl. However, since a small aggregating species, *O. trimeni*, dominated towed camera observations, it is unclear whether the high densities observed were because of this species dominating or whether the towed camera recorded higher densities of all species that were detected by both sampling methods. Since densities were not compared absolutely, due to discrepancies in sampling area between methods (Ellingsen et al., 2007; McIntyre, 1956), densities could be formally investigated in the future using either species accumulation curves (e.g. Williams et al., 2015) or by standardizing sampling effort (area sampled) consistently between methods in the field e.g. shortening trawl tows and increasing camera tows. While increasing the amount of footage to be analysed from towed camera footage is not necessarily feasible due to long processing times (Cailliet et al., 1999; Spencer et al., 2005), it may be feasible if only densities of a single taxa are compared.

The findings from this study were not conclusive on whether patterns in abundance across the assemblages detected were congruent between sampling methods or not, which has implications for marine ecosystem classification and mapping in South Africa. A move towards data-driven bioregionalization approaches has been prioritised for marine classification and mapping in South Africa (Sink et al., 2019b; Sink et al., 2023). Abundance data are more informative for management applications and decision making as they reveal more robust information on species' distributions and relationships with the environment (Stephenson et al., 2021). However, abundance data collected with different sampling efforts cannot easily be combined in analyses or compared directly. Therefore, when informing data-driven bioregionalizations using abundance data, different datasets will likely need to be prioritised or weighted according to which habitat, species, or spatial scales the sampling methods best detect, which has implications for how different datasets are integrated in data-driven approaches (Sink et al., 2023). If significantly similar patterns were observed between sampling methods, their detected patterns could potentially act as surrogates for the other (Mellin et al., 2011; Sink et al., 2023). This could reduce the need for both datasets to inform bioregionalizations, prioritising datasets which are available. However, significantly different patterns detected between sampling methods would imply that the assemblages are not structured the same across scales or habitats, either due to different drivers, interactions or life histories, and datasets would need to be prioritised or integrated accordingly.

Although findings from this study did not definitively detect congruence or non-congruence, similarities and differences were observed. Both sampling methods appeared to detect similar broad patterns between sites, such as depth or ecosystem type. It should be noted that these were the known variables in this study, but any other variable correlated with depth or ecosystem type (e.g. temperature, salinity, substratum) may be more important in driving the similar patterns observed at broad spatial scales. However, at sites where one of the dominant species (*O. trimeni* or *S. dimorphus)* was observed, detected patterns differed the most between sampling methods, since neither sampling method fully detected both species. Previous studies have also found greater similarities at broader spatial scales when comparing different assemblages, attributable to similar environmental drivers identified at broader scales compared to finer ones (Reiss et al., 2010; Silberberger et al., 2019). Due to the different dispersion patterns known for these species, findings seem to suggest that a significant relationship was not detected due to variations in congruency across spatial scales or habitats.

As such, findings may suggest that trawl datasets could be prioritised over towed camera datasets in areas across the outer shelf where *S. dimorphus* was highly abundant, while towed camera datasets could be prioritised across the shelf edge and upper canyons, where *O. trimeni* tended to dominate. However, *Ophiura* aggregations have been observed to be highly variable from one year to the next (Gage & Tyler, 1982), so this species may not represent stable long-term patterns usually required for bioregionalizations. However, due to limited knowledge of offshore epifaunal distributions over time, further comparisons and analyses of epifaunal patterns from these sampling methods over longer temporal periods are strongly advised before conclusions are drawn.

Co-correspondence analysis (Co-CA, ter Braak & Schaffers, 2004) has been shown to be a useful tool for comparing patterns of assemblage structure between sampling methods, especially when methods are challenging to compare due to discrepancies in sampling effort (Brandt, 2022). However, comparing diversity and composition between datasets are advised to accompany Co-CA, to aid determining the direction of correlated patterns, since Co-CA does not indicate if patterns are negatively correlated (Hanson et al., 2015). Another eigenvector-based analysis, Moran's Eigenvector Maps (MEMs, Dray et al., 2006), has been shown to be useful when comparing assemblages across broad, meso and fine spatial scales in the marine environment (Silberberger et al., 2019). Similar to Co-CA, the first MEMs extracted indicate high positive eigenvalues and spatial autocorrelation in broad scale structure. However, further negative eigenvalues can be extracted to reveal spatial structure at finer scales (Silberberger et al., 2019). Such an analysis may be better suited at clarifying congruence when it is suspected that similarities may differ depending on the spatial scale.

These findings have implications for bioregionalizations based on abundance data, however, univariate comparisons of species richness were almost significantly similar in patterns across sites in this study. As such, it is possible that bioregionalizations based purely on species richness may provide similar patterns regardless of which sampling method is used.

Irrespective of the degree of congruence in abundance data collected between sampling methods, trawl surveys cover a much greater extent across the South African shelf both spatially and temporally. Their long-term, systematic sampling design across the west and south coasts on an annual basis makes these datasets ideal for deriving a regional scale bioregionalization using abundance data (e.g. Murillo et al., 2016; Pitcher et al., 2018). Despite the relatively greater invasive nature of trawl sampling (Hiddink et al., 2017; Sink et al., 2012a) and recent global calls to phase this research approach out (Trenkel et al., 2019), in a South African context, sampling with both camera and trawl methods is mostly restricted to sandy shelf ecosystems, having less of an impact on the seafloor compared to hard ground ecosystems (Sink et al., 2012a). While it is noted that trawling in this context is assumed to have a minimal impact, towed cameras are acknowledged as having a lower impact in comparison (Cailliet et al., 1999; Lirman et al., 2007; McCormick & Choat, 1987; McIntyre et al., 2015; Spencer et al., 2005; Williams et al., 2015). However, even towed cameras are too destructive for highly sensitive ecosystems or marine protected areas, which are better sampled by ROVs (e.g. Adams et al., 2020) or AUVs (e.g. Doherty et al., 2018; Ferrari et al., 2018). By applying a data-driven approach to bioregionalization for the southern Benguela shelf (western margin) of South Africa, this study has shown that epifaunal abundance data collected by trawl surveys can provide reasonable estimates of bioregions, finding similarity with previously observed distributions on the western margin (Atkinson et al., 2011b; Karenyi, 2014; Lange & Griffiths, 2014; Roel, 1987; Roeleveld et al., 1992; Shah, 2018; Sink et al., 2012b; Sink et al., 2019b; Smale et al., 1993).

Since this study was intended as a baseline analysis using limited biological and environmental datasets, further investigations into optimal combinations of environmental predictors and species are strongly advised. Low temperatures and low values of dissolved oxygen at the seafloor were shown to be useful at predicting the upper slope and inner shelf bioregions respectively, while bioregions across intermediate depths were not as well defined by the environmental predictors included in this study. Therefore, a wider suite of environmental predictors should be tested which may better explain biological patterns across intermediate depth ranges. Examples of environmental variables which have been found to predict epifaunal patterns include sediment particle size or substratum type (Buhl-Mortensen et al., 2012; Callaway et al., 2002; de Juan et al., 2013; Ganesh & Raman, 2007; Makwela,

2017; Pitcher et al., 2012), sediment organic matter (Ganesh & Raman, 2007), particulate organic carbon (Levin et al., 2001; O'Hara et al., 2020; Woolley et al., 2016), current speeds (Stephenson et al., 2022) and trawling intensity (de Juan et al., 2007; de Juan et al., 2013).

It would also be good practice to compare the outputs from the RCP method with other statistical techniques which can produce bioregionalizations, such as classifying outputs of gradient forest models ('predict, then classify' approach) which have successfully been applied to produce marine bioregionalizations for Australia (Pitcher et al., 2018) and New Zealand (Stephenson et al., 2018; Stephenson et al., 2022). Where towed camera surveys have been conducted on the shelf, data-driven bioregionalizations could be produced based on towed camera data for those locations. This will further serve to compare patterns between sampling methods. If strong differences are found it is likely that sampling methods are detecting patterns at different spatial scales, and towed cameras can therefore be prioritised to inform patterns at finer scales than trawls.

Though seemingly apparent, it is worth noting that the relative importance of various environmental predictors will depend on the number and type of species used as response variables, since epifaunal species respond differently to their environment (Ellingsen et al., 2007). As such, care should be taken to select relevant environmental predictors for the species used. This may be determined from pre-existing literature or by using statistical tools such as generalized additive models (GAMs) for each species (Hill et al., 2017; Hui et al., 2013). Additionally, the number and type of environmental predictors included in models tend to influence the number of bioregions delineated (i.e. the spatial scale of the bioregionalization). Future efforts should take care to consider covariates which are important for driving biological patterns at the relevant scale and are represented by data layers at the appropriate resolution (Rowden et al., 2018). A greater number of environmental variables is likely to delineate bioregions at smaller spatial scales, since more gradients of responses (e.g. RCPs in this study) are identified. Variables which are less varied over fine scales, such as temperature and salinity, tend to be better predictors at broad spatial scales and delineate fewer bioregions, while those which are more variable over fine spatial scales, such as sediment and terrain characteristics, would be better predictors of species at fine spatial scales and delineate a greater number of bioregions (e.g. Buhl-Mortensen et al., 2020). Including relevant environmental variables is also advised from a perspective of reducing values of dispersion which result in highly variable estimates of abundance, as seen in this study. Further investigation into species-environment relationships is therefore recommended to explain the high variability across sites observed for some species.

Bioregionalizations are most beneficial when they can provide information for as many applications as possible. Failing to incorporate measures of uncertainty into mapped outputs is a limitation of expert-derived maps (Woolley et al., 2019) which may have inaccuracies due to limited spatial detail (Jetz et al., 2019). RCP models overcome this challenge by providing maps of spatial uncertainty in predicted bioregions through simultaneous classification and prediction (Foster et al., 2013). Measures of spatial uncertainty are informative for communicating to decision makers and managers and for identifying areas where relationships between biological assemblages and their predictors may not be as well understood, thereby enabling prioritisation of future research needs (Woolley et al., 2019). Whichever approach or statistical method is chosen to derive bioregionalizations, it is clear that measures of uncertainty should be incorporated. This study found greater uncertainty attributed to intermediate depths, highlighting that further investigation into species-environment relationships should be prioritised in these areas.

Limitations

This study was mostly limited by a lack of data available to quantify patterns between sampling methods and determine bioregions. Towed camera and trawl sampling methods have not intentionally been deployed at the same location, resulting in a limited number of trawl and towed camera sites which were deemed suitably comparable. Although sites compared were relatively close in location and sampled at similar depths and within the same classified ecosystem type, it is possible that some of the sites compared were not truly from the same assemblage of species. This could have resulted in patterns which appeared more different than they truly are. Furthermore, the small sample size (18 sites) may have been insufficient to detect congruence, if patterns were indeed significantly similar.

A lack of suitable environmental data layers limited the number of bioregions which were adequately defined. Freely available and comprehensive benthic data layers at appropriate resolutions are limited in South Africa (Sink et al., 2023). Therefore, only environmental variables collected *in-situ* during trawl surveys, and a variable easily derived from bathymetry, were considered. Since only three of these variables were not highly collinear, they were all included for modelling. However, ideally covariate selection should be supported by data, using only the covariates which best explain patterns in biological assemblages. While variable selection is not always straightforward and can be a downside to data-driven bioregionalizations (Rowden et al., 2018), various approaches can be utilised. These may include exploring species-environment relationships prior to modelling with e.g. GAMs (Hill et al., 2017; Hui et al., 2013), incorporating a forward selection routine (e.g. Hill et al., 2017) or

using a modelling method which is more robust to highly collinear variables (e.g. gradient forests, Pitcher et al., 2012). Model validation was similarly not able to be performed due to the unavailability of additional verified trawl datasets, which is acknowledged as a limitation to being able to fully assess model performance.

Conclusion

This pilot study on the western margin of South Africa produced the first data-driven bioregionalization using trawl collected epifaunal abundance. Data-driven bioregionalizations, particularly when informed by abundance data, provide valuable information for management and decision-making and are able to include quantified uncertainty measures. Expert-derived approaches, using only occurrence records, are limited by their inability to assess uncertainty (Woolley et al., 2019). Though it is acknowledged that inputs derived from experts are invaluable, and data-driven maps should ideally still be verified with expert opinion and validated against independent datasets (Bowden et al., 2021; Limongi et al., 2023), this study highlights the feasibility of using quantitative data from trawl surveys to produce data-driven bioregionalizations in South Africa.

An initial investigation into the congruence of epifaunal abundance patterns collected using trawl and towed camera sampling methods established a baseline for further comparisons. Comparisons can be necessary in order to optimize methods of sampling for effective management and quantifying differences in patterns between methods of sampling should be prioritized before important management decisions are made (Przeslawski et al., 2018). Ultimately, the quality and quantity of data available and used affect the outcome of any analyses and the detection of patterns (Bowden et al., 2021; Strong, 2020). Careful consideration should always be taken when selecting a method to collect or analyse data, depending on the aims of the study (Uzmann et al., 1977; Williams et al., 2015). While general advantages and limitations of using different methods may be expected, the ecological congruence of patterns detected between sampling methods appears to be dependent on the species or habitat being sampled (Flannery & Przeslawski, 2015; Mellin et al., 2011). This study suggests both trawl and towed camera sampling methods offer valid information about epifaunal patterns when informing data-driven bioregionalizations in South Africa.

The knowledge gleaned from this study has provided an initial quantitative exploration on the use of epifaunal abundance data for informing data-driven marine bioregionalizations in South Africa. This study provides a useful foundation on which to build upon and conduct further research into data-driven marine bioregionalization and ecosystem classification in South Africa.

References

Abelló, P. & Macpherson, E. 1990. Influence of environmental conditions on the distribution of Pterygosquilla armata capensis (Crustacea: Stomatopoda) off Namibia. *South African Journal of Marine Science.* 9(1):169-175. DOI:10.2989/025776190784378934.

Adams, L.A., Maneveldt, G.W., Green, A., Karenyi, N., Parker, D., Samaai, T. & Kerwath, S. 2020. Rhodolith Bed Discovered off the South African Coast. *Diversity.* 12(4):1-125. Available: https://www.mdpi.com/1424-2818/12/4/125.

Adams, R. 2017. Optimal sampling and spatiotemporal change in epibenthos at a sub-Antarctic Marine Protected Area. Master of Science. Stellenbosch University. 1-103.

Aitchison, J. 1982. The Statistical Analysis of Compositional Data. *Journal of the Royal Statistical Society. Series B (Methodological).* 44(2):139-177. Available: http://www.jstor.org.ezproxy.uct.ac.za/stable/2345821.

Alric, B., ter Braak, C.J.F., Desdevises, Y., Lebredonchel, H. & Dray, S. 2020. Investigating microbial associations from sequencing survey data with co-correspondence analysis. *Molecular ecology resources.* 20(2):468-480. DOI:https://doi.org/10.1111/1755-0998.13126.

Assis, J., Tyberghein, L., Bosh, S., Verbruggen, H., Serrão, E.A. & De Clerck, O. 2017. Bio-ORACLE v2.0: Extending marine data layers for bioclimatic modelling. *Global Ecology and Biogeography.* 27:277-284.

Atkinson, L., Attwood, C., Karenyi, N., Sink, K., von der Meden, C. & van der Heever, G. 2022. *A Benthic Trawl Experiment: Measuring faunal change in a southern Benguela slope after cessation of trawling.* Presentation at the 14th Southern African Marine Science Symposium, 21-24 June 2022, Durban.

Atkinson, L.J. & Sink, K.J. 2008. *User profiles for the South African offshore environment*. SANBI biodiversity series 10. South African National Biodiversity Institute. Pretoria. 1-66.

Atkinson, L.J. 2009. Effects of demersal trawling on marine infaunal, epifaunal and fish assemblages: studies in the southern Benguela and Oslofjord. PhD. University of Cape Town. 1-141.

Atkinson, L.J., Field, J.G. & Hutchings, L. 2011a. Effects of demersal trawling along the west coast of southern Africa: multivariate analysis of benthic assemblages. *Marine Ecology Progress Series.* 430:241-256. Available: http://www.jstor.org.ezproxy.uct.ac.za/stable/24874514.

Atkinson, L.J., Leslie, R.W., Field, J.G. & Jarre, A. 2011b. Changes in demersal fish assemblages on the west coast of South Africa, 1986–2009. *African Journal of Marine Science.* 33(1):157-170. Available: https://doi.org/10.2989/1814232X.2011.572378.

Atkinson, L.J. & Sink, K.J. 2018. *Field Guide to the Offshore Marine Invertebrates of South Africa.* Pretoria: Malachite Marketing and Media. 10.15493/SAEON.PUB.10000001.

Austin, M.P. 1998. An Ecological Perspective on Biodiversity Investigations: Examples from Australian Eucalypt Forests. *Annals of the Missouri Botanical Garden.* 85(1):2-17. DOI:10.2307/2991991.

Austin, M.P. 2002. Spatial prediction of species distribution: an interface between ecological theory and statistical modelling. *Ecological Modelling.* 157(2):101-118. DOI:https://doi.org/10.1016/S0304-3800(02)00205-3.

Awad, A.A., Griffiths, C.L. & Turpie, J.K. 2002. Distribution of South African marine benthic invertebrates applied to the selection of priority conservation areas. *Diversity and Distributions.* 8(3):129-145. DOI:https://doi.org/10.1046/j.1472-4642.2002.00132.x.

Badenhorst, A. & Smale, M.J. 1991. The distribution and abundance of seven commercial trawlfish from the Cape south coast of South Africa, 1986–1990. *South African Journal of Marine Science.* 11(1):377-393. DOI:10.2989/025776191784287565.

Basford, D., Eleftheriou, A. & Raffaelli, D. 1990. The infauna and epifauna of the northern North Sea. *Netherlands Journal of Sea Research.* 25(1):165-173. DOI:https://doi.org/10.1016/0077-7579(90)90017-B.

Bouchet, P.J., Meeuwig, J.J., Salgado Kent, C.P., Letessier, T.B. & Jenner, C.K. 2015. Topographic determinants of mobile vertebrate predator hotspots: current knowledge and future directions. *Biological Reviews.* 90(3):699-728. DOI:https://doi.org/10.1111/brv.12130.

Bowden, D.A. 2011. *Benthic invertebrate samples and data from the Ocean Survey 20/20 voyages to the Chatham Rise and Challenger Plateau, 2007*. Ministry of Fisheries. Wellington. 1-46.

Bowden, D.A., Anderson, O.F., Rowden, A.A., Stephenson, F. & Clark, M.R. 2021. Assessing Habitat Suitability Models for the Deep Sea: Is Our Ability to Predict the Distributions of Seafloor Fauna Improving? *Frontiers in Marine Science.* 8:632389. DOI:10.3389/fmars.2021.632389.

Brandt, S. 2022. The influence of sampling method on detecting benthic biodiversity patterns at the ecoregion scale on the South African west coast. Master of Science. University of Cape Town. 1-85.

Breiman, L. 2001. Random Forests. *Machine Learning.* 45(1):5-32. DOI:10.1023/A:1010933404324.

Brown, C.J., Smith, S.J., Lawton, P. & Anderson, J.T. 2011. Benthic habitat mapping: A review of progress towards improved understanding of the spatial ecology of the seafloor using acoustic techniques. *Estuarine, Coastal and Shelf Science.* 92(3):502-520. DOI:https://doi.org/10.1016/j.ecss.2011.02.007.

Buhl-Mortensen, L., Vanreusel, A., Gooday, A.J., Levin, L.A., Priede, I.G., Buhl-Mortensen, P., Gheerardyn, H., King, N.J. & Raes, M. 2010. Biological structures as a source of habitat heterogeneity and biodiversity on the deep ocean margins. *Marine Ecology.* 31(1):21-50. DOI:https://doi.org/10.1111/j.1439-0485.2010.00359.x.

Buhl-Mortensen, L., Buhl-Mortensen, P., Dolan, M.F.J., Dannheim, J., Bellec, V. & Holte, B. 2012. Habitat complexity and bottom fauna composition at different scales on the continental shelf and slope of northern Norway. *Hydrobiologia.* 685(1):191-219. DOI:10.1007/s10750-011-0988-6.

Buhl-Mortensen, L., Buhl-Mortensen, P., Dolan, M.F.J. & Holte, B. 2015. The MAREANO programme – A full coverage mapping of the Norwegian off-shore benthic environment and fauna. *Marine Biology Research.* 11(1):4-17. DOI:10.1080/17451000.2014.952312.

Buhl-Mortensen, P., Dolan, M.F.J., Ross, R.E., Gonzalez-Mirelis, G., Buhl-Mortensen, L., Bjarnadóttir, L.R. & Albretsen, J. 2020. Classification and Mapping of Benthic Biotopes in Arctic and Sub-Arctic Norwegian Waters. *Frontiers in Marine Science.* 7:271. DOI:10.3389/fmars.2020.00271.

Bustamante, R.H., Branch, G.M., Eekhout, S., Robertson, B., Zoutendyk, P., Schleyer, M., Dye, A., Hanekom, N., Keats, D., Jurd, M. & McQuaid, C. 1995. Gradients of intertidal primary productivity around the coast of South Africa and their relationships with consumer biomass. *Oecologia.* 102(2):189-201. DOI:10.1007/BF00333251.

Cailliet, G.M., Andrews, A.H., Wakefield, W.W., Moreno, G. & Rhodes, K.L. 1999. Fish faunal and habitat analyses using trawls, camera sleds and submersibles in benthic deep-sea habitats off central California. *Oceanologica Acta.* 22(6):579-592. DOI:https://doi.org/10.1016/S0399-1784(00)88949-5.

Callaway, R., Alsvåg, J., de Boois, I., Cotter, J., Ford, A., Hinz, H., Jennings, S., Kröncke, I., Lancaster, J., Piet, G., Prince, P. & Ehrich, S. 2002. Diversity and community structure of epibenthic invertebrates and fish in the North Sea. *ICES Journal of Marine Science.* 59(6):1199-1214. DOI:10.1006/jmsc.2002.1288.

Cartes, J.E., Rodríguez-Ribas, R., Papiol, V., Valeiras, X., Punzo´n, A., Blanco, M. & Serrano, A. 2021. Biological condition and population structure of benthopelagic shrimps in the Galicia Bank (NE Atlantic): Intra- and interspecific patterns. *Deep-Sea Research Part I.* 168:103434.

Chimienti, G., Angeletti, L., Rizzo, L., Tursi, A. & Mastrototaro, F. 2018. ROV vs trawling approaches in the study of benthic communities: the case of Pennatula rubra (Cnidaria: Pennatulacea). *Journal of the Marine Biological Association of the United Kingdom.* 98(8):1859-1869. DOI:10.1017/S0025315418000851.

Clark, M. & Rowden, A. 2004. BioRoss 2004: expanding our knowledge of marine life in the Ross Sea. *Water & Atmosphere.* 12(3):24-25.

Clark, M.R., Watling, L., Rowden, A.A., Guinotte, J.M. & Smith, C.R. 2011. A global seamount classification to aid the scientific design of marine protected area networks. *Ocean & Coastal Management.* 54(1):19-36. DOI:https://doi.org/10.1016/j.ocecoaman.2010.10.006.

Clark, M.R. & Stewart, R. 2016. The NIWA seamount sled: An effective epibenthic sledge for sampling epifauna on seamounts and rough seafloor. *Deep Sea Research Part I: Oceanographic Research Papers.* 108:32-38. DOI:https://doi.org/10.1016/j.dsr.2015.12.005.

Clarke, K., Gorley, R., Somerfield, P. & Warwick, R. 2014. *Change in marine communities: an approach to statistical analysis and interpretation, 3rd edn.* Plymouth: Primer-E Ltd. Available: http://plymsea.ac.uk/id/eprint/7656/.

Clarke, K.R. & Gorley, R.N. 2015. PRIMER v7: User Manual/Tutorial. Plymouth: PRIMER-E.

Collie, J.S., Escanero, G.A. & Valentine, P.C. 2000. Photographic evaluation of the impacts of bottom fishing on benthic epifauna. *ICES Journal of Marine Science.* 57(4):987-1001. DOI:10.1006/jmsc.2000.0584.

Colquhoun, J., Heyward, A., Rees, M., Twiggs, E., Fitzpatrick, B., McAllister, F. & Speare, P. 2007. Ningaloo Reef Marine Park benthic biodiversity survey. *Western Australian Marine Science Institution, Perth, Western Australia.*1-144.

Connor, D.W., Allen, J.H., Golding, N., Howell, K.L., Lieberknecht, L.M., Northern, K.O. & Reker, J.B. 2004. *The Marine Habitat Classification for Britain and Ireland Version 04.05*. Peterborough: JNCC. 1-49. Available: www.jncc.gov.uk/MarineHabitatClassification.

Cook, R.D. 1979. Influential Observations in Linear Regression. *Journal of the American Statistical Association.* 74(365):169-174. DOI:10.2307/2286747.

Cooper, L.W., Guarinello, M.L., Grebmeier, J.M., Bayard, A., Lovvorn, J.R., North, C.A. & Kolts, J.M. 2019. A video seafloor survey of epibenthic communities in the Pacific Arctic including Distributed Biological Observatory stations in the northern Bering and Chukchi seas. *Deep Sea Research Part II: Topical Studies in Oceanography.* 162:164-179. DOI:https://doi.org/10.1016/j.dsr2.2019.05.003.

Costello, M.J. 2009. Distinguishing marine habitat classification concepts for ecological data management. *Marine Ecology Progress Series.* 397:253-268. Available: http://www.jstor.org.ezproxy.uct.ac.za/stable/24874305.

Costello, M.J., Basher, Z., McLeod, L., Asaad, I., Claus, S., Vandepitte, L., Yasuhara, M., Gislason, H., Edwards, M., Appeltans, W., Enevoldsen, H., Edgar, G.J., Miloslavich, P., De Monte, S., Sousa Pinto, I., Obura, D. & Bates, A.E. 2017. Methods for the Study of Marine Biodiversity. In *The GEO Handbook on Biodiversity Observation Networks.* M. Walters and R.J. Scholes, Eds. 129-163. DOI:10.1007/978-3-319-27288-7_6.

Davies, A.J., Duineveld, G.C.A., Lavaleye, M.S.S., Bergman, M.J.N., van Haren, H. & Roberts, J.M. 2009. Downwelling and deep-water bottom currents as food supply mechanisms to the cold-water coral Lophelia pertusa (Scleractinia) at the Mingulay Reef Complex. *Limnology and Oceanography.* 54(2):620-629. DOI:https://doi.org/10.4319/lo.2009.54.2.0620.

Davies, C.E., Moss, D. & Hill, M.O. 2004. *EUNIS Habitat Classification Revised 2004*. Report to the European Topic Centre on Nature Protection and Biodiversity, European Environment Agency. 1-307.

Davies, J.S., Guillaumont, B., Tempera, F., Vertino, A., Beuck, L., Ólafsdóttir, S.H., Smith, C.J., Fosså, J.H., van den Beld, I.M.J., Savini, A., Rengstorf, A., Bayle, C., Bourillet, J.F., Arnaud-Haond, S. & Grehan, A. 2017. A new classification scheme of European cold-water coral habitats: Implications for ecosystem-based management of the deep sea. *Deep Sea Research Part II: Topical Studies in Oceanography.* 145:102-109. DOI:https://doi.org/10.1016/j.dsr2.2017.04.014.

de Juan, S., Thrush, S.F. & Demestre, M. 2007. Functional changes as indicators of trawling disturbance on a benthic community located in a fishing ground (NW Mediterranean Sea). *Marine Ecology Progress Series.* 334:117-129. Available: http://www.jstor.org.ezproxy.uct.ac.za/stable/24870922.

de Juan, S., Lo Iacono, C. & Demestre, M. 2013. Benthic habitat characterisation of soft-bottom continental shelves: Integration of acoustic surveys, benthic samples and trawling disturbance intensity. *Estuarine, Coastal and Shelf Science.* 117:199-209. DOI:https://doi.org/10.1016/j.ecss.2012.11.012.

de Mendonça, S.N. & Metaxas, A. 2021. Comparing the Performance of a Remotely Operated Vehicle, a Drop Camera, and a Trawl in Capturing Deep-Sea Epifaunal Abundance and Diversity. *Frontiers in Marine Science.* 8:631354. DOI:10.3389/fmars.2021.631354.

de Wet, W.M. & Compton, J.S. 2021. Bathymetry of the South African continental shelf. *Geo-Marine Letters.* 41(3):1-40. DOI:10.1007/s00367-021-00701-y.

DEFF (Department of Environment Forestry and Fisheries). 2020. *Status of the South African marine fishery resources 2020*. DEFF. Cape Town. 1-112.

Diaz, R.J., Solan, M. & Valente, R.M. 2004. A review of approaches for classifying benthic habitats and evaluating habitat quality. *Journal of Environmental Management.* 73(3):165-181. DOI:https://doi.org/10.1016/j.jenvman.2004.06.004.

Dingle, R.V. & Nelson, G. 1993. Sea-bottom temperature, salinity and dissolved oxygen on the continental margin off south-western Africa. *South African Journal of Marine Science.* 13(1):33-49. DOI:10.2989/025776193784287220.

Doherty, B., Johnson, S.D.N. & Cox, S.P. 2018. Using autonomous video to estimate the bottom-contact area of longline trap gear and presence-absence of sensitive benthic habitat. *Canadian Journal of Fisheries & Aquatic Sciences.* 75(5):797-812. DOI:10.1139/cjfas-2016-0483.

Dray, S., Legendre, P. & Peres-Neto, P.R. 2006. Spatial modelling: a comprehensive framework for principal coordinate analysis of neighbour matrices (PCNM). *Ecological Modelling.* 196(3):483-493. DOI:https://doi.org/10.1016/j.ecolmodel.2006.02.015.

Dunn, P.K. & Smyth, G.K. 1996. Randomized Quantile Residuals. *Journal of Computational and Graphical Statistics.* 5(3):236-244. DOI:10.2307/1390802.

Dunstan, P.K., Foster, S.D. & Darnell, R. 2011. Model based grouping of species across environmental gradients. *Ecological Modelling.* 222(4):955-963. DOI:https://doi.org/10.1016/j.ecolmodel.2010.11.030.

Dunstan, P.K., Foster, S.D., Hui, F.K.C. & Warton, D.I. 2013. Finite Mixture of Regression Modeling for High-Dimensional Count and Biomass Data in Ecology. *Journal of Agricultural, Biological, and Environmental Statistics.* 18(3):357-375. Available: http://www.jstor.org.ezproxy.uct.ac.za/stable/26452946.

Durden, J.M., Bett, B.J., Jones, D.O.B., Huvenne, V.A.I. & Ruhl, H.A. 2015. Abyssal hills – hidden source of increased habitat heterogeneity, benthic megafaunal biomass and diversity in the deep sea. *Progress in Oceanography.* 137:209-218. DOI:https://doi.org/10.1016/j.pocean.2015.06.006.

Durden, J.M., Schoening, T., Althaus, F., Friedman, A., García Campos, R., Glover, A.G., Greinert, J., Stout, N.J., Jones, D.O., Jordt, A., Kaeli, J.W., Köser, K., Kuhnz, L.A., Lindsay, D., Morris, K.J., Nattkemper, T.W., Osterloff, J., Ruhl, H.A., Singh, H., Tran, M. & Bett, B.J. 2016a. Perspectives in Visual Imaging for Marine Biology and Ecology: from Acquisition to Understanding. In *Oceanography and Marine Biology: An Annual Review.* R. Hughes, D. Hughes, I. Smith and A. Dale, Eds. Boca Raton: CRC Press. 1-72.

Durden, J.M., Bett, B.J., Schoening, T., Morris, K.J., Nattkemper, T.W. & Ruhl, H.A. 2016b. Comparison of image annotation data generated by multiple investigators for benthic ecology.

Marine Ecology Progress Series. 552:61-70. Available: https://www.int-res.com/abstracts/meps/v552/p61-70/.

Eastwood, P.D., Souissi, S., Rogers, S.I., Coggan, R.A. & Brown, C.J. 2006. Mapping seabed assemblages using comparative top-down and bottom-up classification approaches. *Canadian Journal of Fisheries and Aquatic Sciences.* 63:1536-1548. Available: https://link-gale-com.ezproxy.uct.ac.za/apps/doc/A149662107/AONE?u=unict&sid=bookmark-AONE&xid=996c213a.

Elith, J., Leathwick, J.R. & Hastie, T. 2008. A Working Guide to Boosted Regression Trees. *Journal of Animal Ecology.* 77(4):802-813. Available: http://www.jstor.org.ezproxy.uct.ac.za/stable/20143253.

Ellingsen, K.E., Brandt, A., Ebbe, B. & Linse, K. 2007. Diversity and species distribution of polychaetes, isopods and bivalves in the Atlantic sector of the deep Southern Ocean. *Polar Biology.* 30(10):1265-1273. DOI:10.1007/s00300-007-0287-x.

Ellis, N., Smith, S.J. & Pitcher, C.R. 2012. Gradient forests: calculating importance gradients on physical predictors. *Ecology.* 93(1):156-168. Available: http://www.jstor.org.ezproxy.uct.ac.za/stable/23144030.

Emanuel, B.P., Bustamante, R.H., Branch, G.M., Eekhout, S. & Odendaal, F.J. 1992. A zoogeographic and functional approach to the selection of marine reserves on the west coast of South Africa. *South African Journal of Marine Science.* 12(1):341-354. DOI:10.2989/02577619209504710.

Emery, K.O., Bremner, J.M. & Rogers, J. 1992. Hypsometry of divergent and translational continental margins of southern Africa. *Marine Geology.* 106(1):89-105. DOI:https://doi.org/10.1016/0025-3227(92)90056-N.

Ferrari, R., Marzinelli, E.M., Ayroza, C.R., Jordan, A., Figueira, W.F., Byrne, M., Malcolm, H.A., Williams, S.B. & Steinberg, P.D. 2018. Large-scale assessment of benthic communities across multiple marine protected areas using an autonomous underwater vehicle. *PloS one.* 13(3):e0193711. DOI:10.1371/journal.pone.0193711.

Ferrier, S. & Guisan, A. 2006. Spatial modelling of biodiversity at the community level. *Journal of Applied Ecology.* 43(3):393-404. DOI:https://doi.org/10.1111/j.1365-2664.2006.01149.x.

FGDC (Federal Geographic Data Committee). 2012. *Coastal and Marine Ecological Classification Standard (FGDC-STD-018-2012)*. Federal Geographic Data Committee. USA. 1-342.

Field, J.G., Clarke, K.R. & Warwick, R.M. 1982. A Practical Strategy for Analysing Multispecies Distribution Patterns. *Marine Ecology Progress Series.* 8(1):37-52. Available: http://www.jstor.org.ezproxy.uct.ac.za/stable/24814621.

Filander, Z., Smith, A.N.H., Cawthra, H.C. & Lamont, T. 2022a. Benthic species patterns in and around the Cape Canyon: A large submarine canyon off the western passive margin of South Africa. *Frontiers in Marine Science.* 9:1025113. DOI:10.3389/fmars.2022.1025113.

Filander, Z., Atkinson, L., Wozniak, D. & Snyders, L. 2022b. *Processed imagery data collected off the western margin's deep-sea environment on Algoa Voyage 246, February 2018.*

Department of Forestry, Fisheries and the Environment. Available:https://repository.saeon.ac.za/index.php/s/PzfgExZEQ3ysGKK.

Flannery, E. & Przeslawski, R. 2015. *Comparison of sampling methods to assess benthic marine biodiversity. Are spatial and ecological relationships consistent among sampling gear?* Canberra: G. Australia. 1-65. Available: http://hdl.handle.net/11329/963.

Foster, S.D., Givens, G.H., Dornan, G.J., Dunstan, P.K. & Darnell, R. 2013. Modelling biological regions from multi-species and environmental data. *Environmetrics.* 24(7):489-499. DOI:https://doi.org/10.1002/env.2245.

Foster, S.D., Hill, N.A. & Lyons, M. 2017. Ecological grouping of survey sites when sampling artefacts are present. *Journal of the Royal Statistical Society: Series C (Applied Statistics).* 66(5):1031-1047. DOI:https://doi.org/10.1111/rssc.12211.

Fujita, T. & Ohta, S. 1989. Spatial structure within a dense bed of the brittle starOphiura sarsi (Ophiuroidea: Echinodermata) in the bathyal zone off otsuchi, Northeastern Japan. *Journal of Oceanography.* 45(5):289-300. DOI:10.1007/BF02123483.

Gage, J.D. & Tyler, P.A. 1982. Depth-related gradients in size structure and the bathymetric zonation of deep-sea brittle stars. *Marine Biology.* 71(3):299-308. DOI:10.1007/BF00397046.

Ganesh, T. & Raman, A. 2007. Macrobenthic community structure of the northeast Indian shelf, Bay of Bengal. *Marine Ecology Progress Series.* 341:59-73. Available: https://www.int-res.com/abstracts/meps/v341/p59-73/.

Gibbons, M.J., Macpherson, E. & Barange, M. 1994. Some observations on the pelagic decapod Pasiphaea semispinosa Holthuis 1951 in the Benguela upwelling system. *South African Journal of Marine Science.* 14(1):59-67. DOI:10.2989/025776194784287157.

Gioria, M., Bacaro, G. & Feehan, J. 2011. Evaluating and interpreting cross-taxon congruence: Potential pitfalls and solutions. *Acta Oecologica.* 37(3):187-194. DOI:https://doi.org/10.1016/j.actao.2011.02.001.

González-Irusta, J.M., González-Porto, M., Sarralde, R., Arrese, B., Almón, B. & Martín-Sosa, P. 2015. Comparing species distribution models: a case study of four deep sea urchin species. *Hydrobiologia.* 745(1):43-57. DOI:10.1007/s10750-014-2090-3.

Greene, H.G., Yoklavich, M.M., Starr, R.M., O'Connell, V.M., Wakefield, W.W., Sullivan, D.E., McRea, J.E. & Cailliet, G.M. 1999. A classification scheme for deep seafloor habitats. *Oceanologica Acta.* 22(6):663-678. DOI:https://doi.org/10.1016/S0399-1784(00)88957-4.

Gregr, E.J., Ahrens, A.L. & Perry, R.I. 2012. Reconciling classifications of ecologically and biologically significant areas in the world's oceans. *Marine Policy.* 36(3):716-726. DOI:https://doi.org/10.1016/j.marpol.2011.10.009.

Griffiths, C.L. & Blaine, M.J. 1988. Distribution, population structure and biology of stomatopod Crustacea off the west coast of South Africa. *South African Journal of Marine Science.* 7(1):45-50. DOI:10.2989/025776188784379008.

Griffiths, C.L., Robinson, T.B., Lange, L. & Mead, A. 2010. Marine Biodiversity in South Africa: An Evaluation of Current States of Knowledge. *PloS one.* 5(8):e12008. DOI:10.1371/journal.pone.0012008.

Guisan, A. & Zimmermann, N.E. 2000. Predictive habitat distribution models in ecology. *Ecological Modelling.* 135(2):147-186. DOI:https://doi.org/10.1016/S0304-3800(00)00354-9.

Haley, C., von der Meden, C., Atkinson, L. & Reed, C. 2017. Habitat associations and distribution of the hyperbenthic shrimp, Nauticaris marionis, around the sub-Antarctic Prince Edward Islands. *Deep Sea Research Part I: Oceanographic Research Papers.* 127:41-48. DOI:https://doi.org/10.1016/j.dsr.2017.07.005.

Hanson, M.A., Buelt, C.A., Zimmer, K.D., Herwig, B.R., Bowe, S. & Maurer, K. 2015. Co-correspondence among aquatic invertebrates, fish, and submerged aquatic plants in shallow lakes. *Freshwater Science.* 34(3):953-964. DOI:10.1086/682118.

Harris, L.R., Holness, S.D., Finke, G., Amunyela, M., Braby, R., Coelho, N., Gee, K., Kirkman, S.P., Kreiner, A., Mausolf, E., Majiedt, P., Maletzky, E., Nsingi, K.K., Russo, V., Sink, K.J. & Sorgenfrei, R. 2022a. Practical Marine Spatial Management of Ecologically or Biologically Significant Marine Areas: Emerging Lessons From Evidence-Based Planning and Implementation in a Developing-World Context. *Frontiers in Marine Science.* 9:831678. DOI:10.3389/fmars.2022.831678.

Harris, L.R., Holness, S.D., Kirkman, S.P., Sink, K.J., Majiedt, P. & Driver, A. 2022b. A robust, systematic approach for developing the biodiversity sector's input for multi-sector Marine Spatial Planning. *Ocean & Coastal Management.* 230:106368. DOI:https://doi.org/10.1016/j.ocecoaman.2022.106368.

Harris, P.T. 2020. Chapter 4: Biogeography, benthic ecology and habitat classification schemes. In *Seafloor Geomorphology as Benthic Habitat (Second Edition).* P.T. Harris and E.K. Baker, Eds.: Elsevier. 63-96. DOI:https://doi.org/10.1016/B978-0-12-814960-7.00004-X.

Hiddink, J.G., Jennings, S., Sciberras, M., Szostek, C.L., Hughes, K.M., Ellis, N., Rijnsdorp, A.D., McConnaughey, R.A., Mazor, T., Hilborn, R., Collie, J.S., Pitcher, C.R., Amoroso, R.O., Parma, A.M., Suuronen, P. & Kaiser, M.J. 2017. Global analysis of depletion and recovery of seabed biota after bottom trawling disturbance. *Proc Natl Acad Sci U S A.* 114(31):8301-8306. DOI:10.1073/pnas.1618858114.

Hijmans, R.J., van Etten, J., Sumner, M., Cheng, J., Baston, D., Bevan, A., Bivand, R., Busetto, L., Canty, M., Fasoli, B., Forrest, D., Ghosh, A., Golicher, D., Gray, J., Greenberg, J.A., Hiemstra, P., Hingee, K., Ilich, A., Institute for Mathematics Applied Geosciences, Karney, C., Mattiuzzi, M., Mosher, S., Naimi, B., Nowosad, J., Pebesma, E., Lamigueiro, O.P., Racine, E.B., Rowlingson, B., Shortridge, A., Venables, B. & Wueest, R. 2022. *Geographic Data Analysis and Modeling, R 'raster' package.* Version 3.6-3. Available:https://CRAN.R-project.org/package=raster.

Hill, M.O. 1979. *TWINSPAN: A FORTRAN program for arranging multivariate data in an ordered two-way table by classification of the individuals and attributes.* Ithaca, New York: Cornell University, Section of Ecology and Systematics.

Hill, M.O. & Gauch, H.G. 1980. Detrended Correspondence Analysis: An Improved Ordination Technique. *Vegetatio.* 42(1/3):47-58. Available: http://www.jstor.org/stable/20145789.

Hill, N.A., Foster, S.D., Duhamel, G., Welsford, D., Koubbi, P. & Johnson, C.R. 2017. Model-based mapping of assemblages for ecology and conservation management: A case study of demersal fish on the Kerguelen Plateau. *Diversity and Distributions.* 23(9/10):1216-1230. Available: http://www.jstor.org.ezproxy.uct.ac.za/stable/44896925.

Hill, N.A., Woolley, S.N.C., Foster, S.D., Dunstan, P.K., McKinlay, J., Ovaskainen, O. & Johnson, C.R. 2020. Determining marine bioregions: A comparison of quantitative approaches. *Methods in Ecology and Evolution.* 11(10):1258-1272. DOI:https://doi.org/10.1111/2041-210X.13447.

Howell, K.L. 2010. A benthic classification system to aid in the implementation of marine protected area networks in the deep/high seas of the NE Atlantic. *Biological Conservation.* 143(5):1041-1056. DOI:https://doi.org/10.1016/j.biocon.2010.02.001.

Howell, K.L., Davies, J.S., Allcock, A.L., Braga-Henriques, A., Buhl-Mortensen, P., Carreiro-Silva, M., Dominguez-Carrió, C., Durden, J.M., Foster, N.L., Game, C.A., Hitchin, B., Horton, T., Hosking, B., Jones, D.O.B., Mah, C., Laguionie Marchais, C., Menot, L., Morato, T., Pearman, T.R.R., Piechaud, N., Ross, R.E., Ruhl, H.A., Saeedi, H., Stefanoudis, P.V., Taranto, G.H., Thompson, M.B., Taylor, J.R., Tyler, P., Vad, J., Victorero, L., Vieira, R.P., Woodall, L.C., Xavier, J.R. & Wagner, D. 2019. A framework for the development of a global standardised marine taxon reference image database (SMarTaR-ID) to support image-based analyses. *PloS one.* 14(12):e0218904. DOI:10.1371/journal.pone.0218904.

Hui, F.K.C., Warton, D.I., Foster, S.D. & Dunstan, P.K. 2013. To mix or not to mix: comparing the predictive performance of mixture models vs. separate species distribution models. *Ecology.* 94(9):1913-1919. Available: http://www.jstor.org.ezproxy.uct.ac.za/stable/23597313.

Jacobs, R.A., Jordan, M.I., Nowlan, S.J. & Hinton, G.E. 1991. Adaptive Mixtures of Local Experts. *Neural Computation.* 3(1):79-87. DOI:10.1162/neco.1991.3.1.79.

Jamieson, A.J., Boorman, B. & Jones, D.O.B. 2013. Deep-Sea Benthic Sampling. In *Methods for the Study of Marine Benthos.* 4th ed. A. Eleftheriou, Ed. 285-347. DOI:https://doi.org/10.1002/9781118542392.ch7.

Jarre, A., Hutchings, L., Crichton, M., Wieland, K., Lamont, T., Blamey, L.K., Illert, C., Hill, E. & Berg, M. 2015. Oxygen-depleted bottom waters along the west coast of South Africa, 1950-2011. *Fisheries Oceanography.* 24:56-73. DOI:10.1111/fog.12076.

Jetz, W., McGeoch, M.A., Guralnick, R., Ferrier, S., Beck, J., Costello, M.J., Fernandez, M., Geller, G.N., Keil, P., Merow, C., Meyer, C., Muller-Karger, F.E., Pereira, H.M., Regan, E.C., Schmeller, D.S. & Turak, E. 2019. Essential biodiversity variables for mapping and monitoring species populations. *Nature Ecology & Evolution.* 3(4):539-551. DOI:10.1038/s41559-019-0826-1.

Jørgensen, L.L., Renaud, P.E. & Cochrane, S.K.J. 2011. Improving benthic monitoring by combining trawl and grab surveys. *Marine Pollution Bulletin.* 62(6):1183-1190. DOI:https://doi.org/10.1016/j.marpolbul.2011.03.035.

Kaiser, M.J., Rogers, S.I. & Ellis, J.R. Eds. 1999. Importance of benthic habitat complexity for demersal fish assemblages. 212-223.

Karenyi, N. 2014. Patterns and drivers of benthic macrofauna to support systematic conservation planning for marine unconsolidated sediment ecosystems. PhD. Nelson Mandela Metropolitan University. 1-252.

Karenyi, N., Sink, K. & Nel, R. 2016a. Defining seascapes for marine unconsolidated shelf sediments in an eastern boundary upwelling region: The southern Benguela as a case study.

Estuarine, Coastal and Shelf Science. 169:195-206. DOI:https://doi.org/10.1016/j.ecss.2015.11.030.

Karenyi, N., Sink, K. & Nel, R. 2016b. Defining seascapes for marine unconsolidated shelf sediments in an eastern boundary upwelling region: The southern Benguela as a case study. *Estuarine Coastal and Shelf Science.* 169:1-195. DOI:https://doi.org/10.1016/j.ecss.2015.11.030.

Kassambara, A. 2020. *ggpubr: 'ggplot2' Based Publication Ready Plots.* Available:https://CRAN.R-project.org/package=ggpubr.

Keith, D.A., Ferrer-Paris, J.R., Nicholson, E. & Kingsford, R.T.e. Eds. 2020. *The IUCN Global Ecosystem Typology 2.0: Descriptive profiles for biomes and ecosystem functional groups.* Gland, Switzerland: IUCN. 1-170. DOI:https://doi.org/10.2305/IUCN.CH.2020.13.en.

Kenchington, E., Callery, O., Davidson, F., Grehan, A.J., Morato, T., Appiott, J., Davis, A., Dunstan, P.K., Du Preez, C., Finney, J., González-Irusta, J.M., Howell, K.L., Knudby, A., Lacharité, M., Lee, J., Murillo, F.J., Beazley, L., Roberts, J.M., Roberts, M., Rooper, C.N., Rowden, A.A., Rubidge, E.M., Stanley, R., Stirling, D., Tanaka, K.R., Vanhatalo, J.P., Weigel, B., Woolley, S.N.C. & Yesson, C. 2019. *Use of Species Distribution Modeling in the Deep Sea*. Canadian Technical Report of Fisheries and Aquatic Sciences 3296. ix+76. Available: http://hdl.handle.net/10026.1/13729.

Kenkel, N.C. 2006. On selecting an appropriate multivariate analysis. *Canadian Journal of Plant Science.* 86(3):663-676. DOI:10.4141/P05-164.

Kensley, B. 1981. On the zoogeography of southern African decapod Crustacea, with a distributional checklist of the species. *Smithsonian Contributions to Zoology, Number 338.*1-64.

Kensley, B. 2006. Pelagic shrimp (Crustacea: Decapoda) from shelf and oceanic waters in the southeastern Atlantic Ocean off South Africa. *Proceedings of the Biological Society of Washington.* 119(3):384-394. DOI:10.2988/0006-324X(2006)119[384:PSCDFS]2.0.CO;2.

Keribin, C. 2000. Consistent Estimation of the Order of Mixture Models. *Sankhyā: The Indian Journal of Statistics, Series A (1961-2002).* 62(1):49-66. Available: http://www.jstor.org/stable/25051289.

Kirkman, S.P., Holness, S., Harris, L.R., Sink, K.J., Lombard, A.T., Kainge, P., Majiedt, P., Nsiangango, S.E., Nsingi, K.K. & Samaai, T. 2019. Using Systematic Conservation Planning to support Marine Spatial Planning and achieve marine protection targets in the transboundary Benguela Ecosystem. *Ocean & Coastal Management.* 168:117-129. DOI:https://doi.org/10.1016/j.ocecoaman.2018.10.038.

Kirkman, S.P., Mann, B.Q., Sink, K.J., Adams, R., Livingstone, T.C., Mann-Lang, J.B., Pfaff, M.C., Samaai, T., van der Bank, M.G., Williams, L. & Branch, G.M. 2021. Evaluating the evidence for ecological effectiveness of South Africa's marine protected areas. *African Journal of Marine Science.* 43(3):389-412. DOI:10.2989/1814232X.2021.1962975.

Kreft, H. & Jetz, W. 2013. Comment on "An Update of Wallace's Zoogeographic Regions of the World". *Science.* 341(6144):343-343. DOI:10.1126/science.1237471.

Lacharité, M. & Metaxas, A. 2018. Environmental drivers of epibenthic megafauna on a deep temperate continental shelf: A multiscale approach. *Progress in Oceanography.* 162:171-186. DOI:https://doi.org/10.1016/j.pocean.2018.03.002.

Lange, L. & Griffiths, C.L. 2014. Large-scale spatial patterns within soft-bottom epibenthic invertebrate assemblages along the west coast of South Africa, based on the Nansen trawl survey. *African Journal of Marine Science.* 36(1):111-124. DOI:10.2989/1814232X.2014.894943.

Last, P.R., Lyne, V.D., Williams, A., Davies, C.R., Butler, A.J. & Yearsley, G.K. 2010. A hierarchical framework for classifying seabed biodiversity with application to planning and managing Australia's marine biological resources. *Biological Conservation.* 143(7):1675-1686. DOI:https://doi.org/10.1016/j.biocon.2010.04.008.

Leaper, R., Dunstan, P.K., Foster, S.D., Barrett, N.S. & Edgar, G.J. 2014. Do communities exist? Complex patterns of overlapping marine species distributions. *Ecology.* 95(7):2016-2025. Available: http://www.jstor.org.ezproxy.uct.ac.za/stable/43494880.

Leathwick, J.R., Elith, J. & Hastie, T. 2006a. Comparative performance of generalized additive models and multivariate adaptive regression splines for statistical modelling of species distributions. *Ecological Modelling.* 199(2):188-196. DOI:https://doi.org/10.1016/j.ecolmodel.2006.05.022.

Leathwick, J.R., Elith, J., Francis, M.P., Hastie, T. & Taylor, P. 2006b. Variation in demersal fish species richness in the oceans surrounding New Zealand: an analysis using boosted regression trees. *Marine Ecology Progress Series.* 321:267-281. Available: http://www.jstor.org.ezproxy.uct.ac.za/stable/24870850.

Leathwick, J.R., Rowden, A., Nodder, S., Gorman, R., Bardsley, S., Pinkerton, M., Baird, S.J., Hadfield, M., Currie, K. & Goh, A. 2012. *A Benthic-optimised Marine Environment Classification (BOMEC) for New Zealand waters*. New Zealand Aquatic Environment and Biodiversity Report No. 88. 1-54.

Lecours, V., Devillers, R., Schneider, D.C., Lucieer, V.L., Brown, C.J. & Edinger, E.N. 2015. Spatial scale and geographic context in benthic habitat mapping: review and future directions. *Marine Ecology Progress Series.* 535:259-284. Available: https://www.int-res.com/abstracts/meps/v535/p259-284/.

Lemaitre, R. 2004. A worldwide review of hermit crab species of the genus Sympagurus Smith, 1883 (Crustacea: Decapoda: Parapaguridae). In *Tropical Deep-Sea Benthos.* B. Marshall and B. Richer de Forges, Eds. Paris: Memoires du Museum national d'Histoire naturelle. 85-149.

Levin, L.A., Etter, R.J., Rex, M.A., Gooday, A.J., Smith, C.R., Pineda, J., Stuart, C.T., Hessler, R.R. & Pawson, D. 2001. Environmental Influences on Regional Deep-Sea Species Diversity. *Annual Review of Ecology and Systematics.* 32:51-93. Available: http://www.jstor.org.ezproxy.uct.ac.za/stable/2678635.

Levin, L.A. 2003. Oxygen Minimum Zone Benthos: Adaptation and Community Response to Hypoxia. *Oceanography and Marine Biology: An Annual Review.* 41:1-45.

Levin, S.A. 1998. Ecosystems and the Biosphere as Complex Adaptive Systems. *Ecosystems.* 1(5):431-436. DOI:10.1007/s100219900037.

Limongi, P., Ortega, L., Horta, S., Burone, L. & Carranza, A. 2023. Bioregionalization in a data-poor situation: Mapping of Uruguayan marine benthic regions. *Frontiers in Marine Science.* 10:1130827. DOI:10.3389/fmars.2023.1130827.

Lirman, D., Gracias, N.R., Gintert, B.E., Gleason, A.C.R., Reid, R.P., Negahdaripour, S. & Kramer, P. 2007. Development and application of a video-mosaic survey technology to document the status of coral reef communities. *Environmental Monitoring and Assessment.* 125(1):59-73. DOI:10.1007/s10661-006-9239-0.

Lombard, A.T., Strauss, T., Harris, J., Sink, K., Attwood, C. & Hutchings, L. 2004. *South African National Spatial Biodiversity Assessment 2004: Technical Report. Volume 4: Marine Component*. South African National Biodiversity Institute. Pretoria. 1-101.

Lyons, M.B., Foster, S.D. & Keith, D.A. 2017. Simultaneous vegetation classification and mapping at large spatial scales. *Journal of Biogeography.* 44(12):2891-2902. DOI:https://doi.org/10.1111/jbi.13088.

Magorrian, B.H., Service, M. & Clarke, W. 1995. An Acoustic Bottom Classification Survey of Strangford Lough, Northern Ireland. *Journal of the Marine Biological Association of the United Kingdom.* 75(4):987-992. DOI:10.1017/S0025315400038315.

Magorrian, B.H. 1997. The extent and temporal variation of disturbance to epibenthic communities in Strangford Lough, Northern Ireland. *Journal of the Marine Biological Association of the United Kingdom.* 77(4):1151-1164. DOI:10.1017/S0025315400038686.

Maiorano, P., D'Onghia, G., Capezzuto, F. & Sion, L. 2002. Life-history traits of Plesionika martia (Decapoda: Caridea) from the eastern-central Mediterranean Sea. *Marine Biology.* 141(3):527-539. DOI:10.1007/s00227-002-0851-4.

Makwela, M.S. 2017. An Investigation of Benthic Epifauna to Support Classification and Mapping of Outer Shelf Ecosystems in KwaZulu-Natal. University of the Western Cape. 1-108.

McArthur, M.A., Brooke, B.P., Przeslawski, R., Ryan, D.A., Lucieer, V.L., Nichol, S., McCallum, A.W., Mellin, C., Cresswell, I.D. & Radke, L.C. 2010. On the use of abiotic surrogates to describe marine benthic biodiversity. *Estuarine, Coastal and Shelf Science.* 88(1):21-32. DOI:https://doi.org/10.1016/j.ecss.2010.03.003.

McCormick, M.I. & Choat, J.H. 1987. Estimating total abundance of a large temperate-reef fish using visual strip-transects. *Marine Biology.* 96(4):469-478. DOI:10.1007/BF00397964.

McIntyre, A.D. 1956. The use of trawl, grab and camera in estimating marine benthos. *Journal of the Marine Biological Association of the United Kingdom.* 35(2):419-429. DOI:10.1017/S0025315400010249.

McIntyre, F.D., Neat, F., Collie, N., Stewart, M. & Fernandes, P.G. 2015. Visual surveys can reveal rather different 'pictures' of fish densities: Comparison of trawl and video camera surveys in the Rockall Bank, NE Atlantic Ocean. *Deep Sea Research Part I: Oceanographic Research Papers.* 95:67-74. DOI:https://doi.org/10.1016/j.dsr.2014.09.005.

McQuaid, K.A., Attrill, M.J., Clark, M.R., Cobley, A., Glover, A.G., Smith, C.R. & Howell, K.L. 2020. Using Habitat Classification to Assess Representativity of a Protected Area Network in a Large, Data-Poor Area Targeted for Deep-Sea Mining. *Frontiers in Marine Science.* 7:558860. DOI:10.3389/fmars.2020.558860.

McQuaid, K.A., Bridges, A.E.H., Howell, K.L., Gandra, T.B.R., de Souza, V., Currie, J.C., Hogg, O.T., Pearman, T.R.R., Bell, J.B., Atkinson, L.J., Baum, D., Bonetti, J., Carranza, A., Defeo, O., Furey, T., Gasalla, M.A., Golding, N., Hampton, S.L., Horta, S., Jones, D.O.B., Lombard, A.T., Manca, E., Marin, Y., Martin, S., Mortensen, P., Passadore, C., Piechaud, N., Sink, K.J. & Yool, A. 2023. Broad-scale benthic habitat classification of the South Atlantic. *Progress in Oceanography.* https://doi.org/10.1016/j.pocean.2023.103016. DOI:https://doi.org/10.1016/j.pocean.2023.103016.

Mellin, C., Delean, S., Caley, J., Edgar, G., Meekan, M., Pitcher, R., Przeslawski, R., Williams, A. & Bradshaw, C. 2011. Effectiveness of Biological Surrogates for Predicting Patterns of Marine Biodiversity: A Global Meta-Analysis. *PloS one.* 6(6):e20141. DOI:10.1371/journal.pone.0020141.

Meyer, H.K., Roberts, E.M., Rapp, H.T. & Davies, A.J. 2019. Spatial patterns of arctic sponge ground fauna and demersal fish are detectable in autonomous underwater vehicle (AUV) imagery. *Deep Sea Research Part I: Oceanographic Research Papers.* 153:103137. DOI:https://doi.org/10.1016/j.dsr.2019.103137.

Mohn, C. & Beckmann, A. 2002. Numerical studies on flow amplification at an isolated shelfbreak bank, with application to Porcupine Bank. *Continental Shelf Research.* 22(9):1325-1338. DOI:https://doi.org/10.1016/S0278-4343(02)00004-3.

Montefalcone, M., Tunesi, L. & Ouerghi, A. 2021. A review of the classification systems for marine benthic habitats and the new updated Barcelona Convention classification for the Mediterranean. *Marine Environmental Research.* 169:105387. DOI:https://doi.org/10.1016/j.marenvres.2021.105387.

Murillo, F.J., Kenchington, E., Beazley, L., Lirette, C., Knudby, A., Guijarro, J., Benoît, H., Bourdages, H. & Sainte-Marie, B. 2016. *Distribution Modelling of Sea Pens, Sponges, Stalked Tunicates and Soft Corals from Research Vessel Survey Data in the Gulf of St. Lawrence for Use in the Identification of Significant Benthic Areas*. Canadian Technical Report of Fisheries and Aquatic Sciences vi + 132.

Murillo, F.J., Kenchington, E., Koen-Alonso, M., Guijarro, J., Kenchington, T.J., Sacau, M., Beazley, L. & Rapp, H.T. 2020a. Mapping benthic ecological diversity and interactions with bottom-contact fishing on the Flemish Cap (northwest Atlantic). *Ecological Indicators.* 112:106135. DOI:https://doi.org/10.1016/j.ecolind.2020.106135.

Murillo, F.J., Weigel, B., Bouchard Marmen, M. & Kenchington, E. 2020b. Marine epibenthic functional diversity on Flemish Cap (north-west Atlantic)—Identifying trait responses to the environment and mapping ecosystem functions. *Diversity and Distributions.* 26(4):460-478. DOI:https://doi.org/10.1111/ddi.13026.

Nefdt, L. 2022. Marine ecosystem classification and conservation targets within the Agulhas ecoregion, South Africa. Master of Science. University of Cape Town. 1-134.

Neumann, H., Diekmann, R., Emeis, K., Kleeberg, U., Moll, A. & Kröncke, I. 2017. Full-coverage spatial distribution of epibenthic communities in the south-eastern North Sea in relation to habitat characteristics and fishing effort. *Marine Environmental Research.* 130:1-11. DOI:https://doi.org/10.1016/j.marenvres.2017.07.010.

Norberg, A., Abrego, N., Blanchet, F.G., Adler, F.R., Anderson, B.J., Anttila, J., Araújo, M.B., Dallas, T., Dunson, D., Elith, J., Foster, S.D., Fox, R., Franklin, J., Godsoe, W., Guisan, A., O'Hara, B., Hill, N.A., Holt, R.D., Hui, F.K.C., Husby, M., Kålås, J.A., Lehikoinen, A., Luoto,

M., Mod, H.K., Newell, G., Renner, I., Roslin, T., Soininen, J., Thuiller, W., Vanhatalo, J., Warton, D.I., White, M., Zimmermann, N.E., Gravel, D. & Ovaskainen, O. 2019. A comprehensive evaluation of predictive performance of 33 species distribution models at species and community levels. *Ecological monographs.* 89(3):e01370. DOI:https://doi.org/10.1002/ecm.1370.

Nybakken, J., Craig, S., Smith-Beasley, L., Moreno, G., Summers, A. & Weetman, L. 1998. Distribution density and relative abundance of benthic invertebrate megafauna from three sites at the base of the continental slope off central California as determined by camera sled and beam trawl. *Deep Sea Research Part II: Topical Studies in Oceanography.* 45(8):1753-1780. DOI:https://doi.org/10.1016/S0967-0645(98)80016-7.

O'Hara, T.D., Rowden, A.A. & Bax, N.J. 2011. A Southern Hemisphere Bathyal Fauna Is Distributed in Latitudinal Bands. *Current Biology.* 21(3):226-230. DOI:https://doi.org/10.1016/j.cub.2011.01.002.

O'Hara, T.D., Williams, A., Althaus, F., Ross, A.S. & Bax, N.J. 2020. Regional-scale patterns of deep seafloor biodiversity for conservation assessment. *Diversity and Distributions.* 26(4):479-494. DOI:https://doi.org/10.1111/ddi.13034.

Omori, M. & Ohta, S. 1981. The use of underwater camera in studies of vertical distribution and swimming behaviour of a sergestid shrimp, Sergia lucens. *Journal of Plankton Research.* 3(1):107-121. DOI:10.1093/plankt/3.1.107.

Osman, R.W. & Whitlatch, R.B. 2004. The control of the development of a marine benthic community by predation on recruits. *Journal of Experimental Marine Biology and Ecology.* 311(1):117-145. DOI:https://doi.org/10.1016/j.jembe.2004.05.001.

Ovaskainen, O. & Soininen, J. 2011. Making more out of sparse data: hierarchical modeling of species communities. *Ecology.* 92(2):289-295. Available: http://www.jstor.org.ezproxy.uct.ac.za/stable/41151138.

Ovaskainen, O., Tikhonov, G., Norberg, A., Guillaume Blanchet, F., Duan, L., Dunson, D., Roslin, T. & Abrego, N. 2017. How to make more out of community data? A conceptual framework and its implementation as models and software. *Ecology letters.* 20(5):561-576. DOI:https://doi.org/10.1111/ele.12757.

Ovaskainen, O. & Abrego, N. 2020. *Joint Species Distribution Modelling: With Applications in R.* United Kingdom: Cambridge University Press. 1-372. DOI:10.1017/9781108591720.

Payne, A.I., Crawford, R.J.M. & Van Dalsen, A.P. 1989. *Oceans of life off southern Africa.* Vlaeberg Publishers.

Pebesma, E.J. 2004. Multivariable geostatistics in S: the gstat package. *Computers & Geosciences.* 30:683-691.

Phillips, S., Dudík, M. & Schapire, R. 2004. A Maximum Entropy Approach to Species Distribution Modeling. *Proceedings of the Twenty-first International Conference on Machine Learning (ICML 2004)*. Banff, Alberta, Canada, July 4-8 2004.

Pillar, S.C. & Barange, M. 1997. Diel variability in bottom trawl catches and feeding activity of the Cape hakes off the west coast of South Africa. *ICES Journal of Marine Science.* 54(3):485-499. DOI:10.1006/jmsc.1996.0169.

Pitcher, C.R., Lawton, P., Ellis, N., Smith, S.J., Incze, L.S., Wei, C.-L., Greenlaw, M.E., Wolff, N.H., Sameoto, J.A. & Snelgrove, P.V.R. 2012. Exploring the role of environmental variables in shaping patterns of seabed biodiversity composition in regional-scale ecosystems. *Journal of Applied Ecology.* 49(3):670-679. DOI:https://doi.org/10.1111/j.1365-2664.2012.02148.x.

Pitcher, R., Rochester, W., Dunning, M., Courtney, T., Broadhurst, M., Noell, C., Tanner, J., Kangas, M., Newman, S., Semmens, J., Rigby, C., Saunders, T., Martin, J. & Lussier, B. 2018. *Putting potential environmental risk of Australia's trawl fisheries in landscape perspective.* Fisheries Research and Development Corporation. 1-62. DOI. Available: https://apo.org.au/node/204281.

Przeslawski, R., Currie, D.R., Sorokin, S.J., Ward, T.M., Althaus, F. & Williams, A. 2011. Utility of a spatial habitat classification system as a surrogate of marine benthic community structure for the Australian margin. *ICES Journal of Marine Science.* 68(9):1954-1962. DOI:10.1093/icesjms/fsr106.

Przeslawski, R., Foster, S.D., Monk, J., Langlois, T.J., Lucieer, V.L. & Stuart-Smith, R.D. 2018. *Comparative assessment of seafloor sampling platforms*.

Przeslawski, R., Foster, S., Monk, J., Barrett, N., Bouchet, P., Carroll, A., Langlois, T., Lucieer, V., Williams, J. & Bax, N. 2019. A Suite of Field Manuals for Marine Sampling to Monitor Australian Waters. *Frontiers in Marine Science.* 6. DOI:10.3389/fmars.2019.00177.

R Core Team. 2021. *R: A language and environment for statistical computing.* Vienna, Austria: R Foundation for Statistical Computing. Available:https://www.R-project.org/.

Rees, H.L., Pendle, M.A., Waldock, R., Limpenny, D.S. & Boyd, S.E. 1999. A comparison of benthic biodiversity in the North Sea, English Channel, and Celtic Seas. *ICES Journal of Marine Science.* 56(2):228-246. DOI:10.1006/jmsc.1998.0438.

Reiss, H., Degraer, S., Duineveld, G.C.A., Kröncke, I., Aldridge, J., Craeymeersch, J.A., Eggleton, J.D., Hillewaert, H., Lavaleye, M.S.S., Moll, A., Pohlmann, T., Rachor, E., Robertson, M., Vanden Berghe, E., van Hoey, G. & Rees, H.L. 2010. Spatial patterns of infauna, epifauna, and demersal fish communities in the North Sea. *ICES Journal of Marine Science.* 67(2):278-293. DOI:10.1093/icesjms/fsp253.

Reiss, H., Birchenough, S., Borja, A., Buhl-Mortensen, L., Craeymeersch, J., Dannheim, J., Darr, A., Galparsoro, I., Gogina, M., Neumann, H., Populus, J., Rengstorf, A.M., Valle, M., van Hoey, G., Zettler, M.L. & Degraer, S. 2014. Benthos distribution modelling and its relevance for marine ecosystem management. *ICES Journal of Marine Science.* 72(2):297-315. DOI:10.1093/icesjms/fsu107.

Renaud, P.E., Morata, N., Ambrose, W.G., Bowie, J.J. & Chiuchiolo, A. 2007. Carbon cycling by seafloor communities on the eastern Beaufort Sea shelf. *Journal of Experimental Marine Biology and Ecology.* 349(2):248-260. DOI:https://doi.org/10.1016/j.jembe.2007.05.021.

Rex, M.A. 1981. Community Structure in the Deep-Sea Benthos. *Annual Review of Ecology and Systematics.* 12:331-353. Available: http://www.jstor.org.ezproxy.uct.ac.za/stable/2097115.

Rex, M.A. 1983. Geographic patterns of species diversity in the deep-sea benthos. In *Deep-sea biology.* New York: John Wiley and Sons. 453-472.

Ringvold, H. & Moum, T. 2020. On the genus Crossaster (Echinodermata: Asteroidea) and its distribution. *PloS one.* 15(1):e0227223. DOI:10.1371/journal.pone.0227223.

Roel, B.A. 1987. Demersal communities off the west coast of South Africa. *South African Journal of Marine Science.* 5(1):575-584. DOI:10.2989/025776187784522135.

Roeleveld, M.A.C., Lipiński, M.R., Augustyn, C.J. & Stewart, B.A. 1992. The distribution and abundance of cephalopods on the continental slope of the eastern South Atlantic. *South African Journal of Marine Science.* 12(1):739-752. DOI:10.2989/02577619209504738.

Roff, J.C. & Taylor, M.E. 2000. National frameworks for marine conservation — a hierarchical geophysical approach. *Aquatic Conservation: Marine and Freshwater Ecosystems.* 10(3):209-223. DOI:https://doi.org/10.1002/1099-0755(200005/06)10:3<209::AID-AQC408>3.0.CO;2-J.

Roff, J.C., Taylor, M.E. & Laughren, J. 2003. Geophysical approaches to the classification, delineation and monitoring of marine habitats and their communities. *Aquatic Conservation: Marine and Freshwater Ecosystems.* 13(1):77-90. DOI:https://doi.org/10.1002/aqc.525.

Rogers, J. & Bremner, J.M. 1991. The Benguela ecosystem, Part VII Marine-geological aspects. *Oceanography and Marine Biology: An Annual Review.* 29:1-85.

Ross, R.E. & Howell, K.L. 2013. Use of predictive habitat modelling to assess the distribution and extent of the current protection of 'listed' deep-sea habitats. *Diversity and Distributions.* 19(4):433-445. DOI:https://doi.org/10.1111/ddi.12010.

Rowden, A.A., Anderson, O.F., Georgian, S.E., Bowden, D.A., Clark, M.R., Pallentin, A. & Miller, A. 2017. High-Resolution Habitat Suitability Models for the Conservation and Management of Vulnerable Marine Ecosystems on the Louisville Seamount Chain, South Pacific Ocean. *Frontiers in Marine Science.* 4. DOI:10.3389/fmars.2017.00335.

Rowden, A.A., Lundquist, C.J., Hewitt, J.E., Stephenson, F. & Morrison, M.A. 2018. *Review of New Zealand's coastal and marine habitat and ecosystem classification*. NIWA Client Report 2018115WN, prepared for Department of Conservation. 1-75.

RStudio Team. 2021. *RStudio: Integrated Development Environment for R.* Boston, MA: PBC. Available: http://www.rstudio.com/.

Rubidge, E.M., Gale, K.S.P. & Curtis, J.M.R. 2016. Community ecological modelling as an alternative to physiographic classifications for marine conservation planning. *Biodiversity and Conservation.* 25(10):1899-1920. DOI:10.1007/s10531-016-1167-x.

Rubin, D.B. 1981. The Bayesian Bootstrap. *The Annals of Statistics.* 9(1):130-134. Available: http://www.jstor.org/stable/2240875.

Rybakova, E., Galkin, S., Gebruk, A., Sanamyan, N. & Martynov, A. 2020. Vertical distribution of megafauna on the Bering Sea slope based on ROV survey. *PeerJ.* 8:e8628. Available: https://doi.org/10.7717/peerj.8628.

SANBI (South African National Biodiversity Institute). 2022. *National Marine Ecosystem Map beta, Version 2022 beta 1 (2006-2022)*. South African National Biodiversity Institute. Cape Town.

Schmidt-Nielsen, K. 1990. *Animal physiology: adaptation and environment.* New York: Cambridge University Press.

Sea-Bird Electronics Inc. 2017. *Seasoft V2: SBE Data Processing - CTD Data Processing and Plotting Software for Windows.* Washington. Available:https://epic.awi.de/id/eprint/38965/.

Sea-Bird Scientific. 2017. Module 13: Advanced Data Processing. In *Sea-Bird University: Sea-Bird Scientific Training for Data Collection in the Ocean.* K. Martini, Ed. 1-21.

Sea-Bird Scientific. 2022. *SBE 19plus V2 SeaCAT Profiler CTD.* Available:https://www.seabird.com/sbe-19plus-v2-seacat-profiler-ctd/product?id=60761421596.

Shah, A. 2018. Distribution of epifauna in offshore benthic environments along the west and south coast of South Africa. University of Cape Town. 1-75.

Shannon, L.V. 1985. The Benguela ecosystem part 1. Evolution of the Benguela, physical features and processes. *Oceanography and Marine Biology, Annual Review.* 23:105-182.

Shannon, L.V. & Nelson, G. 1996. The Benguela: Large Scale Features and Processes and System Variability. In *The South Atlantic: Present and Past Circulation.* Berlin, Heidelberg: Springer Berlin Heidelberg. 163-210. DOI:10.1007/978-3-642-80353-6_9.

Shumchenia, E.J. & King, J.W. 2010. Comparison of methods for integrating biological and physical data for marine habitat mapping and classification. *Continental Shelf Research.* 30(16):1717-1729. DOI:https://doi.org/10.1016/j.csr.2010.07.007.

Siberchicot, A., Julien-Laferrière, A., Dufour, A.-B., Thioulouse, J. & Dray, S. 2017. *adegraphics: An S4 Lattice-Based Package for the Representation of Multivariate Data.* The R Journal. Available:https://journal.r-project.org/archive/2017/RJ-2017-042/index.html.

Silberberger, M.J., Renaud, P.E., Buhl-Mortensen, L., Ellingsen, I.H. & Reiss, H. 2019. Spatial patterns in sub-Arctic benthos: multiscale analysis reveals structural differences between community components. *Ecological monographs.* 89(1):e01325. DOI:https://doi.org/10.1002/ecm.1325.

Simpson, G.L. 2009. *cocorresp: Co-correspondence analysis ordination methods.* R package version 0.4-3. Available:https://cran.r-project.org/package=cocorresp.

Sink, K.J., Wilkinson, S., Atkinson, L.J., Sims, P.F., Leslie, R.W. & Attwood, C.G. 2012a. *The potential impacts of South Africa's demersal hake trawl fishery on benthic habitats: Historical perspectives, spatial analyses, current review and potential management actions*. South African National Biodiversity Institute. Unpublished report. 1-84.

Sink, K.J., Holness, S., Harris, L.R., Majiedt, P.A., Atkinson, L.J., Robinson, T., Kirkman, S.P., Hutchings, L., Leslie, R., Lamberth, S. & al., e. 2012b. *South African National Biodiversity Assessment 2011: Technical Report. Marine and coastal component. Technical Report 4*. South African National Biodiversity Institute. Pretoria. 1-332.

Sink, K.J., van der Bank, M.G., Majiedt, P.A., Harris, L.R., Atkinson, L.J., Kirkman, S.P. & Karenyi, N.e. Eds. 2019a. *South African National Biodiversity Assessment 2018 Volume 4: Marine Realm.* Pretoria, South Africa: South African National Biodiversity Institute. 1-555. Available: http://hdl.handle.net/20.500.12143/6372.

Sink, K.J., Harris, L.R., Skowno, A.L., Livingstone, T., Franken, M., Porter, S., Atkinson, L.J., Bernard, A., Cawthra, H., Currie, J., Dayaram, A., de Wet, W.M., Dunga, L.V., Filander, Z., Green, A., Herbert, D., Karenyi, N., Palmer, R., Pfaff, M., Makwela, M., Mackay, F., van Niekerk, L., van Zyl, W., Bessinger, M., Holness, S., Kirkman, S.P., Lamberth, S. & Lück-Vogel, M. 2019b. Chapter 3: Marine Ecosystem Classification and Mapping. In *South African National Biodiversity Assessment 2018 Technical Report Volume 4: Marine Realm.* K.J. Sink, M.G. van der Bank, P.A. Majiedt, L.R. Harris, L.J. Atkinson, S.P. Kirkman and N. Karenyi, Eds. South African National Biodiversity Institute, Pretoria. South Africa. 49-108. Available: http://hdl.handle.net/20.500.12143/6372.

Sink, K.J., McQuaid, K., Atkinson, L.J., Palmer, R.M., Van der Heever, G., Majiedt, P.A., Dunga, L.V., Currie, J.C., Adams, R., Wahome, M., Howell, K.L. & Patterson, A.W. 2021. *Challenges and Solutions to develop capacity for Deep-sea Research and Management in South Africa*. South African National Biodiversity Institute. 1-35.

Sink, K.J., Adams, L.A., Franken, M., Harris, L.R., Currie, J., Karenyi, N., Dayaram, A., Porter, S., Kirkman, S., Pfaff, M., van Niekerk, L., Atkinson, L.J., Bernard, A., Bessinger, M., Cawthra, H., de Wet, W., Dunga, L., Filander, Z., Green, A., Herbert, D., Holness, S., Lamberth, S., Livingstone, T., Lück-Vogel, M., Mackay, F., Makwela, M., Palmer, R., Van Zyl, W. & Skowno, A. 2023. Iterative mapping of marine ecosystems for spatial status assessment, prioritization, and decision support. *Frontiers in Ecology and Evolution.* 11:1108118. DOI:10.3389/fevo.2023.1108118.

Smale, M.J., Roel, B.A., Badenhorst, A. & Field, J.G. 1993. Analysis of the demersal community of fish and cephalopods on the Agulhas Bank, South Africa. *Journal of Fish Biology.* 43(sA):169-191. DOI:https://doi.org/10.1111/j.1095-8649.1993.tb01186.x.

Smith, C.R., Jumars, P.A. & DeMaster, D.J. 1986. In situ studies of megafaunal mounds indicate rapid sediment turnover and community response at the deep-sea floor. *Nature.* 323(6085):251-253.

Snelder, T.H., Leathwick, J.R., Dey, K.L., Rowden, A.A., Weatherhead, M.A., Fenwick, G.D., Francis, M.P., Gorman, R.M., Grieve, J.M., Hadfield, M.G., Hewitt, J.E., Richardson, K.M., Uddstrom, M.J. & Zeldis, J.R. 2007. Development of an Ecologic Marine Classification in the New Zealand Region. *Environmental Management.* 39(1):12-29. DOI:10.1007/s00267-005-0206-2.

Snelgrove, P.V.R. & Butman, C.A. 1995. Animal-sediment relationships revisited: cause versus effect. *Oceanographic Literature Review.* 42(8):1-668.

Solan, M., Germano, J.D., Rhoads, D.C., Smith, C., Michaud, E., Parry, D., Wenzhöfer, F., Kennedy, B., Henriques, C., Battle, E., Carey, D., Iocco, L., Valente, R., Watson, J. & Rosenberg, R. 2003. Towards a greater understanding of pattern, scale and process in marine benthic systems: a picture is worth a thousand worms. *Journal of Experimental Marine Biology and Ecology.* 285-286:313-338. DOI:https://doi.org/10.1016/S0022-0981(02)00535-X.

Spalding, M.D., Fox, H.E., Allen, G.R., Davidson, N., Ferdaña, Z.A., Finlayson, M., Halpern, B.S., Jorge, M.A., Lombana, A., Lourie, S.A., Martin, K.D., McManus, E., Molnar, J., Recchia, C.A. & Robertson, J. 2007. Marine Ecoregions of the World: A Bioregionalization of Coastal and Shelf Areas. *BioScience.* 57(7):573-583. DOI:10.1641/B570707.

Spencer, M.L., Stoner, A.W., Ryer, C.H. & Munk, J.E. 2005. A towed camera sled for estimating abundance of juvenile flatfishes and habitat characteristics: Comparison with beam

trawls and divers. *Estuarine, Coastal and Shelf Science.* 64(2):497-503. DOI:https://doi.org/10.1016/j.ecss.2005.03.012.

Stephenson, F., Leathwick, J.R., Geange, S.W., Bulmer, R.H., Hewitt, J.E., Anderson, O.F., Rowden, A.A. & Lundquist, C.J. 2018. Using Gradient Forests to summarize patterns in species turnover across large spatial scales and inform conservation planning. *Diversity and Distributions.* 24(11):1641-1656. DOI:https://doi.org/10.1111/ddi.12787.

Stephenson, F., Bowden, D.A., Finucci, B., Anderson, O.F. & Rowden, A.A. 2021. *Developing updated predictive models for benthic taxa and communities across Chatham Rise and Campbell Plateau using photographic survey data*. New Zealand Aquatic Environment and Biodiversity Report No. 276. 1-82.

Stephenson, F., Rowden, A.A., Brough, T., Petersen, G., Bulmer, R.H., Leathwick, J.R., Lohrer, A.M., Ellis, J.I., Bowden, D.A., Geange, S.W., Funnell, G.A., Freeman, D.J., Tunley, K., Tellier, P., Clark, D.E., Lundquist, C.J., Greenfield, B.L., Tuck, I.D., Mouton, T.L., Neill, K.F., Mackay, K.A., Pinkerton, M.H., Anderson, O.F., Gorman, R.M., Mills, S., Watson, S., Nelson, W.A. & Hewitt, J.E. 2022. Development of a Seafloor Community Classification for the New Zealand Region Using a Gradient Forest Approach. *Frontiers in Marine Science.* 8:792712. DOI:10.3389/fmars.2021.792712.

Strong, J.A., Clements, A., Lillis, H., Galparsoro, I., Bildstein, T. & Pesch, R. 2019. A review of the influence of marine habitat classification schemes on mapping studies: inherent assumptions, influence on end products, and suggestions for future developments. *ICES Journal of Marine Science.* 76(1):10-22. DOI:10.1093/icesjms/fsy161.

Strong, J.A. 2020. An error analysis of marine habitat mapping methods and prioritised work packages required to reduce errors and improve consistency. *Estuarine, Coastal and Shelf Science.* 240:106684. DOI:https://doi.org/10.1016/j.ecss.2020.106684.

Sutton, T.T., Clark, M.R., Dunn, D.C., Halpin, P.N., Rogers, A.D., Guinotte, J., Bograd, S.J., Angel, M.V., Perez, J.A.A., Wishner, K., Haedrich, R.L., Lindsay, D.J., Drazen, J.C., Vereshchaka, A., Piatkowski, U., Morato, T., Błachowiak-Samołyk, K., Robison, B.H., Gjerde, K.M., Pierrot-Bults, A., Bernal, P., Reygondeau, G. & Heino, M. 2017. A global biogeographic classification of the mesopelagic zone. *Deep Sea Research Part I: Oceanographic Research Papers.* 126:85-102. DOI:https://doi.org/10.1016/j.dsr.2017.05.006.

ter Braak, C.J.F., Hoijtink, H., Akkermans, W. & Verdonschot, P.F.M. 2003. Bayesian model-based cluster analysis for predicting macrofaunal communities. *Ecological Modelling.* 160(3):235-248. DOI:https://doi.org/10.1016/S0304-3800(02)00256-9.

ter Braak, C.J.F. & Schaffers, A.P. 2004. Co-Correspondence Analysis: A New Ordination Method to Relate Two Community Compositions. *Ecology.* 85(3):834-846. Available: http://www.jstor.org.ezproxy.uct.ac.za/stable/3450407.

ter Braak, C.J.F. & Smilauer, P. 2015. Topics in constrained and unconstrained ordination. *Plant Ecology.* 216(5):683-696. Available: https://doi.org/10.1007/s11258-014-0356-5.

Toranza, C. & Arim, M. 2010. Cross-taxon congruence and environmental conditions. *BMC Ecology.* 10(1):1-18. DOI:10.1186/1472-6785-10-18.

Trenkel, V.M., Francis, R.I.C.C., Lorance, P., Mahévas, S., Rochet, M. & Tracey, D.M. 2004. Availability of deep-water fish to trawling and visual observation from a remotely operated

vehicle (ROV). *Marine Ecology Progress Series.* 284:293-303. Available: http://www.jstor.org.ezproxy.uct.ac.za/stable/24868944.

Trenkel, V.M., Vaz, S., Albouy, C., Brind'Amour, A., Duhamel, E., Laffargue, P., Romagnan, J.B., Simon, J. & Lorance, P. 2019. We can reduce the impact of scientific trawling on marine ecosystems. *Marine Ecology Progress Series.* 609:277-282. Available: https://www-jstor-org.ezproxy.uct.ac.za/stable/26638515.

Turpie, J.K., Beckley, L.E. & Katua, S.M. 2000. Biogeography and the selection of priority areas for conservation of South African coastal fishes. *Biological Conservation.* 92(1):59-72. DOI:https://doi.org/10.1016/S0006-3207(99)00063-4.

Tyberghein, L., Verbruggen, H., Pauly, K., Troupin, C., Mineur, F. & De Clerck, O. 2012. Bio-ORACLE: A global environmental dataset for marine species distribution modelling. *Global Ecology and Biogeography.* (21):272–281.

Tyler, P. & Gage, J. 1980. Reproduction and growth of the deep-sea brittlestar ophiura-ljungmani (lyman). *Oceanologica Acta.* 3(2):177-185. Available: https://archimer.ifremer.fr/doc/00323/43424/.

UNESCO (United Nations Educational Scientific and Cultural Organization). 2009. *Global Open Oceans and Deep Seabed (GOODS) - Biogeographic Classification*. Paris, UNESCO-IOC. (IOCTechnical Series, 84). 1-87.

Uthicke, S., Schaffelke, B. & Byrne, M. 2009. A Boom-Bust Phylum? Ecological and Evolutionary Consequences of Density Variations in Echinoderms. *Ecological monographs.* 79(1):3-24. Available: http://www.jstor.org.ezproxy.uct.ac.za/stable/27646164 [2023/09/05/].

Uzmann, J.R., Cooper, R.A., Theroux, R.B. & Wigley, R.L. 1977. Synoptic comparison of three sampling techniques for estimating abundance and distribution of selected megafauna: submersible vs camera sled vs otter trawl. *Marine Fisheries Review.* 39(12):11-19.

van der Heever, G.M., Atkinson, L.J. & von der Meden, C.E.O. 2021. Comparison of the particle size distributions of sediment collected from sandy seafloor using a Van Veen grab and cone dredge. *African Journal of Marine Science.* 43(2):259-264. DOI:10.2989/1814232X.2021.1902855.

Vanhatalo, J., Foster, S.D. & Hosack, G.R. 2021. Spatiotemporal clustering using Gaussian processes embedded in a mixture model. *Environmetrics.* 32(7):e2681. DOI:https://doi.org/10.1002/env.2681.

Vasquez, M., Allen, H., Manca, E., Castle, L., Lillis, H., Agnesi, S., Al Hamdani, Z., Annunziatellis, A., Askew, N., Bekkby, T., Bentes, L., Doncheva, V., Drakopoulou, V., Duncan, G., Gonçalves, J., Inghilesi, R., Laamanen, L., Loukaidi, V., Martin, S., McGrath, F., Mo, G., Monteiro, P., Muresan, M., Nikilova, C., O'Keeffe, E., Pesch, R., Pinder, J., Populus, J., Ridgeway, A., Sakellariou, D., Teaca, A., Tempera, F., Todorova, V., Tunesi, L. & Virtanen, E. 2021. *EUSeaMap 2021. A European broad-scale seabed habitat map.* 1-25.

von der Meden, C.E.O., Atkinson, L.J., Branch, G.M., Asdar, S., Ansorge, I.J. & van den Berg, M. 2017. Long-term change in epibenthic assemblages at the Prince Edward Islands: a comparison between 1988 and 2013. *Polar Biology.* 40(11):2171-2185. DOI:10.1007/s00300-017-2132-1.

von der Meden, C.E.O., Snyders, L., van der Heever, G., Haupt, T. & Bernard, A. 2021. *Video demonstrating how to set-up, deploy and operate a Ski-Monkey III towed benthic camera system.* Cape Town, South Africa: Octopi Africa (Pty) Ltd and Array Media (Pty) Ltd.

Warton, D.I., Wright, S.T. & Wang, Y. 2012. Distance-based multivariate analyses confound location and dispersion effects. *Methods in Ecology and Evolution.* 3:89-101. DOI:10.1111/j.2041-210X.2011.00127.x.

Weller, B.E., Bowen, N.K. & Faubert, S.J. 2020. Latent Class Analysis: A Guide to Best Practice. *Journal of Black Psychology.* 46(4):287-311. DOI:10.1177/0095798420930932.

Williams, A., Althaus, F. & Schlacher, T.A. 2015. Towed camera imagery and benthic sled catches provide different views of seamount benthic diversity. *Limnology and Oceanography: Methods.* 13(2):e10007. DOI:https://doi.org/10.1002/lom3.10007.

Williams, G.C. 2011. The Global Diversity of Sea Pens (Cnidaria: Octocorallia: Pennatulacea). *PloS one.* 6(7):e22747. DOI:10.1371/journal. pone.0022747.

Wilson, M.F.J., O'Connell, B., Brown, C.J., Guinan, J.C. & Grehan, A.J. 2007. Multiscale Terrain Analysis of Multibeam Bathymetry Data for Habitat Mapping on the Continental Slope. *Marine Geodesy.* 30(1-2):3-35. DOI:10.1080/01490410701295962.

Woolley, S.N.C., Tittensor, D.P., Dunstan, P.K., Guillera-Arroita, G., Lahoz-Monfort, J.J., Wintle, B.A., Worm, B. & O'Hara, T.D. 2016. Deep-sea diversity patterns are shaped by energy availability. *Nature.* 533:393+. Available: https://link-gale-com.ezproxy.uct.ac.za/apps/doc/A453506227/AONE?u=unict&sid=bookmark-AONE&xid=f441be07.

Woolley, S.N.C., Foster, S.D., Bax, N.J., Currie, J.C., Dunn, D.C., Hansen, C., Hill, N.A., O'Hara, T.D., Ovaskainen, O., Sayre, R., Vanhatalo, J.P. & Dunstan, P.K. 2019. Bioregions in Marine Environments: Combining Biological and Environmental Data for Management and Scientific Understanding. *BioScience.* 70(1):48-59. DOI:10.1093/biosci/biz133.

Woolley, S.N.C. 2021. *'ecomix'.* Statistical Methods Seminar Series, Ecological Forecasting Initiative. Available:https://github.com/eco4cast/Statistical-Methods-Seminar-Series/tree/main/woolley_ecomix.

Woolley, S.N.C. 2022. *'ecomix' R package.* Available:https://github.com/skiptoniam/ecomix.

WoRMS Editorial Board. 2023. *World Register of Marine Species*. Available: https://www.marinespecies.org [10.14284/170, 2023-03-30].

Wright, A.G., Griffiths, C.L. & Fairweather, T.P. 2020. Distribution and abundance patterns of two parapagurid hermit crabs (Crustacea: Decapoda: Anomura) along the west and south coasts of South Africa. *African Journal of Marine Science.* 42(2):177-183. DOI:10.2989/1814232X.2020.1765869.

Yemane, D., Field, J.G. & Leslie, R.W. 2008. Indicators of change in the size structure of fish communities: A case study from the south coast of South Africa. *Fisheries Research.* 93(1):163-172. DOI:https://doi.org/10.1016/j.fishres.2008.03.005.

Yesson, C., Taylor, M.L., Tittensor, D.P., Davies, A.J., Guinotte, J., Baco, A., Black, J., Hall-Spencer, J.M. & Rogers, A.D. 2012. Global habitat suitability of cold-water octocorals. *Journal of Biogeography.* 39(7):1278-1292. DOI:https://doi.org/10.1111/j.1365-2699.2011.02681.x.

Appendices

APPENDIX A – Species conversions from biomass to abundance

Conversions from species biomasses to abundances for selected trawl species where abundance estimation was deemed reasonable and possible. Average weight per individual was estimated based on previous trawls where both biomass and abundance had been recorded for that species. Where weights were variable due to the species being colonial (and weights were small), 1 individual was assumed. Abundances here are unstandardized and represent the total raw abundance estimated per trawl for each species. Weights are rounded off to three decimal places and abundances are rounded up to the nearest individual.

Site	Genus species	Biomass (kg)	Average weight per individual	Estimated abundance (number of individuals)
1	Polychaeta spp.	2.820	0.021	134
1	*Mycale anisochela*	5.100	0.290	18
1	*Haliclona anonyma*	0.050	variable	1
1	*Adeonella* spp.	0.064	variable	1
1	*Melithaea* spp.	0.246	variable	1
5	*Hamacantha esperioides*	0.130	variable	1
6	Cup corals	0.158	0.107	2
6	*Adeonella* spp.	0.002	variable	1
17	Polychaeta spp.	0.964	0.021	46

APPENDIX B – Number of taxa per sampling method

Epifaunal species/morphospecies recorded across the 18 sites by towed camera and trawl sampling methods, showing the overlap in species sampled by both methods (last column). Total species counts for major taxa and sampling methods are shown (S = total number of species/morphotaxa). Major taxa are at the Class level, except for Malacostraca (Decapoda, Isopoda, Stomatopoda) – shown at the Order level due to its large contribution to composition. Major taxa were categorised as 'other' if there were fewer than 3 species in total recorded for that taxon.

Class	Towed camera only (S = 21)	Trawl only (S = 43)	Towed camera and Trawl (S = 41)
Demospongiae (7)	**1**	**5**	**1**
	Polymastia bouryesnaultae	*Haliclona anonyma*	*Tetilla capillosa*
		Hamacantha esperioides	
		Inflatella belli	
		Mycale anisochela	
		Suberites dandelenae	
Anthozoa (14)	**7**	**1**	**6**
	Actinaria spp.	*Halcurias capensis*	*Actinauge granulata*
	Antipatharia spp.		*Actinostola capensis*
	Cerianthidae spp.		*Anthosactis capensis*
	Coral rubble		*Bolocera kerguelensis*
	Seafan spp.		Cup coral
	Soft coral spp.		*Melithaea* spp.
	Thouarella spp.		
Polychaeta (6)	**1**	**1**	**4**
	Praxillura spp.	*Aphrodita alta*	*Chloeia inermis*
			Hyalinoecia tubicola
			Polychaeta spp.
			Polychaete tube
Decapoda (25)	**4**	**14**	**7**
	Ebalia tuberculosa	*Aristaeopsis edwardsiana*	*Chaceon chuni*
	Pagurid spp.	*Chaceon macphersoni*	*Dorhynchus thomsoni*
	Prawn A	*Dromidia hirsutissima*	*Exodromidia spinosa*
	Prawn B	*Haliporoides triarthrus*	*Mursia cristiata*
		Jasus lalandii	*Parapontophilus gracilis*
		Merhippolyte agulhasensis	*Scyramathia hertwigi*
		Miersiograpsus kingsleyi	*Sympagurus dimorphus*
		Neopilumnoplax heterochir	
		Parapagurus bouvieri	
		Plesionika martia	
		Prawn spp.	
		Sergia spp.	
		Solenocera africana	
		Stereomastis sculpta	
Gymnolaemata (4)	**0**	**1**	**3**
		Laminopora jellyae	*Adeonella* spp.
			Flustramorpha spp.
			Phidoloporidae spp.
Gastropoda (8)	**2**	**3**	**3**
	Amalda bullioides	*Africolaria rutila*	*Athleta abyssicola*
	Gastropoda spp.	*Coluzea radialis*	*Fusitriton magellanicus*
		Neptuneopsis gilchristi	Velutinidae spp.
Asteroidea (17)	**0**	**8**	**9**
		Astropecten exilis	Asteroidea spp.
		Cosmasterias felipes	*Astropecten irregularis pontoporeus*
		Diplopteraster multipes	*Cheiraster hirsutus*
		Lophaster quadrispinus	*Crossaster penicillatus*
		Luidia sarsii africana	*Dipsacaster sladeni capensis*
		Perissasterias polyacantha	*Henricia abyssalis*
		Psilaster acuminatus	*Mediaster bairdi capensis*
		Pteraster capensis	*Pseudarchaster tessellatus*
			Toraster tuberculatus
Echinoidea (4)	**0**	**3**	**1**
		Brissopsis lyrifera capensis	*Spatangus capensis*
		Echinus gilchristi	
		Polyechinus agulhensis	

Ophiuroidea (6)	**2**	**1**	**3**
	Ophiomyxa vivipara capensis Ophiuroidea spp.	*Gorgonocephalus pustulatum*	*Ophiothrix aristulata* *Ophiura trimeni* *Ophiuroglypha costata*
Other (14)	4	6	4
Unknown (1)	1	0	0
	Porifera spp.		
Hydrozoa (2)	0	0	2
			Hydroid spp. Stylasteridae spp.
Isopoda (2)	1	1	0
	Munnopsurus mimus	Isopoda spp.	
Pycnogonida (1)	0	1	0
		Pycnogonida spp.	
Stomatopoda (1)	0	0	1
			Pterygosquilla capensis
Stenolaemata (1)	0	1	0
		Hornera erugata	
Rynchonellata (1)	0	1	0
		Terebratulina spp.	
Bivalvia (2)	1	1	0
	Pseudamussium gilchristi	*Limopsis chuni*	
Holothuroidea (1)	1	0	0
	Holothuroidea spp.		
Ascidiacea (1)	0	0	1
			Ascidiacea spp.
Graptolithoidea (1)	0	1	0
		Cephalodiscus gilchristi	

APPENDIX C – Species abundances per site

Epifaunal species/morphospecies abundances recorded at each site (1-18) by the towed camera and trawl sampling methods. Abundances are standardised to individuals.m^{-2} for the towed camera and individuals.1000 m^{-2} for the trawl, rounded off to three decimal places. The most abundant species per site and sampling method are highlighted in bold.

Site	Towed camera		Trawl	
	Species	Abundance (ind.m-2)	Species	Abundance (ind.1000 m-2)
1	Polychaeta spp.	0.744	*Sympagurus dimorphus*	0.034
	Ebalia tuberculosa	3.125	*Mursia cristiata*	0.011
	Munnopsurus mimus	0.050	Pycnogonida spp.	0.034
	Adeonella spp.	0.843	*Miersiograpsus kingsleyi*	0.078
	Cerianthidae spp.	0.050	*Neopilumnoplax heterochir*	0.011
	Stylasteridae spp.	0.050	Isopoda spp.	0.011
	Dipsacaster sladeni capensis	0.198	*Fusitriton magellanicus*	0.045
	Ophiuroglypha costata	0.347	Velutinidae spp.	0.011
	Fusitriton magellanicus	0.050	*Terebratulina* spp.	0.034
	Spatangus capensis	0.050	*Halcurias capensis*	0.011
	Ophiura trimeni	0.099	*Crossaster penicillatus*	0.302
			Cheiraster hirsutus	0.022
			Psilaster acuminatus	1.252
			Pseudarchaster tessellatus	0.011
			Mediaster bairdi capensis	0.011
			Lophaster quadrispinus	0.045
			Pteraster capensis	0.022
			Henricia abyssalis	0.034
			Perissasterias polyacantha	0.022
			Ophiuroglypha costata	0.056
			Ophiothrix aristulata	0.168
			Gorgonocephalus pustulatum	0.201
			Spatangus capensis	0.112
			Echinus gilchristi	0.011
			Polychaeta spp.	1.497
			Mycale anisochela	0.201
			Haliclona anonyma	0.011
			Inflatella belli	0.011
			Tetilla capillosa	0.011
			Adeonella spp.	0.011
			Flustramorpha spp.	0.056
			Phidoloporidae spp.	0.022
			Hornera erugata	0.011
			Ascidiacea spp.	0.436
			Melithaea spp.	0.011
			Cephalodiscus gilchristi	0.011
2	Polychaeta spp.	0.173	*Parapagurus bouvieri*	0.417
	Parapontophilus gracilis	0.635	*Scyramathia hertwigi*	0.011
	Dorhynchus thomsoni	0.288	*Dorhynchus thomsoni*	0.101
	Ebalia tuberculosa	2.135	*Fusitriton magellanicus*	0.011
	Munnopsurus mimus	0.231	*Coluzea radialis*	0.011
	Adeonella spp.	0.231	*Actinauge granulata*	0.135
	Actinaria spp.	1.788	*Actinostola capensis*	0.113
	Cerianthidae spp.	3.692	*Bolocera kerguelensis*	0.270
	Hydroid spp.	0.462	*Cheiraster hirsutus*	0.023
	Asteroidea spp.	0.058	*Luidia sarsii africana*	0.045
	Ophiura trimeni	20.192	*Diplopteraster multipes*	0.169
	Tetilla capillosa	0.231	*Tetilla capillosa*	0.214
3	Polychaeta spp.	0.035	*Parapagurus bouvieri*	0.031
	Ebalia tuberculosa	0.069	*Sympagurus dimorphus*	0.010
	Munnopsurus mimus	3.919	*Mursia cristiata*	0.010
	Actinaria spp.	0.035	*Stereomastis sculpta*	0.010
	Cerianthidae spp.	0.035	Isopoda spp.	0.010
	Cheiraster hirsutus	0.035	Velutinidae spp.	0.021
	Crossaster penicillatus	0.035	*Actinauge granulata*	0.063
	Ophiura trimeni	120.190	*Actinostola capensis*	0.031
			Crossaster penicillatus	0.483
			Cheiraster hirsutus	0.031
			Psilaster acuminatus	0.073
			Perissasterias polyacantha	0.010
			Ophiura trimeni	0.063
			Brissopsis lyrifera capensis	0.010
			Suberites dandelenae	0.031

4	Polychaeta spp.	1.814	*Sympagurus dimorphus*	0.387
	Chloeia inermis	21.589	*Scyramathia hertwigi*	0.022
	Praxillura spp.	0.036	*Mursia cristiata*	0.022
	Mursia cristiata	0.036	*Stereomastis sculpta*	0.011
	Parapontophilus gracilis	0.036	*Actinauge granulata*	0.011
	Scyramathia hertwigi	0.218	*Actinostola capensis*	0.022
	Pagurid spp.	0.036	*Crossaster penicillatus*	2.455
	Sympagurus dimorphus	0.145	*Cheiraster hirsutus*	0.199
	Munnopsurus mimus	0.036	*Psilaster acuminatus*	0.199
	Pterygosquilla capensis	0.036	*Ophiuroglypha costata*	0.055
	Actinaria spp.	0.363		
	Actinauge granulata	0.036		
	Crossaster penicillatus	0.145		
	Ophiura trimeni	0.835		
	Gastropoda spp.	0.036		
	Amalda bullioides	0.036		
5	Polychaeta spp.	0.112	*Parapagurus bouvieri*	0.181
	Mursia cristiata	0.056	*Scyramathia hertwigi*	0.049
	Dorhynchus thomsoni	0.056	*Dorhynchus thomsoni*	0.016
	Ebalia tuberculosa	0.672	*Mursia cristiata*	0.115
	Sympagurus dimorphus	0.056	*Pterygosquilla capensis*	0.033
	Munnopsurus mimus	3.586	*Stereomastis sculpta*	0.033
	Actinaria spp.	0.056	*Fusitriton magellanicus*	0.016
	Dipsacaster sladeni capensis	0.244	*Actinauge granulata*	0.214
	Spatangus capensis	0.112	*Actinostola capensis*	0.066
	Ophiura trimeni	145.011	*Crossaster penicillatus*	1.828
			Cheiraster hirsutus	0.148
			Psilaster acuminatus	0.231
			Diplopteraster multipes	0.033
			Ophiura trimeni	1.515
			Hamacantha esperioides	0.016
6	Polychaeta spp.	0.085	*Sympagurus dimorphus*	0.015
	Exodromidia spinosa	0.057	*Dorhynchus thomsoni*	0.031
	Scyramathia hertwigi	0.028	*Miersiograpsus kingsleyi*	0.015
	Ebalia tuberculosa	4.731	*Neopilumnoplax heterochir*	0.015
	Pagurid spp.	0.057	*Dromidia hirsutissima*	0.015
	Munnopsurus mimus	0.028	*Fusitriton magellanicus*	0.201
	Adeonella spp.	0.708	*Neptuneopsis gilchristi*	0.015
	Flustramorpha spp.	0.085	Velutinidae spp.	0.031
	Phidoloporidae spp.	0.085	*Luidia sarsii africana*	0.046
	Actinaria spp.	0.028	*Psilaster acuminatus*	0.015
	Cerianthidae spp.	2.210	Asteroidea spp.	0.031
	Hydroid spp.	0.340	*Ophiuroglypha costata*	0.355
	Spatangus capensis	0.397	*Ophiothrix aristulata*	0.448
	Ophiothrix aristulata	0.198	*Gorgonocephalus pustulatum*	0.108
	Ophiuroglypha costata	2.153	*Spatangus capensis*	0.293
	Ophiura trimeni	0.142	*Echinus gilchristi*	0.015
	Fusitriton magellanicus	0.028	Polychaeta spp.	0.278
	Amalda bullioides	0.028	Cup coral	0.031
			Isopoda spp.	0.093
			Adeonella spp.	0.015
			Melithaea spp.	0.015
7	Pagurid spp.	0.029	*Sympagurus dimorphus*	49.053
	Sympagurus dimorphus	1.758	*Mursia cristiata*	0.045
	Actinaria spp.	0.029	*Exodromidia spinosa*	0.080
	Bolocera kerguelensis	0.029	*Bolocera kerguelensis*	0.011
	Astropecten irregularis pontoporeus	0.059	*Astropecten irregularis pontoporeus*	0.170
	Spatangus capensis	0.088	*Luidia sarsii africana*	0.011
			Spatangus capensis	0.102
			Brissopsis lyrifera capensis	0.023
8	Polychaeta spp.	1.664	*Sympagurus dimorphus*	61.726
	Exodromidia spinosa	0.128	*Mursia cristiata*	0.427
	Pterygosquilla capensis	0.192	*Exodromidia spinosa*	0.427
	Adeonella spp.	0.256	*Neptuneopsis gilchristi*	0.014
	Astropecten irregularis pontoporeus	0.128	*Bolocera kerguelensis*	0.014
	Ophiuroglypha costata	1.664	*Crossaster penicillatus*	0.028
	Ophiura trimeni	0.064	*Luidia sarsii africana*	0.028
	Gastropoda spp.	0.192	*Dipsacaster sladeni capensis*	0.043
	Hydroid spp.	0.064	*Pseudarchaster tessellatus*	0.057
			Psilaster acuminatus	0.071
			Mediaster bairdi capensis	0.014
			Diplopteraster multipes	0.028

			Cosmasterias felipes	0.028
			Ophiuroglypha costata	0.057
			Brissopsis lyrifera capensis	0.028
			Polyechinus agulhensis	0.071
			Aphrodita alta	0.057
			Ascidiacea spp.	0.085
9	Polychaeta spp.	0.607	*Chaceon chuni*	0.899
	Hyalinoecia tubicola	0.373	*Chaceon macphersoni*	0.011
	Praxillura spp.	0.840	*Aristaeopsis edwardsiana*	0.011
	Parapontophilus gracilis	0.513	*Plesionika martia*	0.493
	Munnopsurus mimus	0.467	*Fusitriton magellanicus*	0.011
	Crossaster penicillatus	0.887	*Actinostola capensis*	0.066
	Prawn A	0.093	*Crossaster penicillatus*	0.033
	Chaceon chuni	0.047	*Hyalinoecia tubicola*	0.110
	Fusitriton magellanicus	0.047		
10	Polychaeta spp.	1.635	*Parapagurus bouvieri*	0.034
	Parapontophilus gracilis	0.889	*Sympagurus dimorphus*	0.011
	Dorhynchus thomsoni	0.029	*Scyramathia hertwigi*	0.034
	Ebalia tuberculosa	0.029	*Dorhynchus thomsoni*	0.011
	Pagurid spp.	0.115	*Mursia cristiata*	0.023
	Munnopsurus mimus	0.057	Isopoda spp.	0.011
	Adeonella spp.	0.803	Velutinidae spp.	0.045
	Phidoloporidae spp.	0.143	*Actinauge granulata*	0.011
	Ascidiacea spp.	0.029	*Actinostola capensis*	0.011
	Actinaria spp.	0.086	*Luidia sarsii africana*	0.011
	Seafan spp.	0.201	*Dipsacaster sladeni capensis*	0.011
	Melithaea spp.	0.086	*Diplopteraster multipes*	0.090
	Thouarella spp.	0.029	*Cosmasterias felipes*	0.011
	Antipatharia spp.	0.029	*Chloeia inermis*	0.011
	Cerianthidae spp.	0.029	Hydroid spp.	0.011
	Coral rubble	0.488		
	Cup coral	0.115		
	Hydroid spp.	0.545		
	Stylasteridae spp.	0.402		
	Henricia abyssalis	0.029		
	Spatangus capensis	0.029		
	Holothuroidea spp.	0.057		
	Ophiomyxa vivipara capensis	1.463		
	Ophiuroglypha costata	0.057		
	Ophiura trimeni	23.870		
	Pseudamussium gilchristi	0.029		
	Porifera spp.	0.230		
	Polymastia bouryesnaultae	0.086		
11	*Sympagurus dimorphus*	0.489	*Sympagurus dimorphus*	0.701
	Adeonella spp.	0.061	*Mursia cristiata*	0.023
	Actinaria spp.	0.061	*Exodromidia spinosa*	0.069
	Hydroid spp.	0.122	*Fusitriton magellanicus*	0.115
	Ophiuroglypha costata	0.183	*Athleta abyssicola*	0.023
	Gastropoda spp.	0.122	*Limopsis chuni*	0.011
	Fusitriton magellanicus	0.122	*Actinauge granulata*	0.011
			Crossaster penicillatus	0.046
			Luidia sarsii africana	0.046
			Dipsacaster sladeni capensis	0.023
			Psilaster acuminatus	0.023
			Pseudarchaster tessellatus	0.184
			Toraster tuberculatus	0.138
			Mediaster bairdi capensis	0.126
			Perissasterias polyacantha	0.011
			Ophiuroglypha costata	0.034
			Stylasteridae spp.	0.011
12	*Pterygosquilla capensis*	0.065	*Sympagurus dimorphus*	0.023
	Actinaria spp.	0.196	*Dorhynchus thomsoni*	0.023
	Pseudarchaster tessellatus	0.065	*Exodromidia spinosa*	0.046
	Sympagurus dimorphus	0.196	*Pterygosquilla capensis*	4.944
	Toraster tuberculatus	0.065	*Fusitriton magellanicus*	0.046
			Africolaria rutila	0.023
			Velutinidae spp.	0.046
			Luidia sarsii africana	0.138
			Pseudarchaster tessellatus	0.069
			Toraster tuberculatus	0.069
			Mediaster bairdi capensis	0.023
			Brissopsis lyrifera capensis	0.484

13	*Praxillura* spp.	0.387	*Parapagurus bouvieri*	0.011
	Parapontophilus gracilis	0.258	*Chaceon chuni*	1.346
	Pagurid spp.	0.129	*Chaceon macphersoni*	0.011
	Munnopsurus mimus	1.033	*Scyramathia hertwigi*	0.011
	Actinaria spp.	0.065	*Plesionika martia*	1.163
	Anthosactis capensis	0.065	*Haliporoides triarthrus*	0.011
	Actinauge granulata	0.065	*Fusitriton magellanicus*	0.043
	Ophiura trimeni	440.802	*Actinauge granulata*	0.011
	Amalda bullioides	0.065	*Actinostola capensis*	0.011
			Anthosactis capensis	0.011
			Crossaster penicillatus	0.743
			Psilaster acuminatus	0.011
			Diplopteraster multipes	0.140
14	*Chloeia inermis*	20.183	*Parapagurus bouvieri*	0.139
	Praxillura spp.	0.274	*Sympagurus dimorphus*	0.043
	Prawn B	0.205	*Scyramathia hertwigi*	0.043
	Parapontophilus gracilis	0.205	*Stereomastis sculpta*	0.032
	Pagurid spp.	0.137	*Plesionika martia*	7.568
	Munnopsurus mimus	0.205	*Haliporoides triarthrus*	0.129
	Actinaria spp.	0.274	*Merhippolyte agulhasensis*	0.021
	Crossaster penicillatus	0.205	*Parapontophilus gracilis*	0.032
	Ophiura trimeni	75.533	*Actinauge granulata*	0.032
	Fusitriton magellanicus	0.068	*Actinostola capensis*	0.011
	Amalda bullioides	0.137	*Crossaster penicillatus*	0.214
	Athleta abyssicola	0.068	*Luidia sarsii africana*	0.011
			Psilaster acuminatus	0.096
			Ophiura trimeni	0.214
			Aphrodita alta	0.021
			Chloeia inermis	3.366
			Fusitriton magellanicus	0.032
15	Polychaeta spp.	0.064	*Sympagurus dimorphus*	1.484
	Adeonella spp.	0.193	*Mursia cristiata*	0.034
	Actinaria spp.	0.064	*Pterygosquilla capensis*	0.101
	Astropecten irregularis pontoporeus	0.064	*Jasus lalandii*	0.067
	Ophiuroglypha costata	0.257	*Solenocera africana*	0.067
	Velutinidae spp.	0.064	Velutinidae spp.	0.191
			Toraster tuberculatus	0.022
			Astropecten exilis	0.011
			Aphrodita alta	0.011
			Laminopora jellyae	0.011
16	Polychaeta spp.	0.143	*Sympagurus dimorphus*	0.035
	Actinaria spp.	0.143	*Luidia sarsii africana*	0.058
	Hydroid spp.	0.071	*Toraster tuberculatus*	0.023
	Toraster tuberculatus	0.071		
	Velutinidae spp.	0.071		
17	Polychaeta spp.	0.298	*Mursia cristiata*	0.012
	Actinaria spp.	0.060	*Pterygosquilla capensis*	0.012
	Mediaster bairdi capensis	0.119	*Astropecten irregularis pontoporeus*	0.012
			Luidia sarsii africana	0.070
			Toraster tuberculatus	0.116
			Mediaster bairdi capensis	0.035
			Brissopsis lyrifera capensis	0.023
			Polychaeta spp.	0.535
18	Polychaeta spp.	0.120	*Sympagurus dimorphus*	0.063
	Hyalinoecia tubicola	0.080	*Chaceon chuni*	1.576
	Praxillura spp.	0.040	*Chaceon macphersoni*	0.011
	Parapontophilus gracilis	0.040	Prawn spp.	10.707
	Chaceon chuni	0.080	Sergia spp.	2.000
	Actinostola capensis	0.040	*Actinauge granulata*	0.011
	Soft coral spp.	0.080	*Actinostola capensis*	0.011
	Thouarella spp.	0.040	*Psilaster acuminatus*	0.011
	Coral rubble	1.277	*Pseudarchaster tessellatus*	0.032
	Cup coral	4.748	*Cosmasterias felipes*	0.011
	Stylasteridae spp.	0.200	*Hyalinoecia tubicola*	1.672
	Crossaster penicillatus	0.080		
	Ophiuroidea spp.	0.200		
	Athleta abyssicola	0.040		

APPENDIX D – *Ophiura trimeni* aggregations

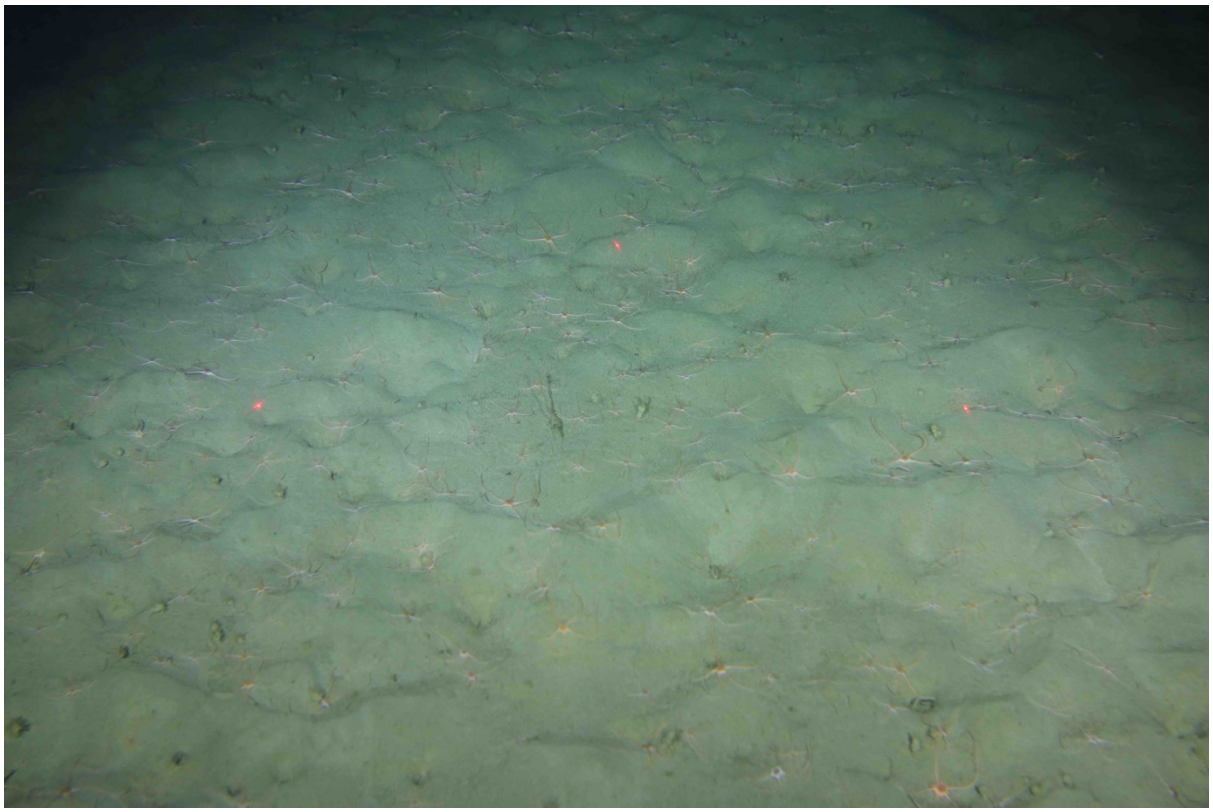

Source: SAEON, Benthic Trawl Experiment, 2018 (site 5)

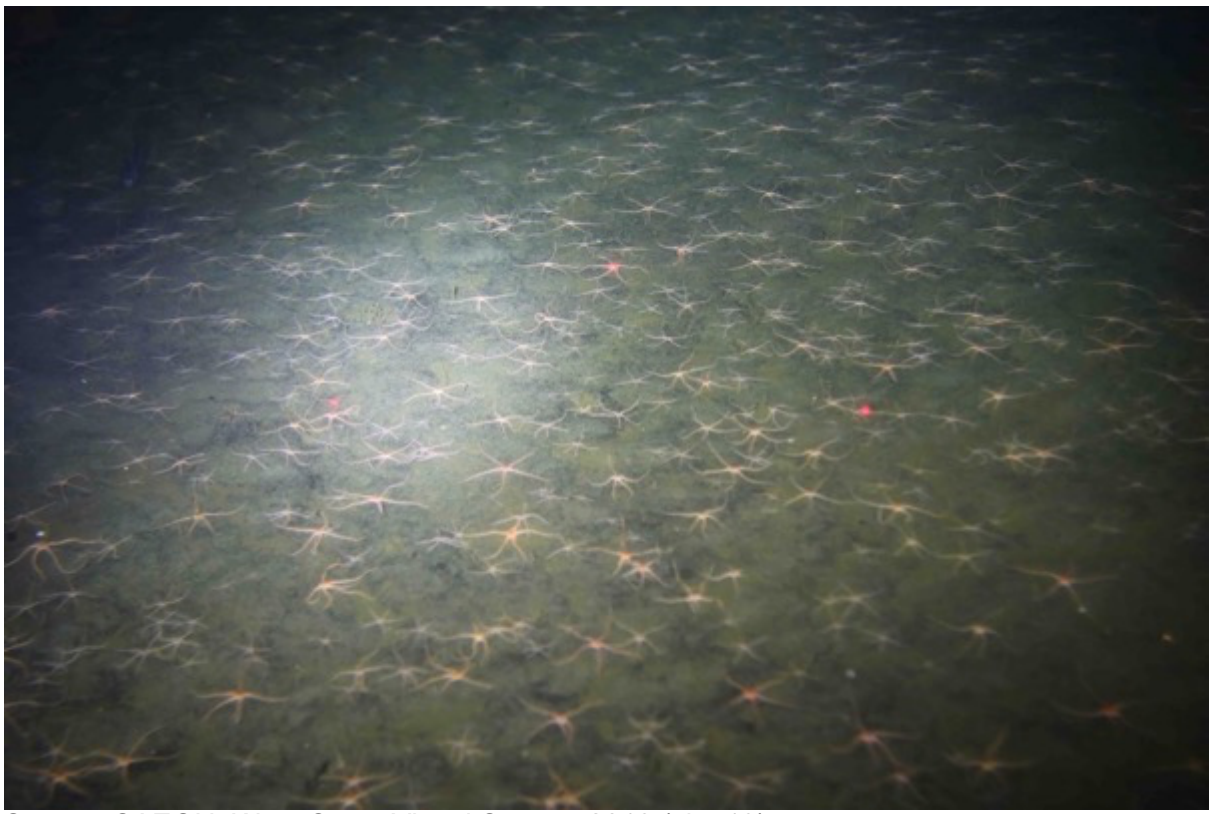

Source: SAEON, West Coast Visual Survey, 2019 (site 13)

APPENDIX E – Environmental data of trawl sites

West coast trawl surveys 2017 – 2020 with environmental data extracted from on board CTD. Slope was derived from a bathymetry layer (de Wet & Compton, 2021). Data will be served through SAEON once examination is complete. Available at this google sheet [Accessed: 2023, 2 April]:

https://docs.google.com/spreadsheets/d/1WsonDY40yAj9iOc5UFW4HVRw8_ratyVS/edit?usp=sharing&ouid=107838058637726807861&rtpof=true&sd=true

APPENDIX F – Estimated RCP model parameters

Species	Dispersion parameter	Alpha parameter	Tau parameter [1,]	[2,]	[3,]	[4,]
Ophiura trimeni	26.1194	-2.2357	3.1063	-5.2148	3.5895	3.1333
Pasiphaea sp 1	17.6527	-2.4897	1.9746	-5.2932	-4.9580	-1.6766
Anthoptilum grandiflorum	16.5105	-3.9270	-4.6666	-1.0436	3.6568	5.2634
Solenocera africana	15.2219	-3.0133	-4.1299	2.8191	0.0260	-0.9878
Bolocera kerguelensis	13.6440	-0.7656	-0.7553	-0.0012	1.0206	2.2102
Pteraster capensis	13.5806	-1.5569	-0.8639	1.1928	0.6254	1.6906
Sergia spp	12.2787	-5.3628	9.6899	-2.6938	-2.1763	-2.4959
Parapagurus bouvieri	12.2568	-1.2159	2.8499	-5.8637	5.6267	3.1622
Cavernularia spp	10.5445	-4.4368	-2.9589	-0.1399	-3.1654	-3.3218
Sympagurus dimorphus	8.8746	3.3279	-3.2127	2.7128	3.2068	2.8168
Hyalinoecia tubicola	8.7696	-5.9872	8.2918	-2.2762	-1.8258	-2.1861
Ophiomyxa vivipara capensis	8.7316	-5.1733	-2.8543	-3.9672	3.8479	5.3201
Funchalia woodwardi	8.7098	-3.9076	6.8363	-3.7713	4.0229	-3.6554
Plesionika martia	8.4841	-2.6757	6.3591	0.7924	1.5868	-4.4422
Echinus gilchristi	8.2934	-2.4014	-0.9409	1.0303	1.9381	2.4916
Brissopsis lyrifera capensis	8.2857	0.8523	-3.7945	1.7999	1.5288	0.4790
Spatangus capensis	6.8231	-0.7191	-6.0997	3.4603	1.2018	4.0039
Velutinid spp	6.5336	-2.0652	-5.2567	1.6273	1.4493	2.9843
Pterygosquilla capensis	6.5155	0.8634	-7.8187	3.6881	-0.0828	-0.4477
Cosmasterias felipes	6.1577	-2.1953	-1.1475	1.3156	1.5537	2.8353
Neptuneopsis gilchristi	6.0193	-5.2954	-3.2710	2.7839	-1.8886	4.4973
Dorhynchus thomsoni	5.9285	-0.0203	0.9061	-1.4925	1.7165	1.2043
Crossaster penicillatus	5.8510	1.0278	4.9825	-1.0900	3.2932	0.3308
Scyramathia hertwigi	5.8064	-1.6098	2.2993	-0.8690	2.5967	1.2809
Ophiuroglypha costata	5.7197	-2.8048	-4.2101	1.4856	2.6980	4.7227
Mediaster bairdi capensis	5.7175	-2.4631	-0.8566	2.5070	0.3606	-0.5664
Cheiraster hirsutus	5.3455	-0.7379	0.4230	-0.6418	4.9016	1.1956
Exodromidia spinosa	4.8683	0.7499	-4.7398	0.5585	2.4840	-0.3088
Ophiothrix aristulata	4.8371	-3.5191	-3.9860	1.4917	-2.9862	4.8746
Diplopteraster multipes	4.7558	-1.5354	2.0814	-0.9475	2.5244	1.7430
Perissasterias polyacantha	4.6365	-2.5376	-1.4668	0.8204	-0.6762	2.0591
Toraster tuberculatus	4.5271	-1.6916	-0.9605	2.8509	1.0311	2.1058
Chaceon chuni	4.4690	-3.6139	7.4827	0.0973	-0.2271	-3.8092
Pseudarchaster tessellatus	4.4341	0.0406	-1.1218	1.1589	0.6593	-1.1297
Athleta lutosa	4.0510	-3.9938	-3.4374	1.6036	-3.3885	0.4861
Actinostola capensis	3.9994	0.0569	1.9273	-2.3513	3.3171	0.5776
Astropecten irregularis pontoporeus	3.8947	-1.5086	-1.8268	2.8211	-5.0470	1.0637
Actinauge granulata	3.6597	-1.4633	2.4081	-0.9313	3.1336	0.6907
Mursia cristiata	3.3682	-0.4604	-2.4396	0.2429	1.9516	0.6337
Aphrodita alta	3.2536	-2.8424	0.7472	0.3609	0.9941	2.1928
Dipsacaster sladeni capensis	2.9816	-1.7182	0.2267	-0.1651	3.2344	1.7756
Psilaster acuminatus	2.8603	0.5017	-0.1689	-0.3640	0.7506	2.4607
Fusitriton magellanicus	2.6770	0.3948	-0.2400	-0.2545	0.2315	0.1861
Henricia abyssalis	2.5345	-2.5130	-3.5946	0.6869	2.0155	1.6538
Athleta abyssicola	2.3726	-2.4245	-4.5354	1.1516	2.1765	1.1722
Luidia sarsii africana	2.0706	0.0566	-1.6956	0.4495	1.7436	1.0622

Environmental covariates	Beta parameter [1,]	[2,]	[3,]	[4,]
(Intercept)	0.5454	1.5715	-0.5499	1.2094
Temperature1	-36.0591	12.8496	-23.5466	5.1490
Temperature2	-16.3986	-21.1524	-68.9020	-19.4601
Oxygen1	26.3791	34.0771	33.2509	62.2986
Oxygen2	4.8247	-10.3701	-15.8252	-12.5741
Slope1	15.5121	-5.3856	12.8549	-6.7362
Slope2	-14.6746	2.0556	-9.1717	0.2061

APPENDIX G – Estimated RCP species profiles

Species catch profiles for each bioregion (RCP 1–5). Profiles based on mean predicted abundances (individuals per 30-minute trawl site) ± lower and upper confidence intervals (CI).

	RCP 1			RCP 2			RCP 3			RCP 4			RCP 5		
Species	**Lower CI**	**Mean**	**Upper CI**	**Lower CI**	**Mean**	**Upper CI**	**Lower CI**	**Mean**	**Upper CI**	**Lower CI**	**Mean**	**Upper CI**	**Lower CI**	**Mean**	**Upper CI**
Actinauge granulata	0.9288	2.3360	4.6827	0.0315	0.0870	0.1777	3.0742	5.0397	7.7647	0.1317	0.4104	0.7953	0.0008	0.0010	0.0013
Actinostola capensis	1.8614	5.1367	15.9404	0.0008	0.0829	0.3087	15.1560	29.4765	57.5661	0.7861	1.7038	2.5729	0.0014	0.0362	0.0965
Anthoptilum grandiflorum	0.0002	0.0006	0.0011	0.0001	0.0045	0.0326	0.0244	1.2747	5.5908	0.5747	3.0789	9.4921	0.0004	0.0006	0.0008
Aphrodita alta	0.0243	0.1288	0.2814	0.0339	0.0867	0.1574	0.0463	0.1970	0.4125	0.1937	0.4549	0.8263	0.0007	0.0008	0.0010
Astropecten irregularis pontoporeus	0.0019	0.0343	0.1056	1.8195	4.0757	9.2476	0.0007	0.0014	0.0037	0.2465	0.7524	1.8441	2.5019	4.1753	6.3886
Athleta abyssicola	0.0006	0.0008	0.0010	0.1682	0.2928	0.5302	0.4905	0.7706	1.1156	0.0736	0.2558	0.6153	0.0035	0.0749	0.2333
Athleta lutosa	0.0004	0.0006	0.0008	0.0128	0.1160	0.3718	0.0004	0.0011	0.0060	0.0004	0.0320	0.1220	1.1471	2.0646	3.3681
Bolocera kerguelensis	0.0876	0.2105	0.3982	0.0019	0.4065	0.9636	0.5032	1.3216	2.5795	1.6034	4.1964	8.1498	0.0024	0.0491	0.1722
Brissopsis lyrifera capensis	0.0044	0.0518	0.1567	2.6344	14.7564	43.8552	1.0600	11.4370	34.3402	1.7301	5.5096	17.4912	0.2541	2.1840	4.4291
Cavernularia spp.	0.0004	0.0005	0.0007	0.0002	0.0133	0.0684	0.0004	0.0006	0.0009	0.0003	0.0008	0.0034	70.7034	183.8137	384.0480
Chaceon chuni	31.1033	48.3005	72.7846	0.0000	0.0217	0.1228	0.0010	0.0381	0.1601	0.0003	0.0005	0.0008	0.0005	0.0006	0.0008
Cheiraster hirsutus	0.1273	0.6451	1.6018	0.0435	0.2760	0.6670	21.2473	61.6623	136.8838	0.5613	1.5057	2.9625	0.0009	0.0011	0.0014
Cosmasterias felipes	0.0047	0.0356	0.0812	0.0747	0.4078	0.8130	0.1301	0.6506	1.4241	0.8489	1.7959	3.3475	0.0007	0.0009	0.0011
Crossaster penicillatus	246.4622	413.2448	667.0117	0.2413	0.9401	3.0243	31.9969	83.8127	168.3416	0.7491	3.2244	6.0502	0.0011	0.0033	0.0353
Diplopteraster multipes	0.7074	1.6336	2.9151	0.0003	0.0858	0.2094	1.7074	2.7741	4.3448	0.2664	1.0469	1.8748	0.0007	0.0010	0.0013
Dipsacaster sladeni capensis	0.0185	0.1729	0.6069	0.0143	0.1448	0.4053	2.5985	4.2514	6.0545	0.4111	1.0402	2.0812	0.0008	0.0010	0.0012
Dorhynchus thomsoni	0.6597	2.2985	5.1567	0.0480	0.2138	0.3838	2.7611	5.8055	11.1603	0.9479	2.7660	5.2853	0.0126	0.0918	0.2202
Echinus gilchristi	0.0018	0.0343	0.1231	0.0141	0.2486	0.6977	0.0321	0.5860	1.5063	0.5910	1.0614	1.8742	0.0007	0.0134	0.1580
Exodromidia spinosa	0.0012	0.0177	0.0693	2.5378	4.6865	12.3036	1.8164	25.9432	79.0344	0.7286	1.4153	2.3836	7.9057	14.5247	23.5145
Funchalia woodwardi	10.5844	18.1284	27.9594	0.0003	0.0004	0.0006	0.0184	1.4652	6.4786	0.0004	0.0005	0.0007	0.0005	0.0006	0.0008
Fusitriton magellanicus	0.5154	1.1673	1.9070	0.7070	1.2051	1.9668	1.2609	1.9583	2.7255	0.7773	1.5892	2.4503	0.8837	1.6131	2.9387
Henricia abyssalis	0.0005	0.0024	0.0173	0.0678	0.1823	0.3327	0.3473	0.6158	0.9482	0.1093	0.3769	0.6743	0.0027	0.0392	0.1110
Hyalinoecia tubicola	5.6984	10.0372	16.3247	0.0002	0.0003	0.0004	0.0003	0.0004	0.0005	0.0002	0.0003	0.0004	0.0003	0.0004	0.0004
Luidia sarsii africana	0.0543	0.1742	0.3277	1.0753	1.6348	2.3183	3.4932	5.9399	9.8210	1.9582	3.0675	4.4954	0.0937	0.2207	0.4207
Mediaster bairdi capensis	0.0005	0.0352	0.1380	0.6336	1.0651	1.6281	0.0142	0.1566	0.5274	0.0065	0.0783	0.4528	0.0005	0.0144	0.0822
Mursia cristiata	0.0119	0.0644	0.1837	0.5502	0.9556	2.6845	1.0223	3.7220	9.5424	0.4582	1.0973	1.7419	0.1427	0.4481	1.2162
Neptuneopsis gilchristi	0.0002	0.0005	0.0007	0.0002	0.0934	0.3223	0.0003	0.0010	0.0073	0.1999	0.4378	0.8023	0.0003	0.0005	0.0006
Ophiomyxa vivipara capensis	0.0003	0.0005	0.0007	0.0002	0.0006	0.0009	0.0228	0.4071	1.0286	0.3163	0.9875	1.7514	0.0004	0.0005	0.0007
Ophiothrix aristulata	0.0005	0.0007	0.0009	0.0215	0.1405	0.3580	0.0006	0.0910	0.5095	1.7120	3.6454	5.7733	0.0074	0.0498	0.1185
Ophiura trimeni	0.8242	2.3277	4.2826	0.0004	0.0006	0.0008	1.1677	4.2115	9.4038	0.0072	2.0935	8.0868	0.0007	0.0009	0.0011
Ophiuroglypha costata	0.0006	0.0008	0.0010	0.1657	0.2837	0.4552	0.4190	1.0148	1.8270	2.8436	6.2734	12.5328	0.0006	0.0009	0.0013
Parapagurus bouvieri	1.4720	4.3314	8.4358	0.0005	0.0007	0.0010	26.1055	79.0278	158.2851	0.0278	6.1807	14.5438	0.0008	0.0010	0.0013

Pasiphaea sp. 1	0.2005	0.6806	1.5518	0.0004	0.0007	0.0017	0.0006	0.0009	0.0016	0.0007	0.0136	0.0470	829.6363	1906.2752	3377.2839
Perissasterias polyacantha	0.0007	0.0176	0.0544	0.0825	0.1938	0.3113	0.0016	0.0501	0.1382	0.3541	0.5980	0.9630	0.0029	0.0323	0.1060
Plesionika martia	20.0917	43.8777	90.3290	0.0416	0.1878	0.5013	0.0303	0.3170	1.2018	0.0005	0.0007	0.0009	0.0007	0.0014	0.0101
Pseudarchaster tessellatus	0.1397	0.3161	0.5747	2.2292	3.6115	5.5322	0.8893	1.9218	3.5165	0.1453	0.3758	0.7473	0.3730	1.4898	3.0276
Psilaster acuminatus	0.6953	1.3119	2.0699	0.3118	1.0616	1.6173	2.1747	3.6133	5.6777	10.8841	18.3722	31.6668	0.0017	0.1218	0.3577
Pteraster capensis	0.0131	0.0932	0.2152	0.1152	0.7314	1.7967	0.1354	0.3363	0.6981	0.3036	1.1883	4.1454	0.0007	0.0164	0.0749
Pterygosquilla capensis	0.0011	0.0031	0.0181	27.0843	110.6239	347.3573	0.4552	2.0422	4.3466	0.7927	1.5985	2.9902	176.9829	246.2346	343.8047
Scyramathia hertwigi	0.5917	1.7484	3.3813	0.0278	0.0900	0.1902	1.5060	2.9157	5.3076	0.0633	0.5524	1.3290	0.0008	0.0010	0.0012
Sergia spp.	43.1463	81.1325	129.5633	0.0002	0.0003	0.0005	0.0003	0.0011	0.0065	0.0003	0.0004	0.0005	0.0004	0.0004	0.0005
Solenocera africana	0.0005	0.0008	0.0010	0.4407	0.9158	1.7210	0.0029	0.0505	0.1464	0.0004	0.0229	0.0658	0.1604	0.5688	1.4727
Spatangus capensis	0.0008	0.0011	0.0014	1.5113	14.7677	27.6727	0.3636	1.5689	3.2740	15.5423	27.4746	44.0561	0.0011	0.0365	0.1187
Sympagurus dimorphus	0.2473	0.9799	2.0289	48.7552	363.2749	683.2187	232.4450	695.5396	1186.9874	153.6235	466.3162	893.7509	0.0153	0.1491	0.7160
Toraster tuberculatus	0.0095	0.0683	0.1688	1.6929	3.2715	4.8773	0.3047	0.7230	1.7342	0.8089	1.5143	2.5842	0.0008	0.0010	0.0012
Velutinid spp.	0.0007	0.0009	0.0012	0.1869	0.6190	1.3702	0.1770	0.5518	1.0984	1.2581	2.4793	3.9117	0.0167	0.0597	0.1493